University of Alabama at Birmingham
UAB Digital Commons

All ETDs from UAB | UAB Theses & Dissertations

2007

A Study Into The Protein/Protein Interactions Involved In HIV-1 Capsid Assembly

Chanel Catherine Douglas
University of Alabama at Birmingham

Follow this and additional works at: https://digitalcommons.library.uab.edu/etd-collection

 Part of the Medical Sciences Commons

Recommended Citation

Douglas, Chanel Catherine, "A Study Into The Protein/Protein Interactions Involved In HIV-1 Capsid Assembly" (2007). *All ETDs from UAB*. 3691.
https://digitalcommons.library.uab.edu/etd-collection/3691

This content has been accepted for inclusion by an authorized administrator of the UAB Digital Commons, and is provided as a free open access item. All inquiries regarding this item or the UAB Digital Commons should be directed to the UAB Libraries Office of Scholarly Communication.

A STUDY INTO THE PROTEIN/PROTEIN INTERACTIONS INVOLVED IN HIV-1 CAPSID ASSEMBLY

by

CHANEL CATHERINE DOUGLAS

PETER E. PREVELIGE, JR., COMMITTEE CHAIR
WILLIAM J. BRITT
BEATRICE H. HAHN
COLLEEN B. JONSSON
MING LUO
RUIWEN ZHANG

A DISSERTATION

Submitted to the graduate faculty of The University of Alabama at Birmingham,
in partial fulfillment of the requirements for the degree of
Doctor of Philosophy

BIRMINGHAM, ALABAMA

2007

A STUDY INTO THE PROTEIN/PROTEIN INTERACTIONS INVOLVED IN HIV-1 CAPSID ASSEMBLY

CHANEL CATHERINE DOUGLAS

MICROBIOLOGY GRADUATE PROGRAM

ABSTRACT

The aim of this work was to build an understanding of the protein/protein interactions involved in HIV-1 capsid assembly as it relates to the condensation of capsid within the virion. This was undertaken in an attempt to (i) understand how capsid subunits recognize and interact with each other, (ii) gain insight into the protein-protein interactions involved in the process, and (iii) determine if the protein-protein interactions involved in virus capsid assembly can be used as a target for viral inhibition.

Within this dissertation you will find two approaches to this investigation. The first examines the role of electrostatics in the in-vitro assembly of HIV-1 capsid through the use of select amino acid mutations. The second searches for small molecules that could inhibit or alter the protein/protein interactions involved in capsid assembly. This was accomplished by screening for restriction of an in-vitro capsid assembly assay as the initial consideration tool.

Of the 10,000 compounds screen 114 compounds were shown to strongly disrupt capsid assembly in-vitro. Ninety-six of the strong inhibitors were screened in a series of cell-culture based assays with fully infectious virus for the ability to inhibit virus infectiv-

ity or viral production. In addition, the degree of toxicity of the compounds to the cells was also monitored. The second selection tool yielded six potential compounds. Attempts to elucidate the mechanism of action of these six compounds are described. Three of the six compounds are shown to primarily exert their anti-viral effect during the second half of the viral life-cycle.

Dedication

…..we also rejoice in our sufferings, because we know that suffering produces perseverance; perseverance, character; and character, hope. And hope does not disappoint us…..Romans 5:3-4 NIV

TABLE OF CONTENTS

Page

LIST OF TABLES

Table *Page*

INVESTIGATION OF N-TERMINAL DOMAIN CHARGED RESIDUES ON THE ASSEMBLY AND STABILITY OF HIV-1CA

IDENTIFICATION OF SMALL MOLECULE INHIBITORS OF HIV-1 ASSEMBLY AND MATURATION

LIST OF FIGURES

Figure *Page*

INVESTIGATION OF N-TERMINAL DOMAIN CHARGED RESIDUES ON THE ASSEMBLY AND STABILITY OF HIV-1CA

IDENTIFICATION OF SMALL MOLECULE INHIBITORS OF HIV-1 ASSEMBLY AND MATURATION

LIST OF ABBREVIATIONS

3TC – cis-1-[2’-Hydroxymethyl-5’-(1,3-oxathiolanyl)] cytosine

AZT -3’-Azido-3’-deoxythymidine

ß-Gal –Beta Galactosidase

Blam-Vpr -β-lactamase- Vpr

CA – Capsid

CAP-1 -1 (N-(3-chloro-4-methylphenyl)-N′-{2-[({5-[(dimethylamino)-methyl]-2-furyl}-methyl)-sulfanyl]-ethyl}urea)

CCF2-AM -

CD –Circular Dichroism

CD8+ - Cytoplasmic Domain 8 positive

CTD – C-terminal domain

CryoEM – Cryogenic Electron Microscopy

Da – Dalton

DEAE Dextran - Diethylamino Ethanol Dextran

DMEM – Dulbecco’s Modified Eagle’s Medium

DMSO – Dimethylsulfoxide

DTT - Dithiothreitol

DSB -3-*O*-{3',3'-dimethylsuccinyl}-betulinic acid

EDTA - Ethylenediaminetetraacetic acid

EGFP – Enhanced Green Fluorescent Protein

ELISA - Enzyme-Linked Immunosorbent Assay

EM – Electron Microscopy

ENV – Envelope Glycoprotein

ESI-TOF – Electron Spray Ionization - Time of Flight

FBS – Fetal Bovine Serum

Gag- Group-specific antigen

Gag-Pol – Group-specific antigen-Polymerase

GFP – Green Fluorescent Protein

H-bond – Hydrogen Bond

HIV-1 –Human Immunodeficiency Virus -1

IC_{50} - 50% inhibitory concentration

IgG – Immunoglobulin G

IL-2 - Interleukin 2

IN – Integrase

IND – Indinavir Sulfate; 4-Hydroxy-N-(2-hydroxy-2,3-dihydro-1H-1-indanyl)-N'-(1,1-dimethylethyl)-2-phenylmethyl-5-[4-(3-pyridylmethyl)-1- piperz-inyl]hexanediamide sulfate

K_d – Dissociation Constant

LTR – Long Terminal Repeat

Luc-M7 - 5.25.GFP.Luc.M7 cells

MA – Matrix Protein

MAGI -

MOI – Multiplicity of Infection

MTS - 3-(4,5-Dimethylthiazol-2-yl)-2,5-diphenyltetrazolium bromide

NC – Nucleocapsid Protein

NF-κβ –Nuclear Factor kappa B

NMR- Nuclear Magnetic Resonance

NTD – N –terminal domain

N-Terminal – Amino Terminal

p24 – Capsid Protein

PA-457 -3-*O*-{3',3'-dimethylsuccinyl}-betulinic acid

PCR – Polymerase Chain Reaction

PBMC - Peripheral Blood Mononuclear Cell

PMT –Photomultiplier tube

Poly-A - Polyadenylation

PR – Protease

Q- Sepharose

RNA – Ribonucleic acid

RPMI 1640 -

RT – Reverse Transcriptase

SEB – Staphylococcal Enterotoxin B

SI – Selectivity Index

SIVcpz- Simian Immunodeficiency Virus chimpanzee

SP-Sepharose -

Tat - Trans-acting regulatory protein

TC_{50} - 50% toxic concentration

TI – Therapeutic Index

UV - Ultraviolet

WT-Wild Type

YK-FH312 - 3-*O*-{3',3'-dimethylsuccinyl}-betulinic acid

INTRODUCTION

Viral Capsid Assembly

Viruses are obligate intracellular parasites whose only purpose is to procreate through replication of their genome. As such there are two essential elements that all viruses have, the viral genome (RNA or DNA) which encodes all of the viral components and the virus capsid which acts to protect the genome during transport from one cell to another. The assembly of virus particles is, even for the simplest of viruses, a complex process. Viruses must be capable of discriminating against an infinite number of cellular components in order to efficiently and correctly assemble fully infectious progeny.

Although the existence of viruses has been known since 1898, it took until 1955 for the process of virus self-assembly to be demonstrated (37). Since then virus capsid assembly has been extensively studied but many unanswered questions still remain. Amongst these are the following: (i) How do capsid subunits recognize and interact with each other? (ii) What protein-protein interactions are involved in this process? (iii) Can the protein-protein interactions involved in virus capsid assembly be used as a target for viral inhibition? Although it is beyond the scope of this dissertation to unequivocally provide the answers for these questions, it is the intent of the author to shed some light on these areas.

Many advances in understanding viruses have been made using those that infect plants and bacteria because of the ability to obtain relative pure samples in high concentrations. As such, many significant discoveries pertaining to virus assembly have also been made in these systems. In fact utilizing the very first isolated virus, tobacco mosaic virus (TMV), the process of self-assembly was discovered in 1955 by Fraenkel-Conrat

and Willams(37). They showed that infectious TMV particles could be reconstituted from the mixing of purified RNA and purified coat protein. The relative simplicity of the plant and bacterial systems has also allowed researchers to decipher many stages of virus assembly through the genetic manipulation of both the host and virus.

The structural biology of viral capsid is another important facet in gaining insight on the nature of virus capsid assembly. Through the ability to directly visualize a virus particle important advances in understanding virus structure and thus virus capsid assembly have been made. Based on what was observed from X-ray diffraction of crystals and under the microscope (electron) Crick and Watson in their 1956 Nature paper proposed that: "a small virus contains identical sub-units, packed together in a regular manner"(22). They also proposed that spherical virus particles would have tetrahedral, octahedral, or icosahedral symmetry. This meant that at most they could have 60 subunits. Expanding on this, Caspar and Klug in their seminal Cold Spring Harbor Symposium paper of 1962 introduced the theory of quasi-equivalence. Quasi-equivalence described the way in which large numbers (>60) of identical protein subunits could build closed virus capsids during a self-assembly process. In the 1962 paper Casper and Klug actually coined the term “self-assembly”. It is an idea that borrows concepts from the process of crystallization and was described as;

> “Self assembly is a process akin to crystallization and is governed by the laws of statistical mechanics. The protein subunits and the nucleic acid chain spontaneously come together to form a simple virus particle because (under appropriate solvent conditions) this is their lowest energy state. It is in the transition from a state in which protein subunits and nucleic acid chains are randomly arranged in space to a state in which they are highly ordered that virus assembly is like crystallization” (17)

Some aspects of quasi-equivalence describe how viruses self –assemble in that it provides a rationale for the differentiation of identical protein subunits into different con-

formations that have essentially the same bonding specificity. It does this by introducing the concept of sub-triangulation, in which there are still only 60 symmetrical units but now each of those units may be composed of multiple identical or non-identical subunits.

Although quasi-equivalence provides us with a way to describe the final state of an assembled capsid complex it does not provide us with a description of how these proteins come together, what interactions keep them together or what drives identical proteins to vary their conformation based on their position in the shell.

To gain a better insight into this we need to develop a dynamic system in which both the proteins and their environment can be manipulated. By being able to vary these conditions we can learn about how viruses assemble and study conditions in which this can be inhibited.

Biochemical and Mutational Analysis

The study of viruses and the study of proteins have an overlapping history. As such, the methods traditionally used to study proteins have also been employed to the study of viruses. These have involved the use of mutations and biochemical manipulations. In essence when we study the assembly of a virus capsid structure we are studying the way in which a protein forms complex structures.

The study of protein folding was launched with the realization that proteins (in particular, enzymes) lost there functionality when precipitated. It was proposed by Chick and Martin in their 1910 paper that precipation was preceded by the process of denaturation(19). In 1929, Hsien Wu hypothesized that denaturation was a form of protein folding in that it was a conformational change of the protein that resulted in the ex-

posure of amino acid side-chains to the solvent. He speculated that the loss of a particular conformation resulted in the loss of enzymatic activity (30). This insight into protein folding was followed by extensive research into the physical interactions that stabilized the folded protein structures. Wrinch and Langmuir, although advocating another theory, discovered hydrophobic interactions (116) (the application to protein chemistry was later expounded by Kauzmann (64)) while Pauling developed models for the secondary structure elements of proteins (85). These structures based on hydrogen bonding were the alpha helix and the beta sheet (91, 92) . In the1960's, Anfinsen put forth the "thermodynamic hypothesis" of protein folding. In his Nobel Lecture on December 11,1972 he articulates:

"This hypothesis-states that the three-dimensional structure of a native protein in its normal physiological milieu is the one in which the Gibbs free energy of the whole system is lowest; that is, that the native conformation is determined by the totality of interatomic interactions and hence by the amino acid sequence, in a given environment(4)."

Or in other words that the folded state represented the global minimum of free energy for the protein.

The ionic nature of proteins was demonstrated by Bjerrum(6), Weber(133), Tiselius(124, 125), and Linderstrom-Lang(77) who demonstrated that the charges were generally accessible to solvent(60). These three characteristics (ionic interactions, hydrophobic and hydrogen bonds) represent major driving forces not only in the folding of proteins but in protein/protein complex such as capsid assemblies.

Mechanisms to modify and manipulate these driving forces have dominated the field of protein engineering. One technique that transformed the study of protein folding is site-directed mutagenesis originated by Smith in 1978 (59). Using this technique we can substitute any amino acid with one of the 20 naturally occurring amino acids and ana-

lyze the protein for the effect of the substitution. However, while much insight can be gained from such a process, substitution of a few carefully chosen amino acids can provide a detailed picture of protein function and simplify data analysis. For example, substitution of a null-charged residue such as glutamine for a negative charge residue such as glutamic acid may reveal the effect of charge at a particular position. While substitution of a positive charge residue such as lysine for the same residue may uncover a special need for a negative charge or simply the need for any charge at the position. Another technique utilized is alanine-scanning mutagenesis. By substituting an amino acid with alanine contributions of individual amino acid side-chains to the stability, fold and functionality of a protein can be examined(87). Substituting a residue with alanine removes all side-chain atoms past the β-carbon. This allows for the role of side-chain functional groups at specific positions to be extrapolated from the alanine mutations. Even though alanine is not the simplest amino acid, glycine, which is (R = H), lacks the presence of carbons in its side-chain. This can introduce conformational flexibility into the protein backbone. Alanine is the next smallest natural amino acid ($R = CH_3$) which with the presence of carbon in the side-chain maintains preferred backbone conformation (backbone dihedral angle) and allows the function of other side-chains to be elucidated (87). Amino acid side-chains can be grouped into four categories; non-polar, uncharged polar, acidic and basic side-chains. Carefully selected substitutions can reveal the role that each type contributes to a position in the overall fold and conformation of the protein.

Assembly Pathways

In 1968 Levinthal pointed out that due to the very large number of degrees of freedom in an unfolded protein, that a polypeptide chain would have an exorbitant number of possible conformations(73). Given the large number of conformations it would be impossible for a protein to sample them all in an attempt to find its correct folded state in a biologically relevant time frame. This thought experiment, called Levinthal's Paradox, lead protein chemist to hypothesize that a protein must reach its native state by a specific folding pathway.

A number of mechanisms have emerged that attempt at providing explanations to how these routes occur. Of note are; the 'framework model' which proposes that local elements of native local secondary structure are formed independent from the tertiary structure. In this model the secondary elements would form first and then diffuse until they collided with each other, formed an interaction, and coalesced to give the tertiary structure(33, 101). The 'hydrophobic-collapse model' suggests that there are two distinct phases involved in protein folding. The first involves a rapid collapsing of the polypeptide around its hydrophobic side-chains. In the second phase the side-chains repack more efficiently as they searched a more limited conformational space in the "molten globule" until finally arriving at the most stable native conformation. In this model, the secondary structure would result as a consequence of native-like tertiary interactions (33). The classical 'nucleation model' or 'nucleation-propagation model' proposes that a few of the adjoining residues of sequence would form native secondary structure. These structures would act as a nucleus from which the native structure, in a stepwise manner, could be formed. In this model the tertiary structure would form as a consequence of the secon-

dary structure(33). The 'nucleation-condensation model' hypothesizes that the process of the formation of the nucleus and the formation of structure elsewhere are concerted. In this model the formation of long range and other native hydrophobic interactions stabilize otherwise weak secondary structure in the nucleus. Which in turn act to formalize tertiary structure(23). The 'jigsaw puzzle model' proposes the existence of multiple protein folding pathways and is analogous to the assembly of a jigsaw puzzle. The analogy is simple; when putting a jigsaw puzzle together there are a number of sequences in which the pieces can be joined to each other that in the end result in the same finished product. In this model, the identification of folding intermediates represents kinetic account rather than a structural one. Each intermediate identified would, in turn, consist of a collection of heterogeneous species in rapid equilibrium (54). In all likelihood the way in which proteins fold is an amalgamation of all of these models (23).

Indeed, the currently accepted model is a unified model of protein folding based on the effective energy surface of a polypeptide chain. This model referred to as the "new view" describes the folding process in terms of an energy landscape and a folding funnel(109, 143). The model describes the thermodynamic and kinetic behavior of the conversion of the nascent polypeptide to a predominantly native state. Putting to rest the debate of whether protein folding is thermodynamically or kinetically driven. It also provides an explanation for the presence of misfolded and aggregated proteins. This 'new view' of protein folding involves the successive ordering of a collection of partially folded structures that occur through multiple pathways. The schematic representation of this model reflects that of a funnel in which the top of the funnel represents the free energy of the nascent polypeptide chain while the bottom of the funnel represents the native

structure. In terms of the conformational possibilities reflected upon by Levinthal; as a protein travels toward the bottom of the folding funnel, the number of accessible protein conformations decreases as does the chain entropy. This model reiterates the fact that proteins fold according to a pathway. However it does not provide for an exclusive pathway. There are many pathways present that lead to the same product and probably just as many that lead to kinetic traps; that is misfolded or aggregated intermediates. Furthermore, it validates the need for folding chaperones in biological organism.

Regardless of which model/s a monomeric protein uses to fold into its correct native structure there seems to be an apparent need for monomers to associate to form larger more complex structures. It is understandable for proteins to develop towards stability and one way in which to do that is to become bigger. This can be rationalized as follows; we know that the stability of proteins depends largely on the multiplicity of weak non-covalent bonds such as hydrophobic interactions that occur mainly in the interior of the protein. If you think of a native protein structure as a sphere of radius R as you increase the size of the sphere the volume (R^3) grows more rapidly than its surface area (R^2)(93). The consequence of this is an increase in the number of stabilizing interactions that occur inside the protein. There are two ways that a protein can increase in size. One way is to increase the size of polypeptide chain. The other is to associate. For viruses it is recognized that there is a very limited amount of space in which to encode proteins(22). It is more efficient to encode smaller proteins that associate than to encode larger ones that don't. This holds true not just for viruses but for biological systems in general.

So far we know that proteins fold according to a progressively directed pathway whose determinates are still questionable. In an analogous way protein complexes such as viruses have been shown to assemble via a preordained pathway. However, while for the folding of nascent polypeptide chains there exists an inexhaustible multitude of successful pathways, the assembly of viruses is a more ordered process in which each steps provides the substrate for the subsequent phase. In the energy-landscape funnel, virus assembly represents the bottom half and is more constricted and directed in its path. For example, in the assembly of the T-even bacteriophages the tailspike cannot be added before the DNA is packaged.

There are three general categories for the final structures of viruses; helical, icosahedral and complex. Although viruses may fall into only one of these three, the ways in which a virus in each class gets there is very divergent. The necessity for an ordered pathway has been extensively demonstrated with each class of virus(16, 32, 106). For the purposes of this dissertation we will only be concerned with that of one virus, HIV-1.

Global Impact of HIV-1

While HIV-1 was not the first retroviruses to be discovered it is the one that is currently having the largest global impact. To date around 65 million people have been infected with HIV, with an estimated 38.6 million people worldwide currently living with some form of HIV. Since recognizing acquired immunodeficiency syndrome (AIDS) as a unique disease in 1981 an estimated 25 million have died from complications associated with the infection (56). Educational programs and antiviral therapy have assisted in impeding the natural spread of HIV-1. With the advent of highly active antiretroviral

therapy (HAART) in 1993 the rate of deaths associated with HIV has declined sharply. Currently HAART therapy targets the processes of reverse transcription, protease cleavage leading to maturation and viral entry. Despite the development of HAART, for those already infected with HIV, the therapy only postpones death. Specifically, these drug regimens are unsuccessful at eradication of the virus. While current circumstances negate eradication, for many, the lyrics to the popular song "Time is on my side" can be seen as an anthem. Introduction of the current regimen has added invaluable years to those infected. Nevertheless, there are complications associated to the administration of the current form of HAART. These include short- and long-term toxicity drawbacks of drug treatments and the emergence of drug resistant mutations in the virus which can then be transmitted. With the emergence of drug resistant strains the requirement of new drug development is imperative. In late 2004, a man in his late 40's was diagnosed with multi-drug-resistant (MDR), dual-tropic HIV-1. The man had no history of antiretroviral treatment prior to diagnosis(81). At diagnosis he was discovered to be resistant to drugs in three out of the four available classes. Although prior cases of MDR have been reported this particular case alarmed health official (who issued an alert in Feb 2005) because of the rapid progression to AIDS (4-20 months versus 10 years). This case heightens the need to not only develop new drugs but new drugs against new targets.

Brief Overview of the HIV-1 Replication Cycle

The infection of a cell with HIV-1 begins with the attachment of the virus to the cell. It is still unclear whether the primary route of infection it due to endocytosis fol-

lowed by viral fusion or simply viral fusion (51, 89). However, it is clear that the virus attachment to the cells is mediated by the interaction of the envelope glycoprotein gp120 with the CD4+ receptor and the use of either the CCR4 or CXCR5 chemokine co-receptors(39, 42). Fusion is catalyzed by the envelope glycoprotein gp41. Upon fusion of the virus with the cell the viral core is released and in a poorly understood procedure undergoes the process of uncoating in which the conical capsid is unassembled. This results in the release of the viral genome in complex with other enzymatic and regulatory viral proteins. The RNA genome is reverse transcribed into linear two-stranded cDNA within the cytoplasm and the incoming viral RNA is destroyed by RNAase H. A complex termed the PIC (pre-integration complex) consisting of the cDNA, NC, RT, Vpr, MA and IN and other host derived proteins is then transported to the nucleus where, utilizing the integrase protein, the viral DNA is inserted into the cells' genome. From here the viral genome is replicated back into full length RNA or transcribed into mRNA. The virally derived nucleic acids are transported out of the nucleus where they can either be packaged into assembling viral particles or translated into viral proteins. The translated proteins are transported to the plasma membrane through the interaction of the p6 domain of Gag with the cellular factor TSG101(49, 127). TSG101 recruitment results in the trafficking of the Gag polyproteins to multivesicular bodies which in turn lead to their interactions with the class E protein through the endosomal trafficking network(115) and their transportation to the plasma membrane. Within this timeframe viral assembly takes place in which, in no well defined order, Gag and Gag-Pol molecules oligomerize, and bind viral genomic RNA. In most cell lines, budding occurs through the plasma membrane. While it is uncertain if budding and maturation occur concomitantly or sequen-

tially, it is recognized that sometime during this period the virus undergoes a self-cleavage event in which the viral poly-proteins are cleaved into the individual proteins resulting in a fully infectious particle(12).

HIV-1 Maturation Results in a Metastable Particle

HIV-1 maturation is an event that is inadequately defined. With the exception of the initial state and the resultant state, little is known of the conformational transitions that take place as the particle converts from an immature to a mature particle.

Maturation commences when the virally encoded protease performs a self-cleavage event, releasing itself from the Gag-pol polyprotein(12, 94). Afterwards, in a preferred sequence, the protease liberates the other viral proteins(12, 97, 136). Disruption or rearrangement of this sequence results in poorly infectious particles(95, 96, 136). This suggests that in a manner akin to protein folding, described previously, subsequent conformational changes depend on those that occur beforehand. Grossly, maturation leads to the liberation of the individual viral proteins. It also leads to the activation of the virus since the cleavage of the envelope protein is required to facilitate viral fusion with a new target cell(141).

With HIV-1 the mature particle is less stable than the immature particle. Evidence supporting this comes from the fact that membrane stripping of the mature particle leads to passive deterioration of a large percentage of the capsid complex while the same process leads to minimal disruption of the spherical structure present in the immature particle(36, 67). The resultant metastability present in the mature particle after protease

cleavage is one mechanism that retroviruses such as HIV-1 use to overcome the paradox of having to assemble and uncoat in the same environment.

There are many intrinsic facets of the mature virus core that infer metastabiliy. To begin with, upon maturation roughly half of the capsid protein is excluded from the conical structure(9, 69). As argued, previously one way in which to form a stable protein complex is for the protein to aggregate and grow in size, such that the interior of the complex and thus stabilizing interactions increase faster than the surface. With HIV-1 maturation results in the reduction of the size of the capsid complex and the reduction of stabilizing interactions present not only in capsid but in the other Gag-derived proteins(12, 66).

Another feature is the inherent structure of the mature core. Continuum elasticity theory asserts, that for large capsids, the energy exerted in the deformation of the individual proteins present in the complex is minimized when the twelve five-fold sites are located as far as away from each other as possible (11, 122). However, as modeled by von Schwedler et al., in order for HIV-1 to adopt its characteristic cone shape the twelve five-fold sites have to be localized on either end of the structure(46).

Furthermore there are mutations that can be engineered into the N-terminal domain of HIV-1 that result in an increase or decrease in stability of the core(36). Either extreme results in an impairment of virus replication suggesting that there is an optimal range of stability required for effective infectivity(48, 131). Enhancing this point is the presence of restriction factors whose primary mechanism of action is through targerting the uncoating process of the capsid complex. Current evidence suggests that the factor

TRIM 5α (previously known as Lv1 and Ref1) acts by destabilizing the capsid core and accelerating uncoating(18, 114).

In general, the process of maturation takes place as a coordinated event on a given particle and is irreversible. Virus maturation most often represents the transition from one local minimum of conformational free energy to another with the majority of the structural changes taking place in the capsid (non-enveloped and enveloped viruses) and surface proteins (enveloped viruses). These conformational changes occur as the result of a triggering event such as nucleic acid packaging (some bacteriophages) or proteolytic processing (retroviruses, picornaviruses).

For the majority of non-enveloped icosahedral viruses the process of maturation results in a more thermodynamically stable particle that is also resistant to nucleases. However for HIV-1 and other retroviruses maturation leads to a capsid complex whose optimum stability resides in a shallow kinetic trap.

Targeting Protein/Protein Interactions

With the evolution of restriction factors nature has devised an effective defensive strategy in combating the zoonosis of retroviral infections. This strategy of targeting the stability of capsid complexes can be re-created synthetically by modulating the means used to generate stability either through disruption or modification of key interactions.

There are two general categories for protein complexes; permanent and temporary complexes. The characteristic of the interface present at the protein/protein junction differs for each type. For permanent complexes the interfaces resemble that of the core

of a monomeric protein. While for temporary complexes the interfaces are analogous to surfaces found in enzyme active sites(1, 2).

As previously described, the central principle in creating stability in protein complexes is the formation of protein/protein interactions. The main factors responsible for protein-protein interactions are; steric complementarity, hydrophobic and electrostatic interactions and hydrogen bonds(1, 2).

Steric complementartity involves the topology of the coalescing interfaces. In general, the interfaces are large flat surfaces with very few cavities (10 % of interacting surface). In permanent complexes the interfaces are strongly complementary while in temporary complexes they are less so.

In permanent complexes the contribution of the hydrophobic interaction to the stability is higher than in temporary complexes. Even so, for both types the hydrophobic regions in the protein/protein interfaces tend to cluster in patches -- the size of which ranges from 1–15 residues.

Two forms of hydrogen bonding take place in protein/protein interactions; those which occur between pairing residues (both backbone and sidechain) and those between amino acid residues and water. The amount of hydrogen bonds resulting from pairing residues in protein/protein interfaces is proportional to the area of the subunit surface. The average ratio is one bond per 100–200 $Å^2$ or about ten bonds per interface. These types of hydrogen bonds in protein/protein interactions tend to not be in there optimal positions and therefore are limited in their contribution to stability. Water is frequently present at the protein/protein interactions of protein complexes. The number of water molecules can vary from 1–50 and can either surround the contacting interfaces or be

buried in them. In the second case, they are located in the cavities of the protein/protein interaction. The water molecules form hydrogen bonds with protein groups and other water molecules, resulting in aqueous networks along the protein/protein interfaces. The overall contribution of water in protein/protein interactions in protein complex is undetermined. However, water molecules theoretically can stabilize protein complexes by forming additional hydrogen bonds, interacting with charges, and enhancing shape and charge complementary.

As mentioned in the "Biochemical and Mutational Analysis" section of the introduction, ionic interactions play an important role in protein folding. In a similar manner the electrostatic makeup of the protein/protein interface has been demonstrated to confer specificity and direct docking orientation (13, 108, 111). In addition, evidence exists suggesting that the electrostatic composition may define the lifetime of proteins in complex with one another(1, 110). The charge density in protein/protein interactions varies from 0–12 charged groups per interaction surface(142). The current evidence suggest that the net electrostatic charge at the interacting protein surfaces is the major determinate of the electrostatic contribution in protein/protein interactions, versus that of charge complementarity between distantly near residues in the interface(82).

Designing targeted molecular structures that can interfere or alter one or more of these essential elements in the formation of protein complexes would be a beneficial therapeutic strategy in combating viral and prion based diseases.

As such another important facet of protein interfaces is the morphology. Unfortunately there is inconclusive evidence for the enrichment of amino acid residues or secondary structure in the sites of protein/protein interactions (1). However, there appear to

be tendencies at these sites. As mentioned above, the interfaces tend to be large and flat. These characteristics pose problems in designing inhibitory molecules. Short peptide sequences mimicking an interacting partner have been successfully used to block interactions or trap complexes in intermediate conformations(14, 113). While these are valid strategies in blocking protein/protein interactions, synthesis and storage of these polypeptides are expensive and not conducive to the wide spread treatment needed for HIV-1. The development of small compounds is a more economically practical and challenging endeavor. Since these interfaces are both flat and large there are very few cavities for a small molecule to bury in and enhance binding. Another concern is the oral bioavailability of compounds which decreases with increasing molecular weight. This poses a problem because upwards of 4900 Å of interacting surface would have to be occluded by compounds with molecular weights $\leq$ 500 Da (2, 79).

Analysis of the morphology of protein/protein interfaces have shown that one-third of protein complexes have interfaces with well-defined hydrophobic cores that are surrounded by a ring of polar groups. The other two-thirds of protein interfaces have a mixture of hydrophilic properties and short hydrophobic patches (1, 2). These morphologies are an outcome of their need to be capable of co-existing either in polar solution or in the bound state in the complex, as such, there is a very delicate balance in the composition of the amino acids in the interface of interacting proteins. This is exemplified by the presence of "hotspots". While there is no doubt that all the amino acids present in protein/protein interfaces contribute in some manner to the development of protein association, it has been shown that for some complexes only a few residues are involved in the majority of stabilizing interactions (20).

While the sporadic distribution of small areas of localized high affinity may not be universal to all protein/protein interfaces. The existence of "hot spots" improves the feasibility of blocking protein/protein interactions with small molecules. Now instead of having to occlude large areas compounds targeted to these much smaller sub-regions in the interface can be designed (or discovered).

Within the virus family the utilization of "hotspots" has been demonstrated in the icosahedral capsid structure of parvovirus(102). There are 28 residues involved in non-covalent interactions between trimeric protein subunits in the parvovirus capsid, of which 7 are shown to be critical to assembly. Alteration of any one of these 7 residues is sufficient to inhibit assembly. Within the HIV-1 system the existence of "hotspots" has also been discovered in both the dimerization of reverse transcriptase and capsid (25, 105). Additionally, small non-peptidic molecules that block or destabilize the dimerization of HIV-1 protease, integrase and reverse transcriptase have been synthesized(5, 14). Furthermore, the therapeutic benefit of blocking protein/protein interactions in HIV-1 has been demonstrated with the entry inhibitor T-20 (Enfuvirtide) (41).

Targeting Protein/Protein Interactions in Viral Capsid Structures

There is growing evidence supporting protein/protein interfaces as viable targets in the treatment of diseases (24, 29, 41, 80). However, the majority of proof as been obtained in systems in which the active complex is dimeric. Targeting protein/protein interactions present in complex structures such as viral capsids introduces a unique problem. Typical icosahedral and complex viruses, as a minimum, consist of 60 subunits forming a closed structure. Each subunit is involved in at least three distinct protein interfaces (17).

Given this knowledge, one must wonder if compounds need to be directed to each of these interfaces or if targeting one interface will suffice. If we narrow down the selection to one interface there are still 60 or more interactions taking place within one complex -- Is it necessary to bind each of these or would interfering with the formation of only a subset be enough to disrupt the function of the complex?

As mentioned previously, the assemblies of viral capsids follow a defined pathway. Using icosahedral viruses it has been shown that compounds can be added during the process of assembly that result in the formation of aberrant non-functional structures (99, 123, 144). It has been proposed that this is due to the incorporation of only a small number of molecules during the process of assembly. This amount is sufficient to alter the intersubunit bonding geometry of a few interfaces resulting in directing the assembly process "off-pathway" with the consequence being a non-functional capsid structure. Therefore, it appears that incorporation of a few molecules can be sufficient to alter the pathway of assembly. However, the assembly of HIV-1 is remarkably different from that of most icosahedral viruses in that the capsid initially oligomerizes within the context of a much bigger protein. Though there is no evidence to support that the interactions made in this context are wholly retained, it is unlikely that all are broken(69, 70). Expressly, that upon maturation (freeing of capsid from Gag) that capsid molecules totally disassociate and then re-oligermerize to form the conical core. It is more likely that the interactions made in the context of the immature particle are the basis for those made in the mature particle. With this in mind; Is it feasible to target the process of HIV-1 assembly? That is to say, can small molecules targeted to capsid be used to obliterate the process of HIV-1 assembly? The likelihood of discovering such a compound is low due to the pres-

ence of compensatory interactions located outside of capsid in Gag. However, there is one known capsid/capsid interface that takes place only in the context of the mature particle. Incorporation of small molecules that can alter or disrupt this interface during the assembly of HIV-1 may direct the second half of capsids assembly "off-pathway" enough to result in a non-functional core as demonstrated by Tang et al (117).

This dissertation can be broken down into two sections. In the first half you will find a study analyzing a number of electrostatic residues located outside of the known protein/protein interfaces and implications for their role in the process of virus capsid assembly and uncoating. In the latter section you will find an article describing the screening of 10,000 small compounds for inhibition of CA assembly through the adaptation of an in-vitro reaction to medium-throughput applications. The subsequent selection of six of these compounds as antiviral leads is corroborated by direct effect on the virus's ability to spread in cell culture.

Taken together these papers represent an analysis into the protein/protein interactions involved in HIV-1 capsid assembly and an investigation into whether these interactions can be altered or inhibited through the use of small molecular compounds.

INVESTIGATION OF N-TERMINAL DOMAIN CHARGED RESIDUES ON THE ASSEMBLY AND STABILITY OF HIV-1 CA

by

CHANEL C. DOUGLAS, DENNIS THOMAS, JASON LANMAN AND PETER E. PREVELIGE JR.

Biochemistry, **43** (32), 10435 -10441, 2004. 10.1021/bi049359g S0006-2960(04)09359-6

Copyright
2004
by
American Chemical Society

Used by permission

Format adapted and errata corrected for dissertation

ABSTRACT

The human immunodeficiency virus type 1 (HIV-1) capsid protein (CA) plays a crucial role in both assembly and maturation of the virion as well as viral infectivity. Previous *in-vivo* experiments generated two N-terminal domain charge change mutants (E45A and E128A/R132A) that showed an increase in stability of the viral core. This increase in core stability resulted in decreased infectivity suggesting the need for a delicate balance of favorable and unfavorable interactions to both allow assembly and facilitate uncoating following infection. Purified CA protein can be triggered to assemble into tube like structures through the use of a high salt buffer system. The requirement for high salt suggests the need to overcome charge/charge repulsion between subunits. The mutations mentioned above lie within a highly charged region of the N-terminal domain of CA away from any of the proposed protein/protein interaction sites. We constructed a number of charge mutants in this region (E45A, E45K, E128A, R132A, E128A/R132A, K131A, K131E) and evaluated their effect on protein stability in addition to their effect on the rate of CA assembly. We find that the mutations alter the rate of assembly of CA without significantly changing the stability of the CA monomer. The changes in rate for the mutants studied are found to be due to varying degrees of electrostatic repulsion between the subunits of each mutant.

INTRODUCTION

Retroviruses such as human immunodeficiency virus type 1 assemble through the polymerization of the Gag and Gag-Pol polyproteins. The Gag protein of HIV-1 is a 55 kDa protein that consists of the structural domains matrix (MA), capsid (CA), p2, nucleocapsid (NC), p1 and p6 (in that order)(38, 58, 84, 88, 126). A -1 ribosomal frame shift results in the Gag-Pol polyprotein which adds the enzymatic proteins which include protease (PR), reverse transcriptase (RT) and integrase (IN)(38, 58, 61). The Gag and Gag-Pol polyproteins together with the Env gene comprise all of the structural and enzymatic proteins needed for viral infectivity. The polyproteins assemble under the plasma membrane and upon budding are found, in the immature virion, radially arranged with the N myristoylated terminus of the matrix domain proximal to the viral envelope(40, 138). During maturation the Gag and Gag-Pol polyproteins are cleaved releasing the structural proteins (MA, CA, and NC) which are then free to form new intersubunit interactions(38, 58). In fact, cleavage results in a profound morphological change in which the capsid and nucleocapsid proteins collapse to form a conical core(38, 58). Formation of the mature viral core is a critical step in the virus life cycle; mutations that block maturation or result in the formation of cores with aberrant morphology inhibit infectivity, in some cases, apparently by blocking the initiation of reverse transcription(27, 34, 103, 104, 120, 129, 132). Stability of the cores is also a factor in infectivity(35). Cores that are too stable may resist the process of uncoating and prevent release of the viral genome. Recent real-time observation of virus movement intra-cellularly showed the migration of intact cores along microtubules towards the nuclear envelope(83). If uncoating can not take place before the core reaches the nuclear envelope the complex may be perceived by

the cell as being an aggregate of misfolded protein and the core may be re-routed, ultimately to a lysosome(112).

A number of studies have demonstrated the ability of the capsid protein to polymerize into dimers, larger oligomers and eventually tubular polymers(15, 31, 52, 129). The presence of small amounts of cones similar in shape and size to viral cores has been described in some of these preparations(45, 75). This indicates that in vitro assembled capsid polymers are capable of forming bonding interactions similar to those found in the virion. The in vitro assembly protocols for CA induce polymerization by utilizing high salt concentrations suggesting the need to overcome charge/charge repulsion between subunits(15, 31, 52, 129).

High resolution structures of CA obtained by X-ray and NMR demonstrate that it is composed of structurally distinct N- and C- terminal domains(43, 44, 50, 119, 139). Merging the crystal structure into cryoEM based reconstructions of in vitro tubes suggested the N-terminal domain forms hexamers stabilized by NTD homotypic interactions, and the hexamers are tied together by CTD dimerization(75). While obtaining high resolution structural information about the interactions driving capsid assembly has proven difficult, this model is well supported by mutational and mass spectroscopic data both of which also provide evidence for an additional intersubunit NTD:CTD interaction(47, 68, 130).

It is known that the C-terminal domain dimer is stable in both low and high salt(44). This suggests that it is either the homotypic N-terminal domain interactions or the heterotypic N/C domain interactions that are salt sensitive. Additionally, mutagenesis studies have uncovered residues away from these sites of interaction that enhance the sta-

bility of the viral core and cause the virion to be less infectious(35). Two of these mutations are found in the N terminal domain at positions E45 and E128/R132 and are located in helix 2 and helix 7 respectively. These mutations replaced charged residues with the neutral amino acid alanine once again suggesting a role for charge/charge repulsion between subunits not only during assembly but during uncoating as well. To determine if the altered capsid stability was due to electrostatic or conformational effects we generated a family of charge change mutants within this region (Fig 1) and evaluated their ability to stably fold and assemble.

MATERIALS AND METHODS

Protein Expression and Purification

A pET based plasmid for expression of wild type (WISP93-73) was obtained from W. Sundquist and transformed into Escherichia coli BL21(DE3). Plasmids for expression of the mutant HIV-CA were obtained by PCR mutagenesis of the wild type plasmid and verified by DNA sequencing. Wild type (WT) and mutant capsid proteins were expressed and purified as previously described except where noted below. The pH of the resuspension buffer for the mutants was increased from 8.0 to 8.5. The minimum percentage of ammonium sulfate used for efficient precipitation varied for each mutant ranging from 20 to 35%. The mutants were eluted from the Q-Sepharose (Amersham Biosciences) column at NaCl concentrations ranging from 70 mM to 90 mM. Most of the K131E protein was found to be irreversibly aggregated after the ammonium sulfate precipitation step and therefore this step was eliminated from the purification protocol. Instead the supernatant from the high speed spin was applied both to an SP and Q-

Sepharose column run in series. CA passed through the SP column, which retained other cellular proteins, and bound to the Q column. The protein was then eluted from the Q-column independently. The eluted proteins were then dialyzed into 50mm Na Phosphate Buffer pH 8.0. The mass of the each mutant protein as determined by ESI-TOF mass spectrometry was within 2 Da of the expected value. Purified protein solutions were stored frozen at -80 ^{0}C at ~ 300-500 μM in 50 mM Na_2PO_4 buffer pH 8.0 until needed.

In Vitro Capsid Assembly

Purified wild type and mutant capsid protein were assembled by rapid dilution into concentrated NaCl solutions at 20 ^{0}C to yield the desired final salt and protein concentration and the course of the reaction was monitored by turbidity. For kinetic analysis, the reaction was rapidly mixed and placed into a 1mm quartz cuvette. Unless otherwise noted, approximately 20 s elapsed between the time of the addition of salt and the first time point measured. The increase in optical density was monitored at 350 nm for one hour as previously described (71), except where noted. The initial rate of assembly was approximated by fitting the early time points to a linear equation

Determination of the Critical Concentration

To determine the fraction of unpolymerized protein present at equilibrium, assembly reactions were performed over a range of starting concentrations (20, 30, 40, 50, 60, 70 μM for WT, E128A, R132A, E128A/R132A; 10 1, 5, 20, 30, 40, 50 μM for E45A, and 30,40, 50, 60, 70, 80 μM for K131A) and allowed to proceed to completion (1 hr). The assembled polymers were collected by centrifugation at 14,000 rpm for 20 mins in a

microfuge. The supernatant was removed and the pellets were resuspended in 400 μL of 50 mM Na_2PO_4 pH 8.0 with 3M GuHCl included to dissociate the tubes and reduce scattering. The concentration of protein in supernatant or pellet was determined spectroscopically at 280nm using an extinction coefficient of 33,460 M^{-1}. The amount of protein present in the supernatant fraction was used to determine the amount of unpolymerized protein in each sample.

Circular Dichroism

CD spectra of WT CA and all mutants were recorded on an AVIV model 620S at 20^o C in 50 mM Na_2HPO_4 pH 8.0 at concentrations ranging from 0.33-0.5 mg/ml. Readings were collected at 1 nm intervals from 195 nm to 260 nm with a 15 second averaging time. Actual concentrations were determined by collecting UV spectra at 280 nm of the sample measured and the CD spectra normalized according to the following equation: $[\theta]=(\theta*100*M_r)/(c*l*N_A)$ The recorded spectra in millidegrees of ellipticity (theta) were converted to mean residue ellipticity [theta] in deg.cm^2.dmol^{-1} by the equation, where c is the protein concentration in mg/ml, l is the pathlength in cm, M_r is the protein molecular weight and N_A is the number of amino acids in the protein. Thermal melting curves were determined for all samples at a concentration of 1 μM in the same buffer using 1 cm path length cells. The temperature was increased in steps of 1.0 deg C with a 12 second equilibration time over a nominal range of 25 – 90 deg. C. The actual temperature was recorded and the observed range was typically ~22 – 83 ^{o}C. Molar ellipticity readings were recorded at 218 nm using a 5 second averaging time and a band width of 2.0 nm. The melting point for each mutant was determined by calculating the first derivative of

the melting curve (ellipticity vs. temperature) to determine the inflection point of the transition.

Sedimentation Equilibrium

Sedimentation equilibrium experiments on wild type and mutant CA protein were performed at protein concentrations of 5.6 μM, 9.8 μM, and 15.8 μM in 50mM sodium phosphate (pH 8.0) at 20 ^{o}C. Data were obtained using a Beckman Optima XL-A analytical ultracentrifuge at rotor speeds of 15,000 rpm, 20,000 rpm and 25,000 rpm using an An-60 Ti rotor equipped with Epon charcoal-filled 12mm 6 channel centerpieces in cells with quartz windows. The absorbance was monitored at 280 nm and ten scans were averaged. The partial specific volume were determined using the public domain software program SEDNTERP (http://www.rasmb.bbri.org/) developed by Hayes, Laue, and Philo(72). Solution densities were obtained from standard tables. The equilibrium data from all nine experiments were fit globally to different models to determine the stoichiometry and association constant that best fit the data(63).

RESULTS

Change in Charge State has Effect on Rate of Assembly

Previous *in vivo* studies have demonstrated that the N-terminal domain mutations E45A and E128A/R132A result in an increase in the stability of the viral core and a decrease in viral infectivity. Should the increased stability result from decreased intersubunit repulsion, the assembly reaction might take place faster because the decreased repulsion could facilitate the close approach of the subunits required for docking. Therefore,

to determine if the increase in stability of these two mutants correlated with an increase in the rate of assembly, the assembly kinetics of purified capsid protein mutants were followed turbidimetrically (Fig. 2) at 50 μM protein concentration. The initial rate of assembly was then estimated from the slope of the linear part of the curve (typically < 10 min). The E45A mutant, which in the *in vivo* studies is 29 fold less infectious(35, 130), assembled 33 times faster than wild type whereas E45K, a charge reversal mutant assembled slower (40% of WT) suggesting the presence of charged residues in this location affects association. The double mutant E128A/R132A displayed kinetic properties similar to wild type although *in vivo* it was 6.2 fold less infectious(35, 130). To determine the relative contributions of E128A and R132A to the assembly kinetics each mutation was examined individually. The E128A mutant assembled approximately twice as fast as wild type while R132A assembled at approximately half the rate of wild type.

The three mutations (E45A, R128A, and E132A) studied previously lie within a 12 Å (most within 7 Å) radius of each other in the NMR structure of CA (Fig., 1), a distance compatible with the formation of long range ion pairs. One other charged residue, K131 lies in the middle of this cluster. To evaluate the role of K131 in assembly this residue was mutated to the opposing and neutral charges and the effect studied. Both K131E (data not shown) and K131A assembled slower (10-20 fold less) than wild type. These results suggest the need for charge balance in this region, a suggestion supported by the fact that sequence comparison between HIV-1 strains shows conservation of the charges at all positions in this cluster. The only exception to this is E128 which had 2 non-conservative changes out of the 380 clones/strains available in the Los Alamos HIV-1/SIVcpz database.

To determine whether the turbidity was proportional to the amount of polymerized CA, assembly reactions were initiated at different initial CA concentrations and allowed to go to completion. The polymerized CA was separated from the unpolymerized subunits by centrifugation and the maximum turbidity observed for each initial concentration was plotted against the amount of polymerized CA found in the pellet fraction after centrifugation (Fig 3). For all the mutants the observed turbidity was directly proportional to the amount of protein polymerized. In the case of the E45A and K131A the absolute amount of turbidity per unit CA was different from the wild type and the other mutants suggesting the structures of the final products might be different. The E45A mutant formed substantially shorter tubes than wild type as determine by thin section electron microscopy (data not shown). The thin section electron microscopy of the mutants with the exception of K131A and K131E were examined and found to all form tubes (data not shown).

If the mutants alter the rate of subunit addition through charge/charge repulsion, the assembly pathway should remain unchanged. A way to measure this would be to look at the dependence of the rate of assembly on protein concentration which provides an indication of the number of molecules involved in the rate determining step. Therefore, assembly reactions were performed with each mutant over a range of concentrations and the log of the rate of the reaction was plotted versus the log of the initial protein concentrations to derive the order of the reaction (Fig 4). The slopes of the mutants are nearly parallel to that of wild type suggesting that for all of the mutants the change in the rate of assembly can be attributed to a change in the rate of subunit association as opposed to a change in the pathway of assembly.

The Change in Rate is Not Due to Altered Folding or Stability

It is possible that the increases or decreases in the rate of assembly are due to changes in the conformation or stability of the protein subunit. Therefore, to determine if the mutations were causing changes in the structure of the capsid protein the CD spectra of each mutant was obtained at low protein concentration where the majority of the capsid protein is monomeric (Fig. 5A) . The CD spectra of the mutants were identical, within experimental error, to that of the wild type suggesting very little (if any) perturbation of the secondary structure. To measure the stability of the capsid monomer the thermal stability of each protein was monitored by melting the protein and recording the molar ellipticity at 218 nm (Table 1). The melting point was determined by taking the first derivative of the melting curve (Fig 5B). With the exception of K131E the mutants have the same or only slightly lower thermal melting transitions suggesting that the mutations have minimal effects on the stability of the monomer. In the case of K131E, the lowered T_m reveals a second thermal transition. Detailed calorimetric studies of the melting of wild type CA demonstrated independent melting of the N and C terminal domains (Protesevich et al, manuscript in preparation). The C-terminal domain melts at a slightly higher temperature than the N-terminal domain. The K131E mutation destabilized the N-terminal domain revealing the underlying C-terminal domain melting transition.

The Change in Rate is Not Due to Altered Dimerization

The ability of the C-terminal domain of CA to dimerize is critical for capsid assembly. C-terminal domain mutants, such as W184A/M185A, which cannot dimerize cannot assemble(71). To ensure that the N-terminal domain charge change mutations did

not affect dimerization the K_d of each mutant was determined using sedimentation equilibrium at three protein concentrations, 5.6 μM, 9.8 μM, and 15.8 μM and for three rotor speeds, 15K, 20K and 25K RPM at 20 ^oC as previously done for wild type. The K_d of all the mutants (Table 1) were within experimental error indicating similar dimerization abilities.

The Magnitude of the Rate Differences Depend on the Salt Concentration

Should the effect of the mutations on assembly rate be strictly electrostatic, the effect of salt on the rate of assembly will vary for each mutant in proportion to the degree of shielding required for effective assembly. At infinite salt concentration the rates of all the mutants should converge as charge shielding completely masks the charge/charge repulsion(108). To test this the dependence of the rate on salt concentration was determined. The mutant capsid proteins were assembled at 50 μM at various salt concentrations ranging from 1 to 3M depending on the mutant. The rate was then determined and the log plotted against the log of the initial salt concentration. From Fig. 6 it can be seen that slopes of the resulting linear fits differ amongst the mutants suggesting that the dependence of the rate of assembly on the salt concentration (i.e. the charge screening capability) is different for each mutant studied. The rates of assembly for the mutants converge at high salt concentrations, as expected. However, one mutant, K131A, appears to have the same dependence on salt concentration as wild type as the slope runs parallel to wild type which suggests the change in rate may not be solely due to electrostatic effects for this mutant. The extent of polymerization as monitored by the final amount of turbidity was found to be salt independent at as previously demonstrated (data not shown).

The Energetics of Assembly Depend on the Charge.

In performing the experiment to determine the correspondence between turbidity and the amount of protein polymerized we noticed that the amount of protein in the supernatant was relatively constant. This represents the critical concentration of the reaction. The critical concentration for polymerization reflects the equilibrium between subunit addition and dissociation and thus serves as an indication of the energetics of intersubunit interactions (3, 53, 90, 100).

To determine if the mutations altered the critical concentration, we measured the amount of unpolymerized protein for each mutant across a range of concentrations (Fig 7). The data demonstrate that the mutants do alter the critical concentration and the alterations correspond to their observed effects on assembly; mutants with lower critical concentration show faster assembly. The alternative model, in which the mutations cause a slight folding defect resulting in a fraction of unassociable protein would result in a constant percentage of unpolymerized protein, rather than a constant concentration. This was not observed.

DISCUSSION

We have previously reported the development of a rapid dilution-induced technique for CA assembly(71). This technique has proven to be useful for the evaluation of the effects of solvent conditions, protein concentration, and mutations on CA assembly. Here we extend the use of this technique to analyze the effect of N-terminal domain charge change mutations on CA assembly. The mutations E45A and E128A/R132A have

been previously reported to result in an increase in core stability(35). Thermodynamically, an increase in stability of a complex is due to an increase in the favorability of the interactions in the complex. Such an increase could lead to an enhancement in the rate of formation of the complex. In the case of E45A we see a corresponding increase in the rate of assembly. For E128A/R132A the observed increase in stability does not result in a corresponding increase in the overall rate of assembly. This seems to arise from a balancing of two opposite effects as can be seen from the analysis of the mutations individually. The E128A mutation results in faster assembly kinetics while the R132A mutation results in slower assembly kinetics. For the mutants studied there is a correlation between the critical concentration and the kinetics of assembly. The exception to this is the E128A/R132A mutant which assembles at a rate similar to wild type but has a higher critical concentration. This concentration is in fact similar to one of its single mutants R132A. The other three mutants studied, E45K K131A and K131E had slower assembly kinetics. K131E was difficult to purify and study, limiting the data obtained, as this charge change destabilized the protein. For E45K and K131A the decrease in assembly kinetics might be due to increased electrostatic repulsion between the subunits as suggested by the critical concentration. Another possibility for the higher critical concentration for these mutants may be difficulty in a nucleation-like step. We have observed that the assembly of K131A is greatly enhanced by the addition of E45A which may serve to nucleate the assembly reaction (data not shown).

There are three protein-protein interactions within CA that are required to stabilize the core. These are the C-terminal domain dimerization mediated by hydrophobic packing of CA helix IX(44, 139), the N-terminal domain homotypic interactions medi-

ated by helices I and II(75), and an N to C domain intersubunit interaction mediated by the loop between helices III and IV and the base of helix IV in the NTD and helices VIII and IX in the CTD(68). As expected, in general mutations at residues within these interfaces prevent capsid assembly. The mutants presented here do not lie within any of these regions but rather within the core of the N domain. However, they affect the kinetics and stability of at least two of these interactions without significantly changing the conformation or stability of the monomeric protein subunit itself. These charged residues are highly conserved in both HIV-1 and SIVcpz. This suggests that the HIV-1 CA may have evolved to be a protein primed for dissociation. In fact, the association constants for each of these interactions is relatively weak. Despite the importance of the homotypic N-terminal domain interactions in the structure of the core, they are unable to form independently of the other stabilizing CA interactions. N-domain carrying the mutation (E45A) which forms a more stable core was also unable to oligomerize in solution independently of the C-terminal domain (data not shown). The C-terminal domain dimer is relatively weak with a K_d of 18 μM(44). Interestingly, point mutation in the C-terminal domain such as Ser-178, Glu-180, Glu-187, and Gln-192 lead to more stable dimers(25). This suggests that the overall stability of the CA domain of HIV-1 is balanced to allow both assembly and disassembly.

An emerging theme is that charge/charge repulsion plays a significant role in HIV-1 assembly and disassembly. Scanning alanine mutagenesis of CA uncovered many charged residues that when neutralized had normal particle production but reduced infectivity(130). Additionally, replacing neutral residues with charged residues resulted in reduced particle production and no infectivity(129). In the context of the virion, assembly

of the capsid protein takes place in two stages. The first involves the association of the Gag polyprotein to form an immature virion while the second involves cleavage of the Gag protein to its constituent structural domains and the condensation of the capsid protein to form the central conical core(10, 38, 58, 84, 88, 126). Assembly of the virion requires a loss of entropy which must be compensated by favorable interactions. There are multiple sites of interaction dispersed throughout the Gag polyprotein which can help promote capsid assembly. The N-terminal matrix (MA) domain is myristylated(21, 118). The myristyl group inserts into the cell membrane increasing the effective concentration of the Gag polyprotein and reduces assembly to a two dimension diffusion problem. The MA domain itself is capable of forming trimeric interactions(55, 86, 118). The NC domain binds the viral RNA tightly through the action of charge clusters and zinc fingers(21). Multiple Gag proteins bind a single RNA molecule, once again providing a mechanism for increasing the concentration and decreasing the entropic penalty of assembly. Mutations in NC which interfere with RNA binding have a deleterious effect on virus assembly. Collectively, these interactions, all of which occur in a single polypeptide chain, are sufficient to overcome both the entropic loss as well as the charge/charge repulsion evident in the CA N-terminal domain.

Having assembled capsid as part of the Gag polyprotein proteolytic cleavage during maturation then liberates CA which collapses to form a conical core(38, 58, 126). Core formation is likely promoted by the high concentration of CA present in the virion which has been estimated to be in the mM range(10). Fusion of the virion with the host cell results in the membrane being stripped away and the naked core entering the cytoplasm. At this point, the concentration of CA drops significantly and uncoating could be

facilitated by electrostatic repulsion between the subunits. Core stability has been shown to play an important role in infectivity but the precise sequence and timing of initiation of reverse transcription, core dissociation, and nuclear transport of the pre-integration complex remains a mystery.

ACKNOWLEDGMENT

We are grateful to Mike Jablonsky for assistance with CD and John Rodgers for assistance with the Analytical Ultracentrifuge. We also wish to acknowledge the support provided by NIH CFAR Core Grant P30AI27767 in construction of the mutants.

REFERENCES

1. Freed, E. O. (1998) HIV-1 gag proteins: diverse functions in the virus life cycle, *Virology 251*, 1-15.

2. Hunter, E. (1994) Macromolecular interactions in the assembly of HIV and other retroviruses, *Seminars in Virology 5*, 71-83.

3. Mervis, R. J., Ahmad, N., Lillehoj, E. P., Raum, M. G., Salazar, F. H., Chan, H. W., and Venkatesan, S. (1988) The gag gene products of human immunodeficiency virus type 1: alignment within the gag open reading frame, identification of posttranslational modifications, and evidence for alternative gag precursors, *J Virol 62*, 3993-4002.

4. Turner, B. G., and Summers, M. F. (1999) Structural biology of HIV1, *Journal of Molecular Biology 285*, 1-32.

5. Nermut, M. V., and Hockley, D. J. (1996) Comparative morphology and structural classification of retroviruses, *Current Topics in Microbiology and Immunology 214*, 1-24.

6. Jacks, T., Power, M. D., Masiarz, F. R., Luciw, P. A., Barr, P. J., and Varmus, H. E. (1988) Characterization of ribosomal frameshifting in HIV-1 gag-pol expression, *Nature 331*, 280-3.

7. Fuller, S. D., Wilk, T., Gowen, B. E., Krausslich, H. G., and Vogt, V. M. (1997) Cryo-electron microscopy reveals ordered domains in the immature HIV-1 particle, *Curr Biol 7*, 729-38.

8. Wilk, T., Gross, I., Gowen, B. E., Rutten, T., de Haas, F., Welker, R., Krausslich, H. G., Boulanger, P., and Fuller, S. D. (2001) Organization of immature human immunodeficiency virus type 1, *J Virol 75*, 759-71.

9. Dorfman, T., Bukovsky, A., Ohagen, A., Hoglund, S., and Gottlinger, H. (1994) Functional domains of the capsid protein of human immunodeficiency virus type 1, *J. Virol. 68*, 8180-8187.

10. Fitzon, T., Leschonsky, B., Bieler, K., Paulus, C., Schroder, J., Wolf, H., and Wagner, R. (2000) Proline Residues in the HIV-1 NH2-Terminal Capsid Domain: Structure Determinants for Proper Core Assembly and Subsequent Steps of Early Replication, *Virology 268*, 294-307.

11. Reicin, A., Paik, S., Berkowitz, R., Luban, J., Lowy, I., and Goff, S. (1995) Linker insertion mutations in the human immunodeficiency virus type 1 gag gene: effects on virion particle assembly, release, and infectivity, *J. Virol. 69*, 642-650.

12. Reicin, A., Ohagen, A., Yin, L., Hoglund, S., and Goff, S. (1996) The role of Gag in human immunodeficiency virus type 1 virion morphogenesis and early steps of the viral life cycle, *J. Virol. 70*, 8645-8652.

13. Tang, S., Murakami, T., Agresta, B. E., Campbell, S., Freed, E. O., and Levin, J. G. (2001) Human Immunodeficiency Virus Type 1 N-Terminal Capsid Mutants That Exhibit Aberrant Core Morphology and Are Blocked in Initiation of Reverse Transcription in Infected Cells, *J. Virol. 75*, 9357-9366.

14. von Schwedler, U. K., Stemmler, T. L., Klishko, V. Y., Li, S., Albertine, K. H., Davis, D. R., and Sundquist, W. I. (1998) Proteolytic refolding of the HIV-1 cap-

sid protein amino-terminus facilitates viral core assembly, *EMBO J. 17*, 1555-1568.

15. Wang, C., and Barklis, E. (1993) Assembly, processing, and infectivity of human immunodeficiency virus type 1 gag mutants, *J. Virol. 67*, 4264-4273.

16. Forshey, B. M., von Schwedler, U., Sundquist, W. I., and Aiken, C. (2002) Formation of a human immunodeficiency virus type 1 core of optimal stability is crucial for viral replication, *J Virol 76*, 5667-77.

17. McDonald, D., Vodicka, M. A., Lucero, G., Svitkina, T. M., Borisy, G. G., Emerman, M., and Hope, T. J. (2002) Visualization of the intracellular behavior of HIV in living cells, *J Cell Biol 159*, 441-52.

18. Sodeik, B. (2002) Unchain my heart, baby let me go--the entry and intracellular transport of HIV, *J Cell Biol 159*, 393-5.

19. Campbell, S., and Vogt, V. (1995) Self-assembly in vitro of purified CA-NC proteins from Rous sarcoma virus and human immunodeficiency virus type 1, *J. Virol. 69*, 6487-6497.

20. Ehrlich, L., Agresta, B., and Carter, C. (1992) Assembly of recombinant human immunodeficiency virus type 1 capsid protein in vitro, *J. Virol. 66*, 4874-4883.

21. Gross, I., Hohenberg, H., and Krausslich, H. (1997) In vitro assembly properties of purified bacterially expressed capsid proteins of human immunodeficiency virus, *Eur J Biochem 249*, 592-600.

22. Ganser, B. K., Li, S., Klishko, V. Y., Finch, J. T., and Sundquist, W. I. (1999) Assembly and Analysis of Conical Models for the HIV-1 Core, *Science 283*, 80-83.

23. Li, S., Hill, C. P., Sundquist, W. I., and Finch, J. T. (2000) Image reconstructions of helical assemblies of the HIV-1 CA protein, *Nature 407*, 409-13.

24. Gamble, T. R., Vajdos, F. F., Yoo, S., Worthylake, D. K., Houseweart, M., Sundquist, W. I., and Hill, C. P. (1996) Crystal structure of human cyclophilin A bound to the amino-terminal domain of HIV-1 capsid, *Cell 87*, 1285-94.

25. Gamble, T. R., Yoo, S., Vajdos, F. F., von Schwedler, U. K., Worthylake, D. K., Wang, H., McCutcheon, J. P., Sundquist, W. I., and Hill, C. P. (1997) Structure of the carboxyl-terminal dimerization domain of the HIV-1 capsid protein, *Science 278*, 849-53.

26. Gitti, R. K., Lee, B. M., Walker, J., Summers, M. F., Yoo, S., and Sundquist, W. I. (1996) Structure of the Amino-Terminal Core Domain of the HIV-1 Capsid Protein, *Science 273*, 231-235.

27. Worthylake, D. K., Wang, H., Yoo, S., Sundquist, W. I., and Hill, C. P. (1999) Structures of the HIV-1 capsid protein dimerization domain at 2.6 A resolution, *Acta Crystallogr D Biol Crystallogr 55 (Pt 1)*, 85-92.

28. Tang, C., Ndassa, Y., and Summers, M. F. (2002) Structure of the N-terminal 283-residue fragment of the immature HIV-1 Gag polyprotein, *Nat Struct Biol 9*, 537-43.

29. von Schwedler, U. K., Stray, K. M., Garrus, J. E., and Sundquist, W. I. (2003) Functional surfaces of the human immunodeficiency virus type 1 capsid protein, *J Virol 77*, 5439-50.

30. Lanman, J., Lam, T. T., Barnes, S., Sakalian, M., Emmett, M. R., Marshall, A. G., and Prevelige, P. E., Jr. (2003) Identification of novel interactions in HIV-1 cap-

sid protein assembly by high-resolution mass spectrometry, *J Mol Biol 325*, 759-72.

31. Ganser-Pornillos, B. K., von Schwedler, U. K., Stray, K. M., Aiken, C., and Sundquist, W. I. (2004) Assembly properties of the human immunodeficiency virus type 1 CA protein, *J Virol 78*, 2545-52.

32. Lanman, J., Sexton, J., Sakalian, M., and Prevelige, P. E., Jr. (2002) Kinetic Analysis of the Role of Intersubunit Interactions in Human Immunodeficiency Virus Type 1 Capsid Protein Assembly In Vitro, *J. Virol. 76*, 6900-6908.

33. Laue, T. M., Shah, B.D., Ridgeway, T.M., and Pelletier, S.L. (1992) in *In Analytical ultracentrifugation in biochemistry and polymer science* (al, S. E. H. e., Ed.) pp 90–125, The Royal Society of Chemistry, Cambridge, UK.

34. Johnson, M. L., Correia, J. J., Yphantis, D. A., and Halvorson, H. R. (1981) Analysis of data from the analytical ultracentrifuge by nonlinear least-squares techniques, *Biophysical Journal 36*, 575-588.

35. Schreiber, G., and Fersht, A. R. (1996) Rapid, electrostatically assisted association of proteins, *Nat Struct Biol 3*, 427-31.

36. Andreu, J. M., and Timasheff, S. N. (1986) The measurement of cooperative protein self-assembly by turbidity and other techniques, *Methods Enzymol 130*, 47-59.

37. Harper, J. D., and Lansbury, P. T. (1997) MODELS OF AMYLOID SEEDING IN ALZHEIMER'S DISEASE AND SCRAPIE:Mechanistic Truths and Physiological Consequences of the Time-Dependent Solubility of Amyloid Proteins, *Annual Review of Biochemistry 66*, 385-407.

38. Prevelige, P. E., Jr., Thomas, D., and King, J. (1993) Nucleation and growth phases in the polymerization of coat and scaffolding subunits into icosahedral procapsid shells, *Biophys J 64*, 824-35.

39. Oosawa, F., and Kasai, M. (1962) A theory of Linear and Helical Aggregations of Macromolecules, *J Mol Biol 4*, 10-21.

40. del Alamo, M., Neira, J. L., and Mateu, M. G. (2003) Thermodynamic dissection of a low affinity protein-protein interface involved in human immunodeficiency virus assembly, *J Biol Chem 278*, 27923-9.

41. Briggs, J. A., Wilk, T., Welker, R., Krausslich, H. G., and Fuller, S. D. (2003) Structural organization of authentic, mature HIV-1 virions and cores, *Embo J 22*, 1707-15.

42. Coffin, J. M., Hughes, S.H., Varmus, H.E. (1997) *Retroviruses*, Cold Spring Harbor Laboratory Press.

43. Tang, C., Loeliger, E., Luncsford, P., Kinde, I., Beckett, D., and Summers, M. F. (2004) Entropic switch regulates myristate exposure in the HIV-1 matrix protein, *Proc Natl Acad Sci U S A 101*, 517-22.

44. Morikawa, Y., Zhang, W. H., Hockley, D. J., Nermut, M. V., and Jones, I. M. (1998) Detection of a trimeric human immunodeficiency virus type 1 Gag intermediate is dependent on sequences in the matrix protein, p17, *J Virol 72*, 7659-63.

45. Hill, C. P., Worthylake, D., Bancroft, D. P., Christensen, A. M., and Sundquist, W. I. (1996) Crystal structures of the trimeric human immunodeficiency virus

type 1 matrix protein: Implications for membrane association and assembly, *PNAS 93*, 3099-3104.

Table 1.

Mutant	Melting Point ^{o}C[a]	Second Point	K_d - μM[b]
Wild Type	**54**	**-**	**16**
E45A	**52**	**-**	**25**
E45K	**52**	**64**	**12**
E128A	**54**	**-**	**18**
R132A	**53**	**-**	**18**
E128A/R132A	**54**	**-**	**31**
K131A	**53**	**-**	**27**
K131E	**45**	**62**	**25**

[a] The melting point was determined by taking the first derivative of the molar ellipticity melting curve recorded at 218 nm (Fig 5B).

[b] The dissociation constant (K_d) of each protein was determined using the sedimentation equilibrium of the mutants at protein concentrations of 5.6 μM, 9.8 μM, and 15.8 μM and for three speeds, 15K, 20K and 25K RPM at 20 ^{o}C. The absorbance spectra were recorded at 280 nm and the data analyzed using Origin 4.1/Beckman analysis program.

FIGURE LEGENDS

Figure 1. The structure of the highly charged region in the N-terminal domain of HIV-1 CA Protein. Close-up view of the N-terminal domain structure as determined by NMR (PDB # 1GWP) showing the amino acids mutated in this study. The distances between amino acids are also indicated. This figure was drawn with DeepView 3.7. E45-Red, E128-blue, K131-cyan, R132-green.

Figure 2. Assembly of wild type and mutant CA proteins at 50 μM as followed by turbidity. CA protein was assembled at 50 μM at final NaCl concentration of 2.25 M. WT (♦), E45A (□), E45K (▲), E128A (◊), R132A (■), E128A/R132A (○), K131A (●). Every other data point is shown for clarity.

Figure 3. The dependence of the turbidity on the concentration of polymerized capsid. Final turbidity versus the concentration of polymerized protein after one hour of assembly at 2.25 M salt and varying initial protein concentrations. The polymerized protein was pelleted and the concentration in the pellet determined by resuspension in 3M GuHCl followed by absorbance spectroscopy. Symbols: WT (♦), E45A (□), E45K (▲), E128A (◊), R132A (■), E128A/R132A (○), K131A (●).

Figure 4. The dependence of the assembly rate on the protein concentration. CA protein was assembled at various protein concentrations at 2.25 M NaCl. The log of the rate are plotted versus the log of the protein concentration and the resulting curves are fit to a

least- squares linear equation. Error bars represent the standard deviation of the measurements. The slope of the curves are similar to wild type for each mutant studied suggesting that the rate limiting step is made up of the same number of subunits for each mutant. Symbols: WT (♦), E45A (□), E45K (▲), E128A (◊), R132A (■), E128A/R132A (○), K131A (●).

Figure 5. Circular dichroism spectra for wild-type and mutants and representative trace of thermal melting. (A) CD spectra of WT capsid and all mutants were recorded at 25^{o} C in 50 mM Na_2HPO_4 pH 8.0 at protein concentrations ranging from 0.33-0.5 mg/ml. The raw spectra were corrected for the concentration differences and background contributed by buffer and normalized using the equation found in the materials and method section. The CD spectra are similar and showed no clear differences in secondary structure under these conditions. (B) Shows the CD signal at 218 nm as the temperature is raised for wild type capsid protein. The melting point was determined by taking the first derivative of the melting curve. The transition temperature for each mutant is found in Table 1.

Figure 6. The dependence of the assembly rate on the salt concentration. CA protein was assembled at 50 μM at various NaCl concentrations. The log of the rate was plotted versus the log $f^{*}_{\pm}$ where $f^{*}_{\pm}$ is the electrostatic component of the mean rational activity coefficient of the ions(108). The resulting data points where fit to a least-squares linear equation. At high ionic strength the lines converge as charge/charge shielding becomes com-

plete. Symbols: WT (♦), E45A (□), E45K (▲), E128A (◊), R132A (■), E128A/R132A (○), K131A (●).

Figure 7. The critical concentration for the mutants at 2.25 M NaCl. CA was induced to assemble at concentrations ranging from 10-80 μM at 2.25M NaCl and allowed to assemble for 1 hr. The polymerized and unpolymerized material were separated by centrifugation and the concentrations of both were determined at 280 nm with an extinction coefficient of 33460 M^{-1}. The values shown in the bar graph depict the concentration of unassembled protein found in the supernatant fraction. The average of 6 – 10 concentrations/samples were used to obtained the values shown. The average sample lost was 13 %.

Figure 1.

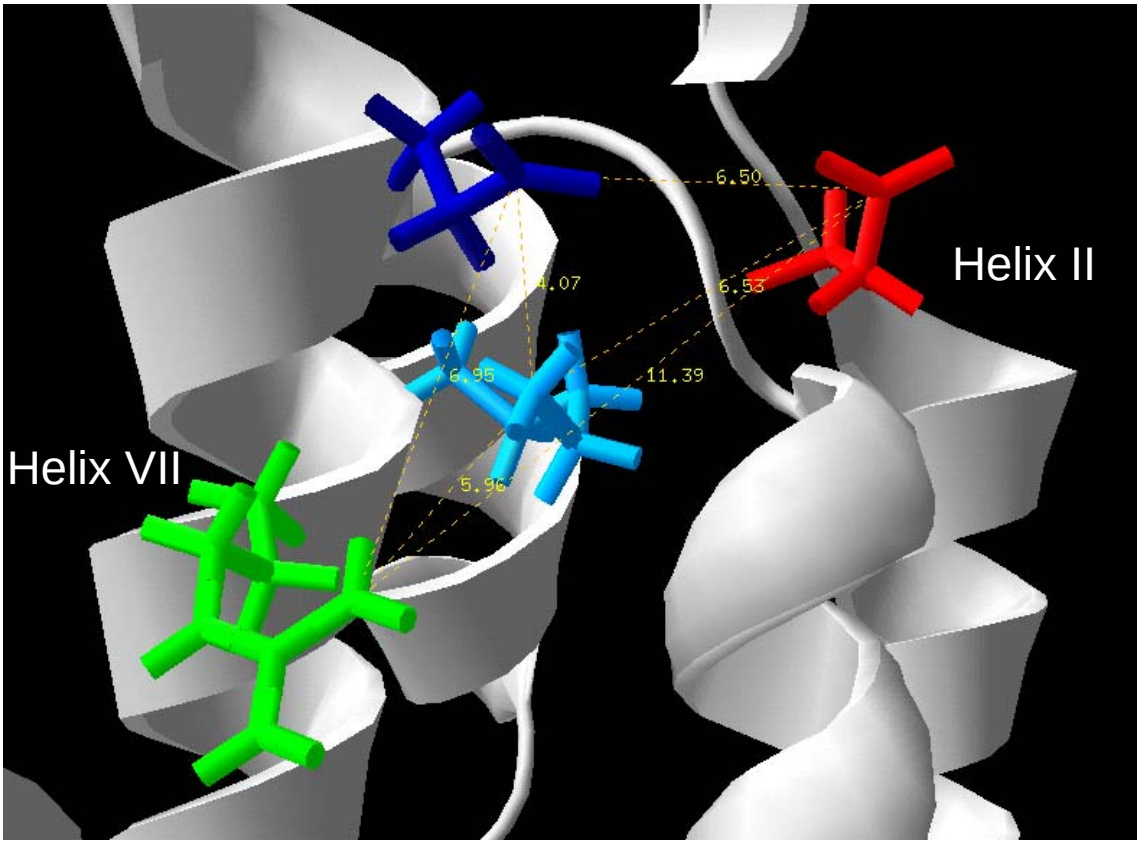

Figure 2.

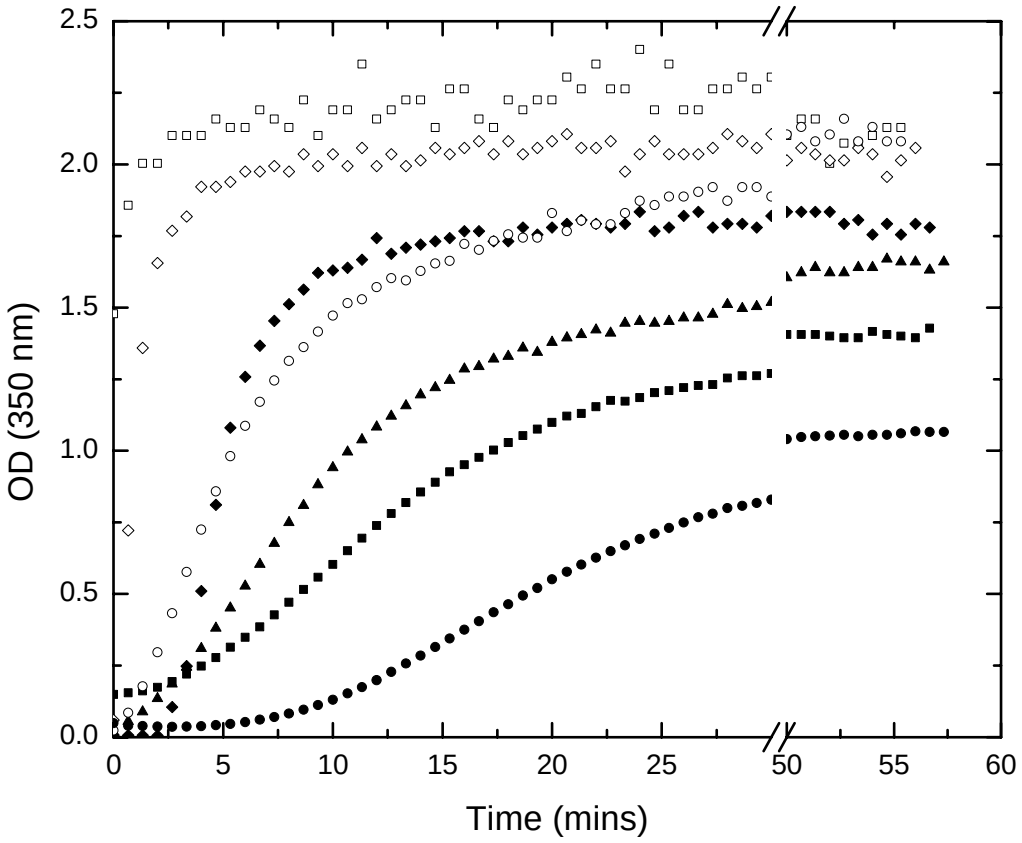

Figure 3.

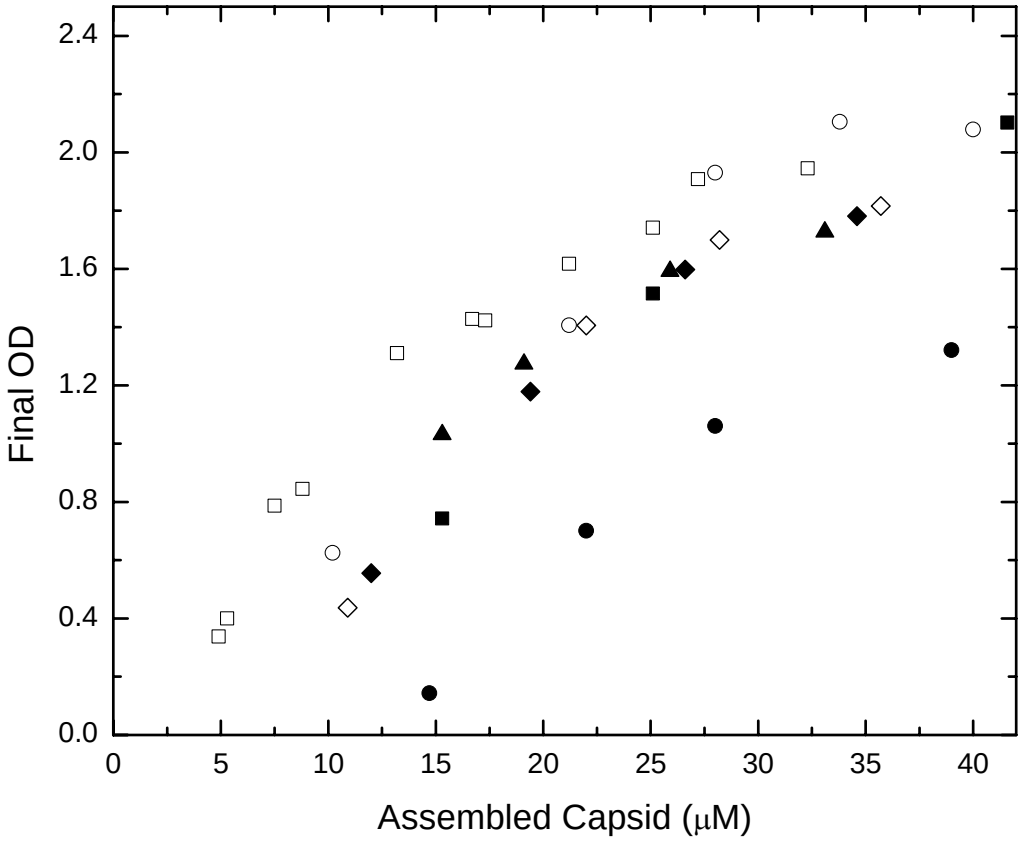
Final OD
Assembled Capsid (μM)
0.0
0.4
0.8
1.2
1.6
2.0
2.4
0
5
10
15
20
25
30
35
40

Figure 4.

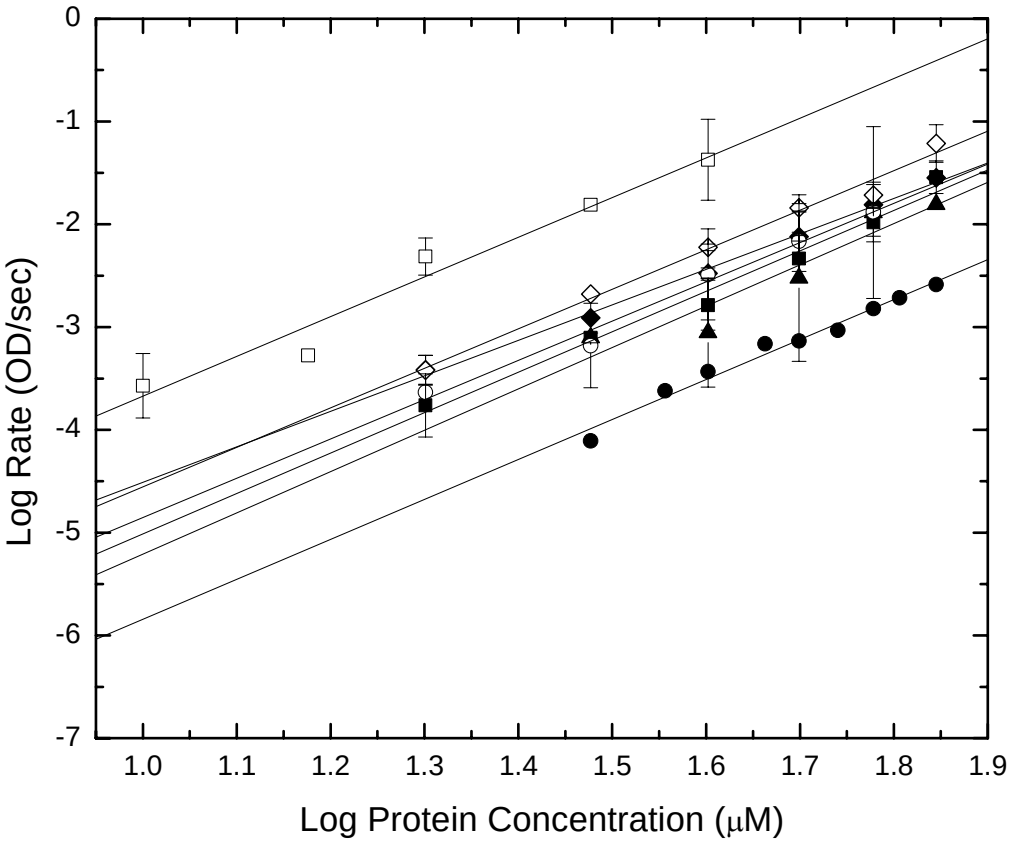
0
-1
-2
-3
-4
-5
-6
-7
Log Rate (OD/sec)
1.0
1.1
1.2
1.3
1.4
1.5
1.6
1.7
1.8
1.9
Log Protein Concentration (μM)

Figure 5.

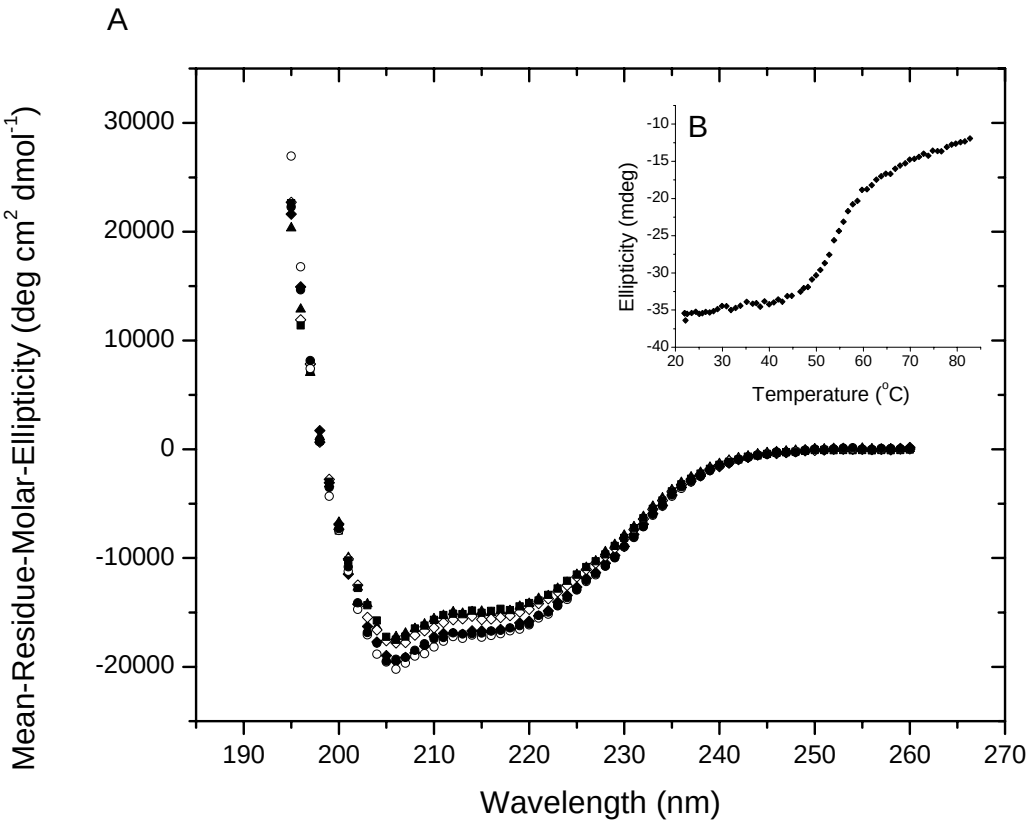
A
B
Mean-Residue-Molar-Ellipticity (deg cm^2 dmol^{-1})
Wavelength (nm)
Ellipticity (mdeg)
Temperature (°C)

Figure 6

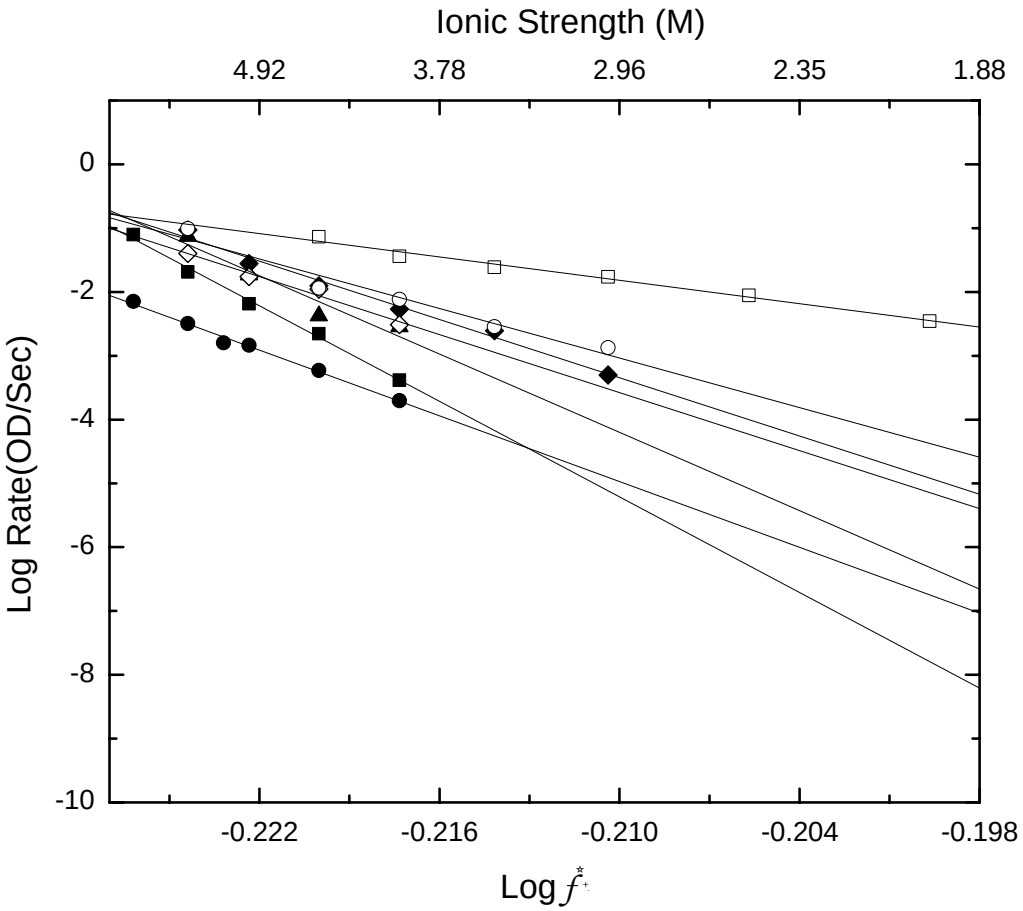
Ionic Strength (M)
4.92
3.78
2.96
2.35
1.88
0
-2
-4
-6
-8
-10
Log Rate(OD/Sec)
-0.222
-0.216
-0.210
-0.204
-0.198
Log $f_{\pm}^{*}$

Figure 7.

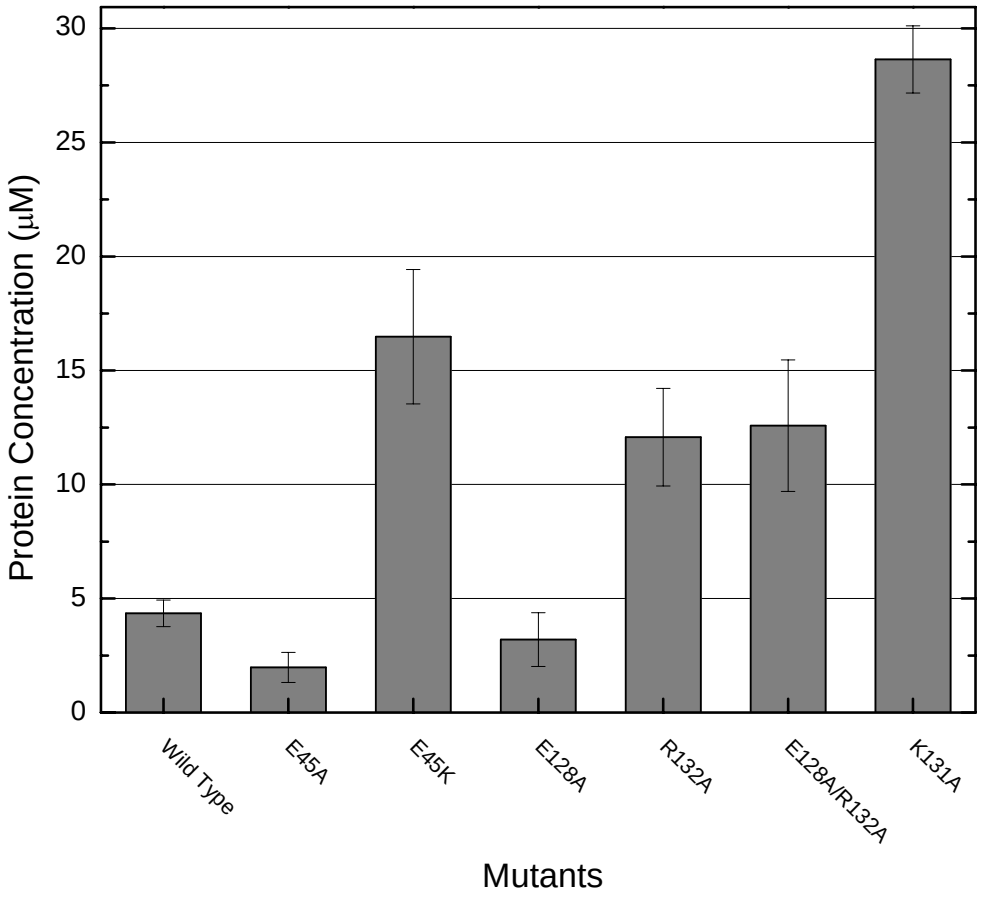
Protein Concentration (μM)
30
25
20
15
10
5
0
Wild Type
E45A
E45K
E128A
R132A
E128A/R132A
K131A
Mutants

Identification of Small Molecule Inhibitors of HIV-1 Capsid Assembly

CHANEL C. DOUGLAS, JENNIFER SEXTON, OLAF KUTSCH, ANJALI JOSHI, ERIC O. FREED, AND PETER E. PREVELIGE JR.

In preparation for Antimicrobial Agents and Chemotherapy

Format adapted for dissertation

ABSTRACT

Here we describe the adaptation of a turbidity-based assay for the *in-vitro* assembly of HIV-1 capsid for medium through-put screening of drug-like compounds. Using this assay we screened 10,000 diverse compounds and selected 116 compounds for the ability to reduce the turbidity associated with capsid assembly. The selected compounds were then screened in a series of cell culture assays which resulted in six compounds showing favorable antiviral effects when compared to their cytotoxicity. Three of these six compounds are shown to primarily exert their antiviral activity after the integration stage in the viral replication cycle.

INTRODUCTION

The current therapeutic regimen for the treatment of human immunodeficiency virus type-1 (HIV-1) infection involves the combined use of potent inhibitors of the reverse transcriptase (RT) and protease (PR) viral enzymes(98). These drugs, while highly effective, often give rise to HIV-1 strains that are not only resistant to the drug used but may also be resistant to other drugs in the same class. The development of drugs effective against new targets will expand treatment options. The most recently approved class of antivirals target virus:host fusion and is typified by the drug FUZEON, a peptide inhibitor of the protein/protein interactions driving the structural rearrangement in HIV-1 gp41 required for viral entry (26, 65, 137). Additionally, an antiviral compound shown to act by targeting the last step in viral maturation known as 3-*O*-{3',3'-dimethylsuccinyl}-betulinic acid (DSB), (also known as PA-457, YK-FH312, or Bevirimat) (74), has shown promising results in clinical trails(62, 135). Together, these suggest that targeting protein/protein interactions and the processes of assembly and maturation represent viable targets.

The assembly of HIV-1 occurs through the polymerization of the Gag and Gag-Pol polyproteins (128). The Gag polyprotein is a 55 KDa protein that consists of the structural domains matrix (MA), capsid (CA), p2, nucleocapsid (NC), p1 and p6 (in that order)(38, 58, 84, 88, 126). A -1 ribosomal frame shift results in synthesis of the Gag-Pol polyprotein which includes the enzymes PR, RT, and integrase (IN) in addition to the aforementioned Gag proteins (38, 58, 61). These proteins, along with the envelope (Env) glycoprotein and several regulatory and accessory factors, comprise all of the structural and enzymatic proteins needed for viral infectivity. HIV-1 assembly is a multi-step proc-

ess in which the Gag and Gag-Pol polyproteins assemble at and bud through the plasma membrane as an immature virion. In the immature virion these polyproteins are arranged radially with the myristoylated MA domain embedded in the viral membrane and the NC/p6 domain in the center (138). Budding activates PR, which cleaves the Gag polyprotein into the individual matrix (MA), capsid (CA), and nucleocapsid (NC) proteins. Upon cleavage, the individual structural proteins undergo a profound morphological rearrangement in which the CA protein collapses to form a conical core which contains the viral RNA in complex with NC, RT, and IN. This structural rearrangement arises from the disruption of existing interdomain interactions and the formation of new ones, particularly with regard to CA (68). In a number of studies, point mutations were introduced into CA. Some of these mutations resulted in the perturbation of core formation. In addition, these viruses had limited or no replication capability, suggesting that proper core formation is required for effective particle infectivity (47, 107, 120, 121, 130). Many of these mutations were located in regions that become protected in CA after assembly, indicating that they existed in regions involved in protein/protein interactions. Thus, small molecule compounds which block the intersubunit interactions involved in either Gag assembly or virion capsid maturation might be expected to have antiviral activity.

Currently, structure-based drug design targeted to CA in the virion is impractical due to the pleiomorphic nature of both the immature and mature HIV-1 virion. This non-uniformity precludes obtaining high-resolution structural information using traditional approaches such as X-ray crystallography or electron microscopy/image reconstruction. Despite this limitation, small molecules that prevent the assembly of the immature or mature CA lattice may still be discovered by using *in-vitro* systems that mimic these bio-

logical processes. In this paper, we describe the adaptation of such an assay capable of mimicking the protein/protein interactions driving virus assembly and CA maturation to medium through-put applications.

A number of studies have demonstrated the ability of recombinant, purified CA protein to polymerize into dimers, larger oligomers and eventually tubular polymers(31, 45, 52, 75). The presence of a small number of cones similar in shape and size to viral cores has been described in some of these preparations (45). Additionally, there are similarities between the hydrogen/deuterium exchange and electron diffraction profiles of *bona fide* viral particles to these *in-vitro* assemblies suggesting that the *in-vitro* assembled CA polymers form bonding interactions similar to those found in the virion.

We have previously described an *in-vitro* procedure in which the assembly kinetics of purified recombinant CA can be monitored by the time-dependent increase in turbidity(71). Here we describe the adaptation of this assay to a ninety-six well format and utilize this assay to screen 10,000 structurally diverse compounds for their ability to inhibit the *in-vitro* assembly of HIV-1 CA. Using cell-based assays, we show that a subset of the compounds identified in the *in vitro* screen are effective at limiting viral replication in cell culture.

MATERIALS AND METHODS

Compounds

A library of 10,000 drug-like molecules, which generally conform to 'Lipinski's Rules of Five' (a molecular weight less than or equal to 500 Da, five or fewer H-bond donors, ten or fewer H-bond acceptors, and a calculated log p [octanol/water partition coefficient] less than or equal to 5)(78), was purchased from ChemBridge Corporation

(San Diego, CA). The average molecular weight was 347 Da (200-596 Da) and this value was used for subsequent calculations of concentration unless otherwise indicated. The compounds came plated in 96-well plates and solubilized in DMSO at 5 mg/mL. One or more of the following reagents were used as reference anti-HIV compounds in cell based assays: Indinavir Sulfate, a protease inhibitor, 3TC and Efavirenz, RT inhibitors were obtained from the National Institutes of Health AIDS Research and Reference Reagent Program. T-20 peptide, an entry inhibitor, was obtained from John Kappes. The following were used as anti-CA HIV-1 compounds: CAP-1 (N-(3-chloro-4-methylphenyl)-N′-{2-[({5-[(dimethylamino)-methyl]-2-furyl}-methyl)-sulfanyl]-ethyl}urea) compound, a gift from Mike Summers and DSB (3-O-{3',3'-dimethylsuccinyl}-betulinic acid), a gift from Chris Aiken.

In-vitro MTS Assay

Recombinant CA protein was purified as previously described and stored at 300 μM at -80 ^{o}C (28, 52, 71). A turbidity-based assembly assay, previously described(71), was adapted to a 96-well, microplate format to allow for medium-throughput screening of compounds in a Nepheloskan Ascent plate reader (Thermo Electron Corp., UK). This was done by first placing 135 μL of 50 mM Na_2HPO_4, 2.25 M NaCl buffer, pH 8 in an optically clear 96-well plate and then initiating assembly by adding 15 μl of recombinant HIV-1 CA to each well using a multi-channel pipette. Since the halftime of the assembly reaction is typically ~5 minutes, the plates were read in thirds to prevent loss of the initial rate data. To accomplish this, CA was added to the first 4 lanes and the reactions followed for 10 minutes, the reading was then paused and CA was added to the next four

lanes, and the process repeated. The instrument was set to have a PMT gain of 500 V, lamp energy was at 10V, and the integration time was 60 ms. The data were visually analyzed using a custom-designed Excel spreadsheet that allowed simultaneous plotting of all kinetic curves. To screen for inhibition of assembly using the compound library, 1.5 μL of compound or DMSO was diluted 90-fold into 50 mM Na_2HPO_4, 2.25 M NaCl buffer, pH 8 in an optically clear 96-well plate. Assembly was then initiated as above by adding 15 μL of the 300 μM stock (in 50 mM Na_2HPO_4 pH 8) of recombinant HIV-1 CA. The final average compound concentration was nominally 142 μM, the CA concentration was 30 μM, and the NaCl concentration was 2.0 M. The compounds were evaluated for their ability to decrease the rate of assembly as monitored by turbidity and scored by eye into strongly inhibitory or weakly inhibitory classes.

Cells and Viruses

293T, a human embryonic kidney cell line and TZM-BL, a HeLa-based cell line, were maintained in DMEM medium supplemented with 10% (vol/vol) heat-inactivated fetal bovine serum (FBS), 100 U/ml penicillin, 100 μg/ml of streptomycin and 292 μg/ml of L-glutamine. 5.25.GFP.Luc.M7 cells (Luc-M7), a CEMx174 based cell line(8), were maintained in RPMI 1640 containing 10% (vol/vol) FBS, 100 U/ml penicillin, 100 μg/ml of streptomycin, 292 μg/ml of L-glutamine, 1% Hepes, 0.5 μg/ml puromycin, 0.3 mg/ml geneticin (G418) and 200 μg/ml hygromycin B. JLTRG-R5 cells, a Jurkat-based cell line stably expressing EGFP under the control of an LTR and CCR5, were cultured in RPMI 1640 1% FBS 1% PSG. Molt4 cells, a human peripheral blood lymphoblastoid T-cell line expressing either NL4-3 or BAL virus, were cultured in RPMI 1640 1% FBS 1% PSG.

CD8+ depleted human peripheral blood mononuclear cells (PBMCs) were obtained from healthy donors (Research Blood Components) and isolated by standard Ficoll-Hypaque technique and depleted using antibody-conjugated magnetic beads (Dynal/Invitrogen). The cells were then stimulated and activated with SEB and IL-2. HIV-1_{NL43}, HIV-1_{YU2}, and HIV-1_{SG3} were prepared by transient transfection of 293T cells with pNL43, pYU2 and pSG3, respectively, using FuGene 6 (Roche) and collecting the viral supernatant 48-72 hours post transfection. Viral infectious units were determined by counting the number of ß-Gal^+ cell colonies in TZM-BL cells as previously described (134).

Anti-HIV Assays (Multiple Round)

The inhibitory effects of the tested compounds on HIV-1_{YU2} replication were determined by the level of luciferase expression after 6 days of infection using Bright-Glo assay (Promega) and a LUMIstar luminometer (BMG Inc.). 1.5×10^4 Luc-M7 (a gift from Ned Landau) cells per ml were infected with HIV-1_{YU2} at a multiplicity of infection (MOI) of 3 (as determined on TZM-BL). The HIV-1 infected (0-75 μM compound) or mock-infected (0-300 μM compound) Luc-M7 cells were placed in 96-well culture plates (100 μl/well) with 100 μl of various concentrations of the compounds with 20μg/ml DEAE Dextran in triplicate and incubated at 37°C under 5% CO_2 at 100% humidity. After 6 days, cell viability was quantified by Cell-Titer Glo or infectivity measured by endogenous luciferase level using Bright-Glo reagent (Promega). The 50% toxic concentration (TC_{50}), 50% inhibitory concentration (IC_{50}), and the therapuetic index ($TI = TC_{50}/IC_{50}$) were then calculated for each of the compounds. The inhibitory effects of the tested compounds on HIV-1_{BAL} and HIV-1_{NL43} viral spread were determined by the

level of EGFP expression after 5 days. 2×10^5/well JLTRG-R5 cells per ml were co-cultured with 1×10^4 Molt4 cells/ml stably infected with either HIV-1_{BAL} or HIV-1_{NL43} in 384-well plates in the presence of 0-75 μM compound in singlet. Cell viability in these cells was determined by comparing them to the level of GFP expression in untreated JLTRG/CUCY cells. Anti-HIV-1 activity was also investigated in PBMCs infected with HIV-1_{SG3} and cultured with various concentrations of test compounds (0-100 μM compound) in triplicate. Cells were infected overnight with SG3 at an MOI of 0.1 in a small volume in the presence of 20 μg/ml DEAE Dextran. The next morning the cells were pelleted and washed five times with media before plating in 96-well plates in the presence of compounds. The activity was evaluated by the level of inhibition of p24 core antigen in the culture supernatant on day 5 as assessed with the HIV-1 p24 enzyme-linked immunosorbent assay (ELISA) (Beckman-Coulter).

Anti-HIV Assays (Single Round)

The inhibitory effect of the compounds on virus production and infectivity was determined by measuring the level of p24 produced in the presence of various concentrations of compounds from 293T cells transiently transfected with pNL43 and by titering the virus on TZM-BL cells. Briefly, 2.5×10^5 293T cells/ml were transfected with pNL43 using FuGene 6. Four hours posttransfection the cells were plated in 96-well plates containing 100 μl of various concentrations of compounds (0-75μM or 0-300μM for mock-transfected cells) in triplicate. 72-hours posttransfection virus supernatant was collected and stored at -80 ^oC until analysis. Cell viability on the mock infected cells was determined using an MTS assay from Promega and compared to DMSO only controls. The

level of p24 produced at each compound concentration was determined relative to the level produced in the presence of the DMSO-only controls using HIV-1 p24 enzyme-linked immunosorbent assay (ELISA) (Beckman-Coulter). To determine virus infectivity, TZM-BL cells were plated at $1x10^5$ cells/well in 100 μL in 96-well plates overnight. The next day, the media were replaced with 75 μL DMEM supplemented with 1% FBS, 1x PSG and 40μg/ml DEAE Dextran and 25 μL of viral supernatant from the 293T cells was added to each well. Three hours later, 100 μL of DMEM with 7% FBS was added to each well. Two days after infection the cells were lysed and the level of luciferase expression was determined using the Bright-Glo (Promega) reagent.

Entry/Early Post-Entry Inhibition

TZM-BL cells were plated at $1x10^5$ cells/well in 96-wells. The next day, the media were replaced with 75 μL DMEM supplemented with 1% FBS, 1x PSG and 40μg/ml DEAE Dextran and infected or mock infected with 25 μL of YU- 2 viral supernatant from transiently transfected 293T cells. Compounds were added at a final concentration of 30 μM for UAB 26,41,59,60,70 or 5 μM of UAB 58, DSB, 3TC, AZT and Indinavir, or 5 μg/ml T-20. Two days after infection, endogenous luciferase activity was measured with the Bright-Glo reagent and cell viability was determined with Cell-titer Glo.

Virus Release Assay

HeLa cells were transfected with the WT HIV-1 molecular clone pNL4-3 (Adachi et al., 1986) using Lipofectamine-2000 in 6-well plates and then cultured in the presence of UAB 58 or 60 (10 and 20 μM) or UAB 26, 60, or 70 (120 μM). Twenty-four hours

posttransfection, cells were metabolically labeled with [35S] Met/Cys (Pro-mix; Amersham). Cell and viral lysates were immunoprecipitated essentially as described (Freed et al., JVI 1994). Briefly, the virus-containing supernatant was pelleted in an ultracentrifuge at 35,000 rpm for 45 min. Cell and viral lysates were immunoprecipitated with HIV-Ig (obtained through the NIH AIDS Reference and Reagent Program) and subjected to SDS-PAGE. Protein levels were quantified by phosphorimager analysis and virus release efficiency was calculated as follows: Virus p24/ (cell p24+cell Pr55+ virus p24).

Time-of-addition assay

JC53BL cells ($1x10^4$ cells/well in 96-well plate) were infected with YU2 at an MOI >1 in 50 μL in the presence of 20μg/ml DEAE Dextran and 0.5 μM Indinivar was present in all wells to limit infection to one round. Compounds were added at 0, 2, 4, 6, and 12 hours post-infection. UAB 41 and 59 were added at a final concentration of 35 μM. 3TC and Indinavir were added at a final concentration of 5 μM. T-20 was added at a final concentration of 8 μg/ml. The cells were lysed and assayed for luciferase expression forty-eight hours post-infection.

Fusion Assay

HIV-1 virions containing the Blam-Vpr chimera were produced by co-transfecting 293T cells with pSG3 and pCMV-Blam-Vpr. 100 μl of virus supernatant was added to$1x10^5$ cells/well in 96-well black clear bottom plates. Compounds were added at various concentrations and the plates were spun at 1200 x g for one hour at 34^o C. After an hour, the plates were incubated for two hours at 37 ^{o}C in 5% CO_2. 20 μl of

CCF2-AM loading solution was added to each well and the plates were incubated for 14 hours at room temperature. The dye was excited at 405 nm and emissions were read at 460 nm and 535 nm on a Victor 3 microplate reader (Perkin Elmer). The background levels of blue fluorescence in wells containing no virus and green fluorescence in wells containing neither virus nor cells were determined at 460 nm and 535 nm, respectively, and were subtracted from the experimental samples. Fluorescence ratios were calculated for each well.

RT Assay

Purified RT was obtained from Calbiochem,. Approximately one unit per well was used in the Enzchek kit (Invitrogen) which measures the amount on RNA-DNA duplex produced from a poly-A template and T-primer. The protein was diluted into enzyme dilution buffer 50 mM Tris-HCl, 20% glycerol, 2 mM DTT, pH 7.6 and incubated for 40 minutes at room temperature in the presence of various concentrations of compounds. The reaction was stopped with EDTA and picogreen supplied with the kit was added to each well. Fluorescence was measured by exciting at 460 nm and reading the emission at 535 nm on the Wallac 1420 Victor 3 microplate reader from Perkin Elmer.

RESULTS

In Vitro Screening of Compound Libraries

The polymerization of recombinant HIV-1 CA into tube-like structures can be followed by monitoring the time-dependent increase of the reactions' turbidity (71). Typically these experiments are performed in a spectrophotometer at a wavelength at

which the protein does not absorb. Light that is scattered does not reach the phototube and is recorded as apparent absorbance. We have adapted this assay to a 96-well format using a nephelometry based plate reader for detection. The assembly reaction is initiated by adding a sodium chloride stock solution to a stock solution of purified CA protein with the final concentrations being 30 μM protein and 2.25 M NaCl. These conditions parallel those that we have used previously to generate tubes of HIV-1 CA in the spectrophotometer-based assays described above (17). Using this 96-well plate assay we screened for assembly inhibitors from a library of ten thousand "druggable" compounds (ChemBridge). The compounds were examined for their ability to inhibit the polymerization of 30 μM CA protein at a nominal compound concentration of 142 μM. The compounds were scored into strongly and weakly inhibitory classes based on visual analysis of their ability to decrease the rate of assembly (Fig. 1).

Of the ten thousand compounds screened, 114 (1.14%) were classified as strongly inhibitory and 1626 (16.26%) were classified as weakly inhibitory. To test for the presence of compounds that non-specifically perturb protein structure, approximately 15% of the strongly inhibitory compounds were selected randomly and screened for their ability to inhibit the *in-vitro* assembly of the bacteriophage P22. Bacteriophage P22 assembly requires the activity of two structural proteins, coat and scaffolding which polymerize in a roughly 2:1 molar ratio. None of the compounds selected inhibited P22 assembly (data not shown) suggesting that their mechanism of action was not non-specific perturbation of protein structure. As the initial screen was performed at high compound concentration, 89 of the compounds classified as strongly inhibitory were then titrated down to determine their IC_{50} for inhibition of *in-vitro* assembly (Fig. 2). In general, the initial screen-

ing data held up well to this scrutiny. There were no instances of false positives and with few exceptions, compounds identified as strongly inhibitory had IC_{50}s in the 20 μM range (Fig 2).

Cell-Based Assays of Activity

Compounds that appear efficacious *in-vitro* can exhibit toxic effects on cells or display problems with membrane permeability that would render them ineffective *in-vivo*. To eliminate the compounds that fall into this category, 75 of the strong inhibitors were screened in cell culture for their ability to inhibit virus particle production as well as for their potential cytotoxicity. To assay for virus replication 293T cells were transiently transfected with proviral DNA. Four hours posttransfection the selected compounds (or the equivalent amount of DMSO as mock treatment) were added to the cells to final concentrations of 10, 30 and 100 μM. Forty-eight hours posttransfection, the culture media were collected and analyzed for p24 levels by ELISA and for virus infectivity using TZM-BL indicator cells. To assay for cytotoxicity, mock-transfected cells were treated with compound in parallel and the cell viability analyzed after forty-eight hours using an MTS assay. Seventeen out of the seventy-five compounds showed either a decrease in p24 production or a decrease in the level of infectious virus in the culture media while maintaining relatively low toxicity (data not shown). Where are the data? These seventeen compounds were chosen for more extensive cell-based analysis.

To identify any compounds that might have been missed, eighty-four of the strong *in-vitro* inhibitors were screened in a multiple-round viral spread assay in which MOLT4 cells stably expressing either NL4-3 or BAL strains of HIV-1 were co-cultured with

JLTRG-R5 indicator cells in the presence of the compound over a 0-75 μM concentration range. Five days after co-culturing, the level of GFP expression from the JLTRG-R5 indicator cells was determined on a fluorescent plate reader (data not shown). The data were normalized for cell viability using untreated JLTRG/CUCY cells which have the same parental derivation as the JLTRG-R5 cells but were designed to stably express GFP. From this assay, an additional ten compounds were identified as reducing the spread of both NL4-3 and BAL. These ten were also advanced for more extensive analysis.

Inhibition of Viral Spread and Selectivity Index Determination

The initial cell-based screens narrowed down the compounds originally selected for inhibition of CA assembly *in- vitro* to twenty-seven possible small molecules, which also appeared to have antiviral activity in cell culture. To more fully assess the effect of the compounds on viral spread, the twenty-seven compounds were further scrutinized in 5.25.EGFP.Luc.M7 indicator cells. The 5.25.EGFP.Luc.M7 cell line carries a luciferase coding sequence under the transcriptional control of the HIV-1 LTR. This cell line was chosen because it requires multiple rounds of virus replication in order to achieve detectable levels of luciferase (8). As such, even a relatively small decrease in viral replication should be detectable. The compounds were tested, in triplicate, at seven concentrations ranging from 0-75 μM. After six days, the extent of virus replication was assayed by measuring the amount of luciferase synthesized by fluorescence (Promega Bright-Glo). To assay for toxicity, uninfected cells were treated with compounds ranging in concentration from 0-300 μM. Six days after treatment, the cells were assayed for metabolic activity (Promega Cell-Titer Glo). The $TC_{50\%}$ and $IC_{50\%}$ values were determined as the con-

centration at which cell viability and reporter gene expression decreased by 50% respectively (Fig 3). This information was then used to calculate the selectivity index (Table 1). Six of the twenty-seven compounds had a selectivity index of ≥ 15. These six (Fig. 4) were advanced for further studies.

Anti-HIV Activity in PBMCs

While laboratory-adapted cell lines provide a reasonably good model for the behavior of physiological events, most, in the processes of being adapted, undergo transformations (which may include mutations) that allow them to grow indefinitely. In addition, laboratory adapted cell-lines tend to be homogenous populations. To study the antiviral effect of the selected compounds in a more clinically relevant cell type human peripheral blood mononuclear cell (PBMCs) from normal donors, depleted of CD8+ cells, were isolated. After stimulation with SEB and activation with IL-2, the cells were infected in the presence of increasing concentrations of compound. The extent of virus replication was determined at five days postinfection by measuring the level of p24 antigen in the media. All but one of the compounds (UAB 60) had an IC_{50} in this assay that was under 20 μM (Table 1). UAB 41 was not assayed here due to a limitation on the availability of the compound. However, UAB 59, which is structurally related to UAB 41 (Fig.4), had an $IC_{50\%}$ of 2.4 μM. To measure cytotoxicity, a mock infection was also performed in the presence of increasing compound concentration. Cell viability was measure six days after mock infection and used to determine the $TC_{50\%}$ for the compounds and subsequently the selectivity index in PBMCs (Table 1). In general, the compounds were

both less toxic and less effective in PBMCs than in the Luc-M7 cells. The one exception was UAB 59 which was less toxic but more effective.

UAB 26, 58, and 60 Target a Late Step in Virus Replication

The compounds were selected for their ability to inhibit the *in-vitro* assembly of purified CA. Nonetheless, in cell culture with fully infectious virus, the compounds could act by inhibiting any number of stages in the virus life cycle. Therefore, to rule out the early steps of infection as the stage at which the compounds act, we performed a single-cycle infectivity assay utilizing the TZM-BL cell line. This is a HeLa-CD4/CCR5 (JC53) cell line that carries both the *Escherichia coli* ß-galactosidase and firefly luciferase coding sequence under the transcriptional control of the HIV-1 long terminal repeat region. Production of luciferase requires entry, reverse transcription, integration, and the expression of the Tat protein. As such, in a single-round assay, only compounds that disrupt an entry or early post-entry event would cause a reduction in luciferase expression. As shown in Fig. 5, the entry inhibitor T-20, and the nucleoside RT inhibitors AZT and 3TC, cause significant reductions in luciferase expression. UAB 41 and 59 also reduced luciferase expression, indicating a possible entry or early post-entry defect. This result was unexpected, since these compounds where selected for the ability to inhibit purified CA assembly. However, compounds have been synthesized that are capable of targeting both the process of capsid maturation and viral cell-entry (57). As expected, the protease inhibitor Indinavir shows no reduction in this system because it acts late in the virus replication cycle. The presence of DSB and UAB 26 during infection resulted in very little reduction in luciferase levels indicating a late post-entry event as the main target.

UAB 60 shows no reduction in luciferase levels, but at the same concentration in uninfected cells is slightly toxic. It is interesting to note that the degree of toxicity of this compound to the cells was abrogated by the presence of virus. This phenomenon is also seen with UAB 58 which was more toxic to the cells than UAB 60 but also showed a significant increase in infectivity when compared to level of viable cells in the mock infection. UAB 70 appears to be highly toxic to this cell line.

Time of Addition

The previous experiments indicated that UAB 41 and 59 may be targeting an entry or early post-entry event. To determine which early stage in the life cycle is targeted, we performed a time-of-addition assay using T-20, 3TC, and indinavir as markers for the processes of viral entry, reverse transcription, and protease-mediated maturation, respectively. Compounds added after the step they target has already occurred will not be effective in blocking replication. TZM-BL cells were infected at an MOI >1. Compounds were added at 0,2,4,6 and 12 hours post-infection in triplicate. Forty-eight hours post-infection, the level of luciferase expression was determined for each time point and compared to the no-compound controls. As indicated in Fig. 6, both UAB 41 and 59 act at an earlier step than does 3TC. This result rules out integration as the viral target for these compounds, suggesting entry, uncoating or reverse transcription as the target. .

UAB 41 and 59 Do Not Affect Virus Entry

To determine whether UAB 41 and 59 act by preventing virus entry, a fusion assay was performed. SG3 virions containing the reporter fusion protein Blam-Vpr (β-

lactamase- Vpr) were produced in 293T cells and used to infect SupT1 cells in the presence of compounds. The cells were then loaded with the β-lactamase substrate CCF2-AM and the level of fluorescence was determined. As seen in Fig. 7, the presence of the entry inhibitor T-20 inhibited fusion of the pseudotyped virus in a dose-dependent manner, whereas the RT inhibitor 3TC did not. At the compound concentrations studied, neither UAB 41 nor 59 inhibited virus fusion.

UAB 41 and 59 Inhibit Reverse Transcriptase

Having ruled out virus entry as the pre-integration target for UAB 41 and 59 we assayed directly for their effect on reverse transcription by determining whether the compounds could inhibit the *in-vitro* transcription of a poly-A template in a dose dependent manner. As positive and negative controls, we used efavirenz and indinavir, respectively. The template and primer were allowed to anneal for one hour prior to the addition of the purified RT and the compounds. As expected, efavirenz inhibited the *in-vitro* transcription in a dose-dependent manner while indinavir did not. UAB 41 and 59 also inhibited RT activity (Fig. 8), suggesting reverse transcription as at least one target for these compounds.

UAB 26, 58, 60 and 70 Do not Reduce Virus Release Efficiency

The previous experiments narrowed down the target for the compounds UAB 26, 58, and 60 to the second half of the viral life cycle; after integration and Tat expression. The possible steps that could be affected include viral protein trafficking, virus assembly, release and maturation. Although, the initial transcription of Tat is most likely mediated

by NF-κβ and not by virally encoded factors, we hypothesize that viral transcription and translation are unlikely targets. This is due to the fact that in-order to obtain high levels of protein expression in the indicator cell lines a continuous supply of Tat must be made. This is only possible if the machinery for viral transcription and translation remain functional. All four of these steps involve processes that require either Gag or CA. To investigate possible effects of the compounds on Gag trafficking, virus assembly and release, HeLa cells were transfected with a WT HIV-1 molecular clone and cultured in the presence of compounds UAB 26, 58, 60 and 70. Twenty-four hours posttransfection, the cells were metabolically labeled with [35S] Met/Cys. Cell and viral lysates were prepared and immunoprecipitated with HIV-IgG and subjected to SDS-PAGE. The virus bands were quantified by phosphorimager analysis and the release efficiency was calculated. The results indicated that the compounds did not affect Gag processing efficiency or virus particle production, compared with DMSO controls (Fig. 6a and b). Interestingly, UAB 70 appears to slightly (2-fold) increase virus particle production in these assays. This effect was also seen in the p24 (ELISA) cell-culture data (data not shown). These observations suggest that a direct interaction between UAB 70 and Gag in the producer cell may cause a modest stimulation in virus particle production .

DISCUSSION

We have previously reported the development of a rapid dilution-induced technique for CA assembly in which the kinetics of assembly can be followed by monitoring turbidity(71). This technique has proven to be useful for the evaluation of the effects of solvent conditions, protein concentration, and mutations on CA assembly. Here we adapt

this technique to allow for medium-through put processing. We further utilize this fairly rapid technique to screen a library of 10,000 small drug-like compounds for the ability to inhibit this assay. In view of the fact that compounds were categorized by visual inspection for the degree of turbidity reduction relative to the DMSO controls, we further titrated the "strong" inhibitors and confirmed their classification. Compounds that significantly reduced CA assembly in this assay were tested in cell culture for the ability to reduce virus production, infectivity and viral spread. Based on these initial results, 26 compounds were chosen for more rigorous testing in cell culture. This analysis included a comparison of the compounds' toxicity and ability to reduce viral spread. While for the majority of the compounds the ability to reduce viral spread could not be separated from their cytotoxicity, there were six compounds for which the antiviral activity could not be attributed to cell death.

The ability of these compounds to inhibit virus replication in tissue culture did not prove that the mechanism by which inhibition was occurring was through targeting CA. To define the step in the virus replication cycle affected by these compounds in cell culture, a number of assays were conducted. We first tried to determine whether the target for the compounds was a step that occurs pre-integration or post-integration by using an indicator cell line (TZM-BL). In this assay three of the six compounds did not inhibit luciferase expression, indicating a post-integration step as their most likely target. For these compounds, radioimmunoprecipitation data suggest that there is no defect in viral protein trafficking, Gag processing, or virus release. Core condensation remains a possible target, though preliminary electron microscopy analysis suggests no overt defect in

virion maturation (unpublished results). Studies are currently underway to elucidate the exact mechanisms by which these compounds disrupt viral spread.

Two compounds, UAB 41 and 59, were shown to inhibit virus infection during an integration or pre-integration step. With the possibility existing that the mechanism could be related to a process involving capsid, in particular uncoating, we set forth to eliminate the steps that did not involve capsid. First, we determined that the primary target was indeed a step that occurred before integration by performing a time-of-addition assay. Next, we eliminated viral entry as a possibility by performing a viral fusion assay. Lastly, we used recombinant, purified RT to determine whether any of the six compounds could inhibit the reverse transcription process. We indeed observed inhibition in the presence of UAB 41 and 59; however, none of the other four candidates tested showed any effect on RT activity. Since these compounds were originally selected because they significantly reduced the *in-vitro* assembly of purified CA, the fact that UAB 41 and 59 also inhibit RT may indicate a possible dual action for these two compounds.

Many questions still remain regarding the exact mechanism of action of these potential lead compounds. Inevitably, answers to these questions will shed light on the characteristic of the binding site(s) for these compounds and determine the feasibility of targeting the protein-protein interactions driving capsid assembly and maturation in a clinical setting.

ACKNOWLEDGEMENTS

This work was supported by NIH Grants AI44626 (PEP) and T32 AI007150 (CCD). We are grateful to John Kappes and Joan Conway for assistance and training in the BSL2+ aspect of this work. We would also like to acknowledge Susan Dubay (1960 -2007) and

Ken Zammit (1957-2007) without their contributions and insights a lot of this work could not have been done. They will be missed.

REFERENCES

1. **Brandt, S. M., R. Mariani, A. U. Holland, T. J. Hope, and N. R. Landau.** 2002. Association of Chemokine-mediated Block to HIV Entry with Coreceptor Internalization10.1074/jbc.M108232200. J. Biol. Chem. **277:**17291-17299.

2. **Derdeyn, C. A., J. M. Decker, J. N. Sfakianos, X. Wu, W. A. O'Brien, L. Ratner, J. C. Kappes, G. M. Shaw, and E. Hunter.** 2000. Sensitivity of human immunodeficiency virus type 1 to the fusion inhibitor T-20 is modulated by coreceptor specificity defined by the V3 loop of gp120. J Virol **74:**8358-67.

3. **Douglas, C. C., D. Thomas, J. Lanman, and P. E. Prevelige, Jr.** 2004. Investigation of N-terminal domain charged residues on the assembly and stability of HIV-1 CA. Biochemistry **43:**10435-41.

4. **Ehrlich, L., B. Agresta, and C. Carter.** 1992. Assembly of recombinant human immunodeficiency virus type 1 capsid protein in vitro. J. Virol. **66:**4874-4883.

5. **Freed, E. O.** 1998. HIV-1 gag proteins: diverse functions in the virus life cycle. Virology **251:**1-15.

6. **Ganser, B. K., S. Li, V. Y. Klishko, J. T. Finch, and W. I. Sundquist.** 1999. Assembly and Analysis of Conical Models for the HIV-1 Core. Science **283:**80-83.

7. **Ganser-Pornillos, B. K., U. K. von Schwedler, K. M. Stray, C. Aiken, and W. I. Sundquist.** 2004. Assembly properties of the human immunodeficiency virus type 1 CA protein. J Virol **78:**2545-52.

8. **Griffin, G. E., K. Leung, T. M. Folks, S. Kunkel, and G. J. Nabel.** 1989. Activation of HIV gene expression during monocyte differentiation by induction of NF-kappa B. Nature **339:**70-3.

9. **Gross, I., H. Hohenberg, and H. Krausslich.** 1997. In vitro assembly properties of purified bacterially expressed capsid proteins of human immunodeficiency virus. Eur J Biochem **249:**592-600.

10. **Huang, L., P. Ho, K.-H. Lee, and C.-H. Chen.** Synthesis and anti-HIV activity of bi-functional betulinic acid derivatives. Bioorganic & Medicinal Chemistry **In Press, Corrected Proof**.

11. **Hunter, E.** 1994. Macromolecular interactions in the assembly of HIV and other retroviruses. Seminars in Virology **5:**71-83.

12. **Jacks, T., M. D. Power, F. R. Masiarz, P. A. Luciw, P. J. Barr, and H. E. Varmus.** 1988. Characterization of ribosomal frameshifting in HIV-1 gag-pol expression. Nature **331:**280-3.

13. **James, J. S.** 2005. PA-457, new kind of antiretroviral: ten-day clinical trial results. AIDS Treat News**:**7-8.

14. **Kevorkov, D., and V. Makarenkov.** 2005. Statistical Analysis of Systematic Errors in High-Throughput Screening 10.1177/1087057105276989. J Biomol Screen **10:**557-567.

15. **Kliger, Y., and Y. Shai.** 2000. Inhibition of HIV-1 entry before gp41 folds into its fusion-active conformation. J Mol Biol **295:**163-8.

16. **Lanman, J., T. T. Lam, S. Barnes, M. Sakalian, M. R. Emmett, A. G. Marshall, and P. E. Prevelige, Jr.** 2003. Identification of novel interactions in HIV-1 capsid protein assembly by high-resolution mass spectrometry. J Mol Biol **325:**759-72.

17. **Lanman, J., J. Sexton, M. Sakalian, and P. E. Prevelige, Jr.** 2002. Kinetic Analysis of the Role of Intersubunit Interactions in Human Immunodeficiency Virus Type 1 Capsid Protein Assembly In Vitro. J. Virol. **76:**6900-6908.

18. **Li, F., R. Goila-Gaur, K. Salzwedel, N. R. Kilgore, M. Reddick, C. Matallana, A. Castillo, D. Zoumplis, D. E. Martin, J. M. Orenstein, G. P. Allaway, E. O. Freed, and C. T. Wild.** 2003. PA-457: A potent HIV inhibitor that disrupts core condensation by targeting a late step in Gag processing10.1073/pnas.2234683100. PNAS **100:**13555-13560.

19. **Li, S., C. P. Hill, W. I. Sundquist, and J. T. Finch.** 2000. Image reconstructions of helical assemblies of the HIV-1 CA protein. Nature **407:**409-13.

20. **Lipinski, C. A., F. Lombardo, B. W. Dominy, and P. J. Feeney.** 1997. Experimental and computational approaches to estimate solubility and permeability in drug discovery and development settings. Advanced Drug Delivery Reviews In Vitro Models for Selection of Development Candidates **23:**3-25.

21. **Mervis, R. J., N. Ahmad, E. P. Lillehoj, M. G. Raum, F. H. Salazar, H. W. Chan, and S. Venkatesan.** 1988. The gag gene products of human immunodeficiency virus type 1: alignment within the gag open reading frame, identification of posttranslational modifications, and evidence for alternative gag precursors. J Virol **62:**3993-4002.

22. **Nabel, G., and D. Baltimore.** 1987. An inducible transcription factor activates expression of human immunodeficiency virus in T cells. Nature **326:**711-3.

23. **Nermut, M. V., and D. J. Hockley.** 1996. Comparative morphology and structural classification of retroviruses. Current Topics in Microbiology and Immunology **214:**1-24.

24. **Piacenti, F. J.** 2006. An update and review of antiretroviral therapy. Pharmacotherapy **26:**1111-33.

25. **Scholz, I., B. Arvidson, D. Huseby, and E. Barklis.** 2005. Virus particle core defects caused by mutations in the human immunodeficiency virus capsid N-terminal domain. J Virol **79:**1470-9.

26. **Tang, S., T. Murakami, B. E. Agresta, S. Campbell, E. O. Freed, and J. G. Levin.** 2001. Human immunodeficiency virus type 1 N-terminal capsid mutants that exhibit aberrant core morphology and are blocked in initiation of reverse transcription in infected cells. J Virol **75:**9357-66.

27. **Tang, S., T. Murakami, N. Cheng, A. C. Steven, E. O. Freed, and J. G. Levin.** 2003. Human immunodeficiency virus type 1 N-terminal capsid mutants containing cores with abnormally high levels of capsid protein and virtually no reverse transcriptase. J Virol **77:**12592-602.

28. **Turner, B. G., and M. F. Summers.** 1999. Structural biology of HIV1. Journal of Molecular Biology **285:**1-32.

29. **Vogt, V. M., and M. N. Simon.** 1999. Mass determination of rous sarcoma virus virions by scanning transmission electron microscopy. J Virol **73:**7050-5.

30. **von Schwedler, U. K., K. M. Stray, J. E. Garrus, and W. I. Sundquist.** 2003. Functional surfaces of the human immunodeficiency virus type 1 capsid protein. J Virol **77:**5439-50.

31. **Wei, X., J. M. Decker, H. Liu, Z. Zhang, R. B. Arani, J. M. Kilby, M. S. Saag, X. Wu, G. M. Shaw, and J. C. Kappes.** 2002. Emergence of Resistant Human Immunodeficiency Virus Type 1 in Patients Receiving Fusion Inhibitor (T-20) Monotherapy 10.1128/AAC.46.6.1896-1905.2002. Antimicrob. Agents Chemother. **46:**1896-1905.

32. **Whelan, J.** 2004. Promising Phase I results against new HIV target. Drug Discovery Today **9:**823.

33. **Wild, C., D. Shugars, T. Greenwell, C. McDanal, and T. Matthews.** 1994. Peptides Corresponding to a Predictive {alpha}-Helical Domain of Human Immunodeficiency Virus Type 1 gp41 are Potent Inhibitors of Virus Infection10.1073/pnas.91.21.9770. PNAS **91:**9770-9774.

34. **Wilk, T., I. Gross, B. E. Gowen, T. Rutten, F. de Haas, R. Welker, H. G. Krausslich, P. Boulanger, and S. D. Fuller.** 2001. Organization of immature human immunodeficiency virus type 1. J Virol **75:**759-71.

Figure 1

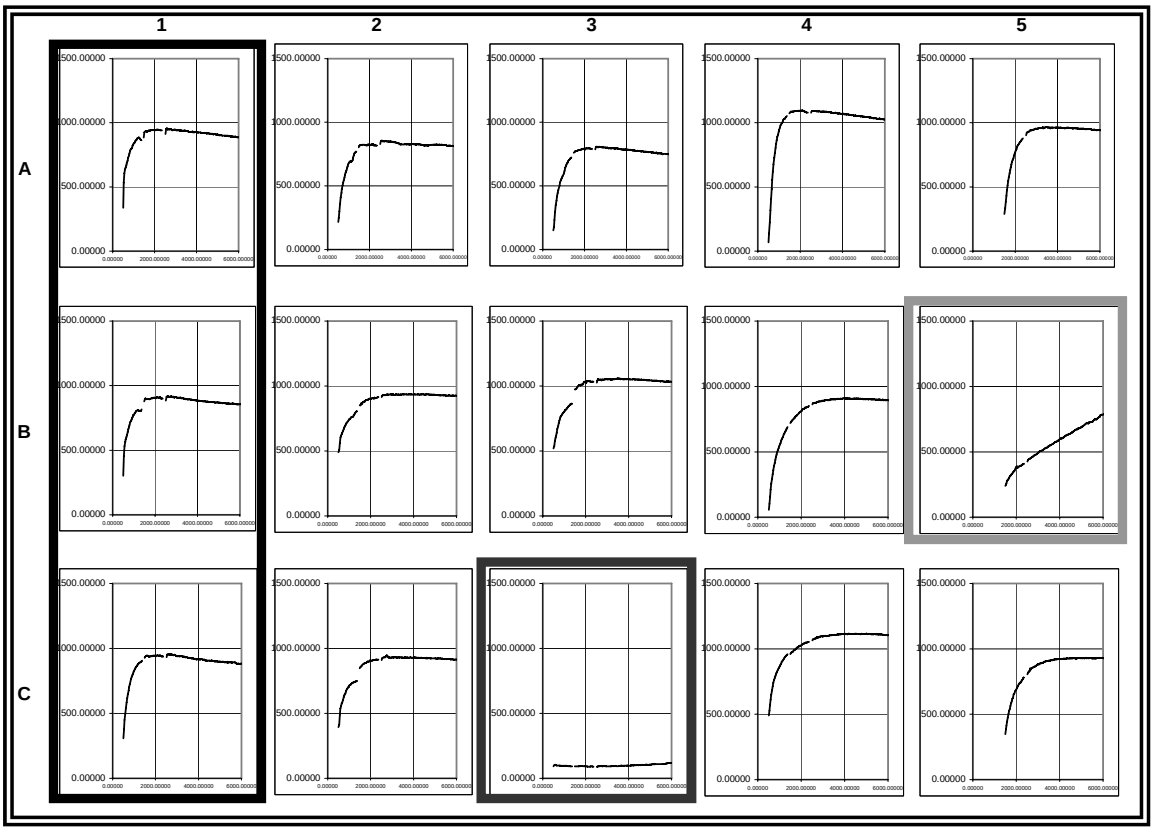

Figure 2

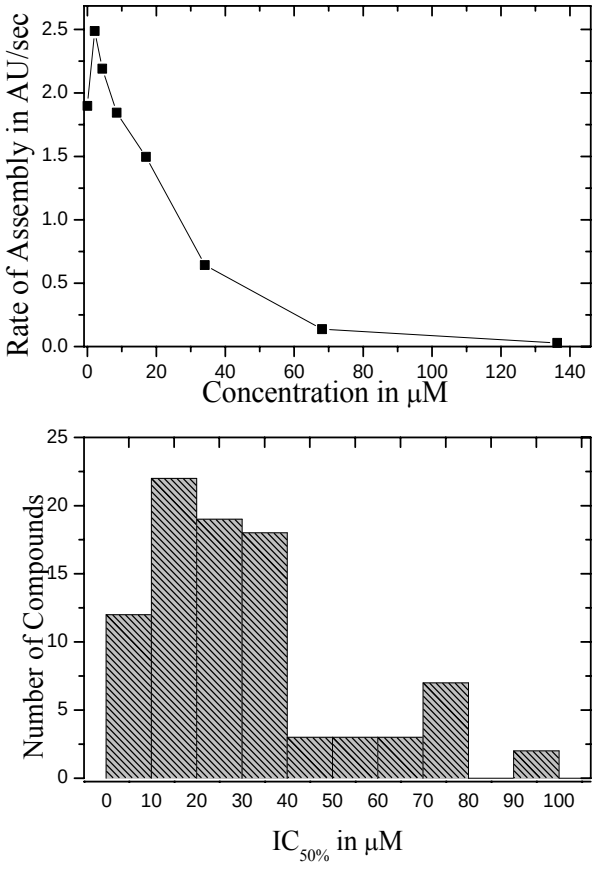
Rate of Assembly in AU/sec
2.5
2.0
1.5
1.0
0.5
0.0
0
20
40
60
80
100
120
140
Concentration in μM
Number of Compounds
25
20
15
10
5
0
0
10
20
30
40
50
60
70
80
90
100
IC50% in μM

Figure 3

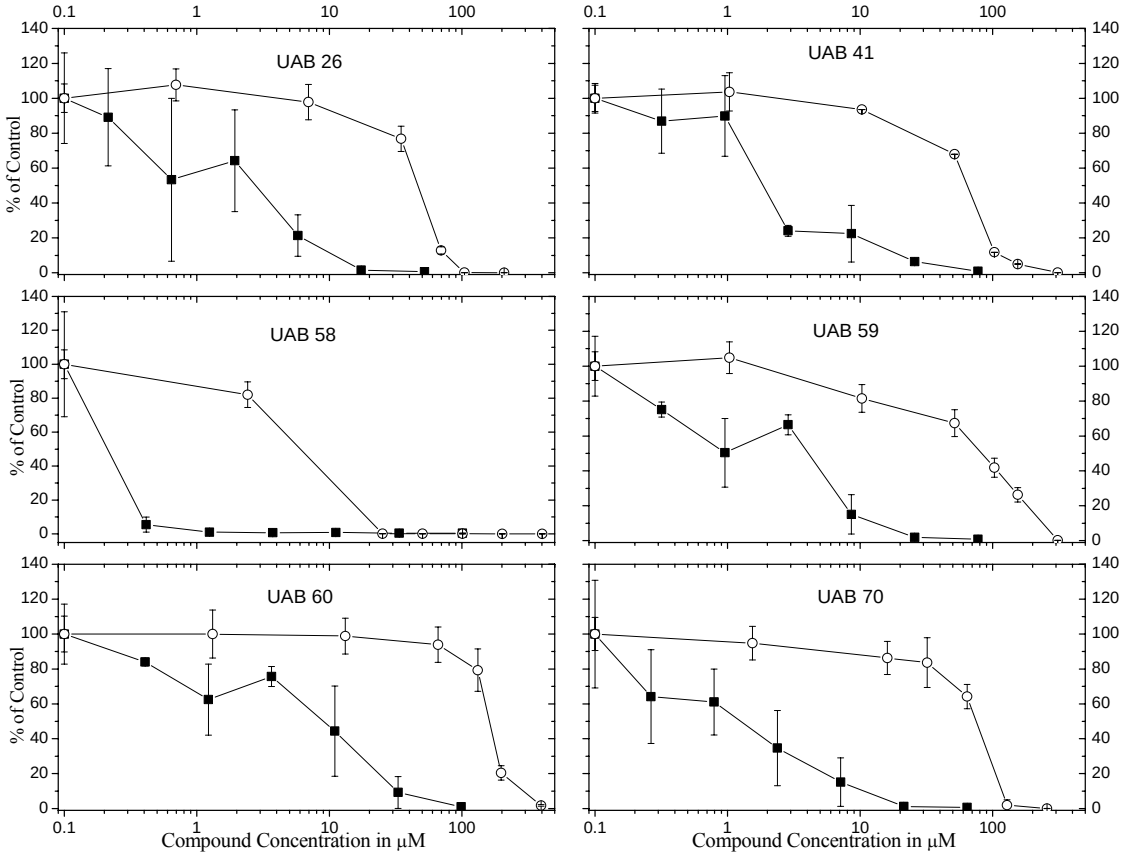
UAB 26
UAB 41
UAB 58
UAB 59
UAB 60
UAB 70
% of Control
Compound Concentration in μM
0.1
1
10
100
0
20
40
60
80
100
120
140

Table 1 – Compiled data of Viral Spread in the Presence of Compounds

	5.25.GFP.Luc.M7 cells			PBMC cells		
Compound	**$IC_{50\%}$**	**$TC_{50\%}$**	**SI**	**$IC_{50\%}$**	**$TC_{50\%}$**	**SI**
UAB 58	0.08	11.7	145.0	7.00	61.5	8.8
UAB 70	1.3	79.2	62.9	4.6	148.4	31.9
UAB 41	2.2	67.9	31.3	n/d	>300	n/d
UAB 59	4.6	86.8	18.7	2.6	272.7	104.9
UAB 60	9.2	165.1	18.0	41.2	>300	>7.3
CAP-1	4.8	76.4	15.8	n/d	60.1	n/d
DSB	n/d	n/d	n/d	0.03	49.3	1896.2
UAB 26	3.12	48.9	15.4	18.4	>300	>16.30
UAB 16	15.2	89.3	5.9	n/d	n/d	n/d
UAB 15	16.9	79.1	4.7	n/d	n/d	n/d
UAB 6	13.2	49.4	3.8	n/d	n/d	n/d
UAB 33	31.5	103.7	3.3	n/d	n/d	n/d
UAB 8	11.4	37.2	3.3	n/d	n/d	n/d

Figure 4

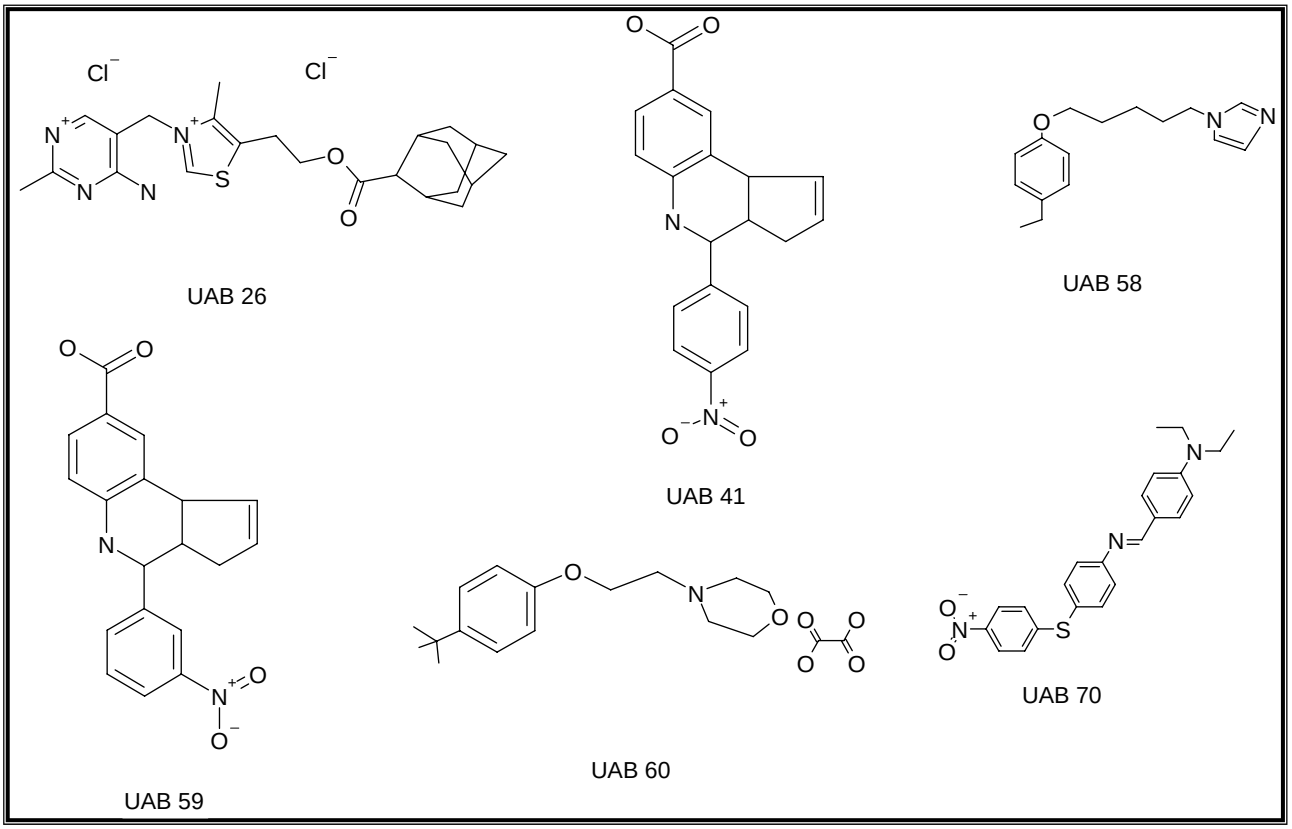

Figure 5

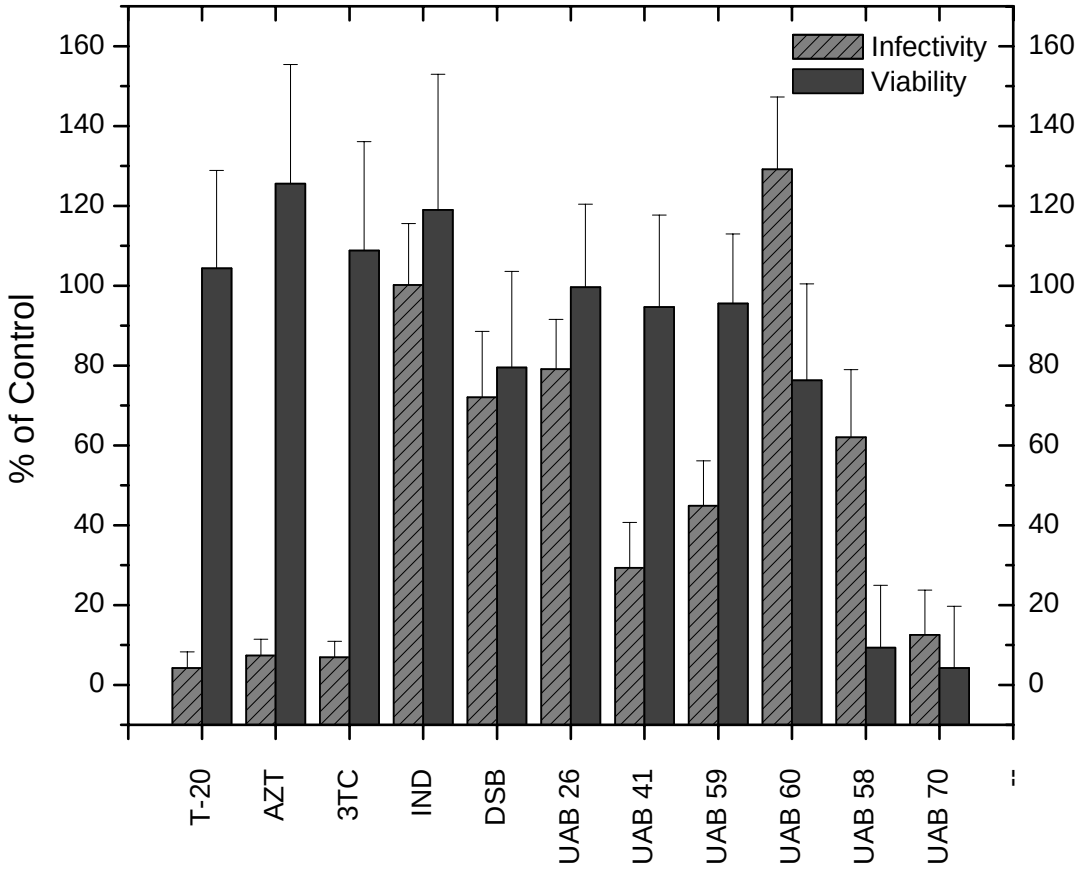
% of Control
Infectivity
Viability
0
20
40
60
80
100
120
140
160
T-20
AZT
3TC
IND
DSB
UAB 26
UAB 41
UAB 59
UAB 60
UAB 58
UAB 70

Figure 6

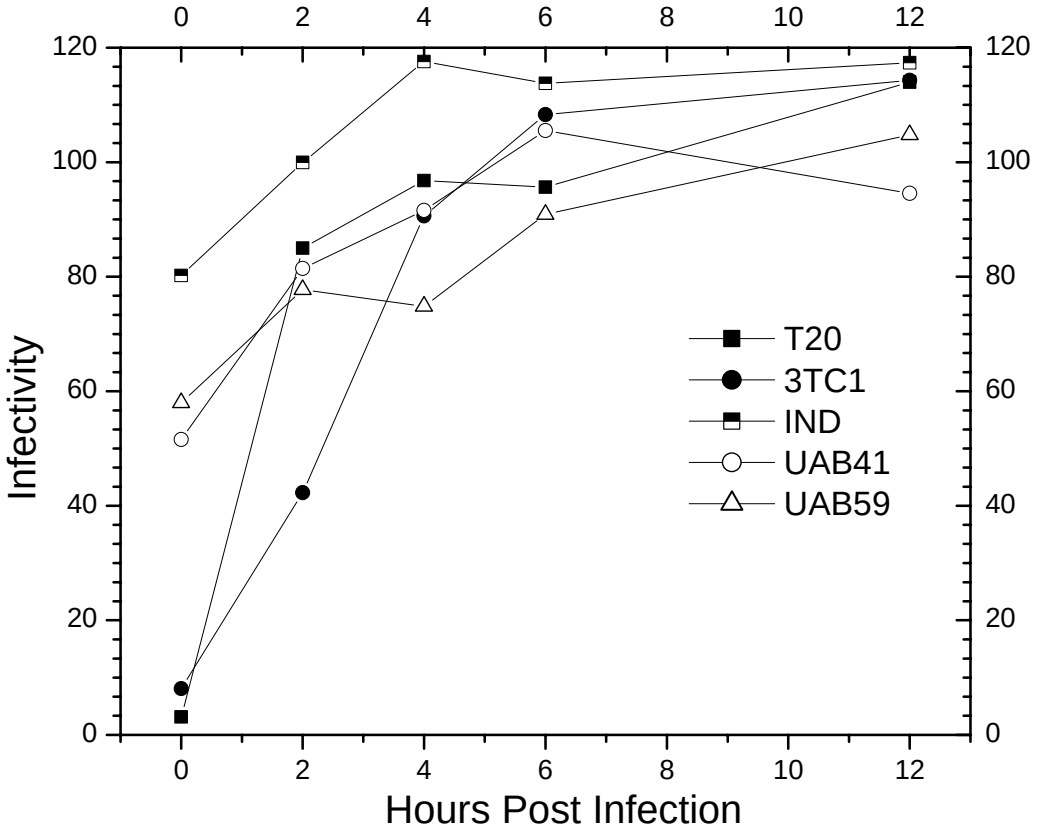
Infectivity
Hours Post Infection
T20
3TC1
IND
UAB41
UAB59
0
20
40
60
80
100
120
0
2
4
6
8
10
12

Figure 7

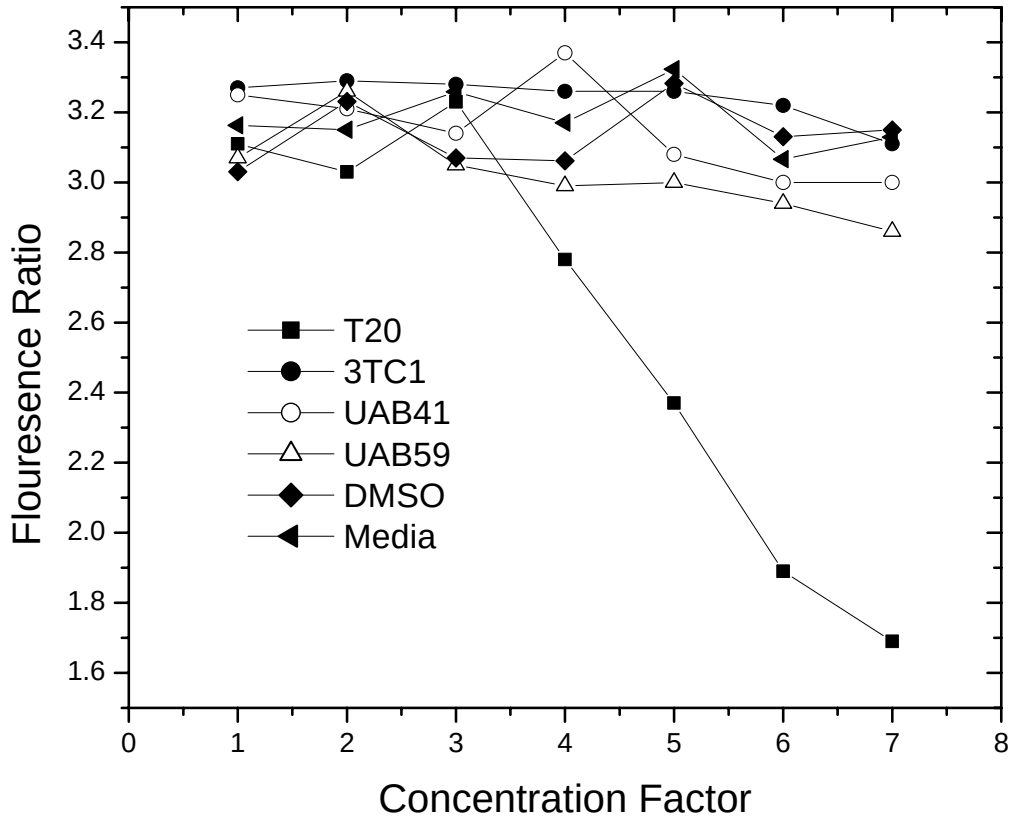
Flouresence Ratio
Concentration Factor
T20
3TC1
UAB41
UAB59
DMSO
Media
3.4
3.2
3.0
2.8
2.6
2.4
2.2
2.0
1.8
1.6
0
1
2
3
4
5
6
7
8

Figure 8

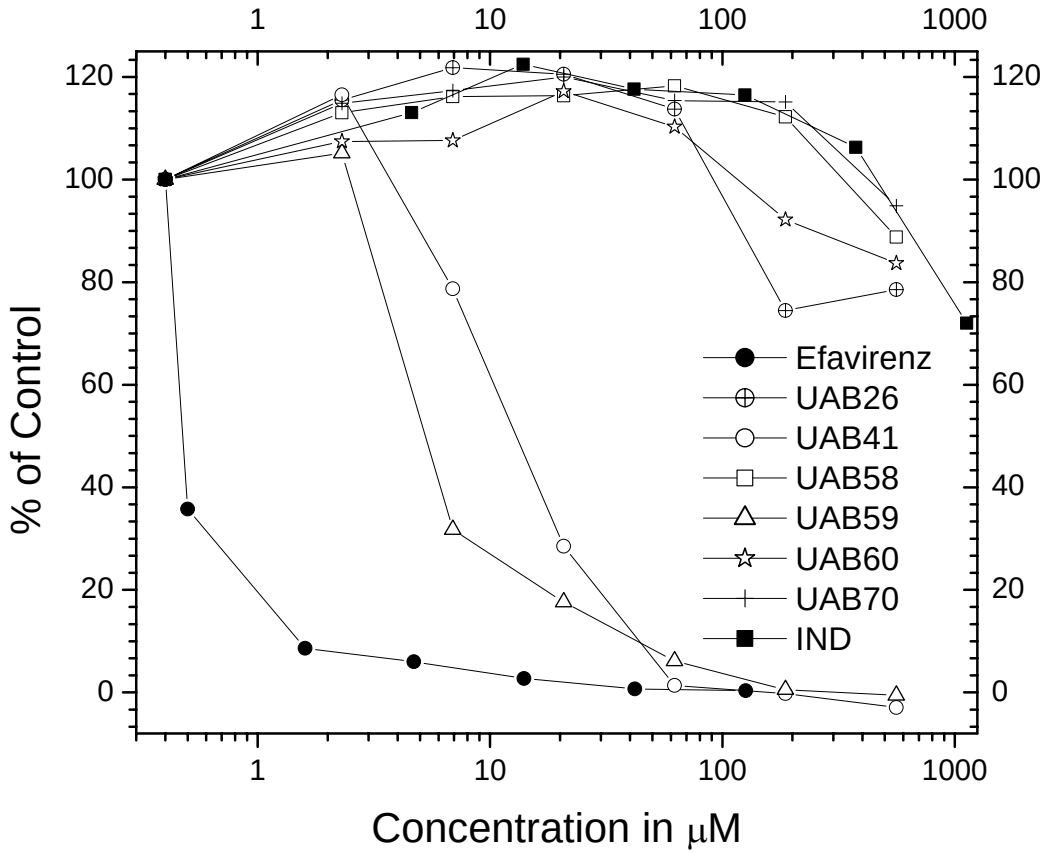
1
10
100
1000
120
100
80
60
40
20
0
% of Control
Efavirenz
UAB26
UAB41
UAB58
UAB59
UAB60
UAB70
IND
Concentration in μM

Figure 9
a)

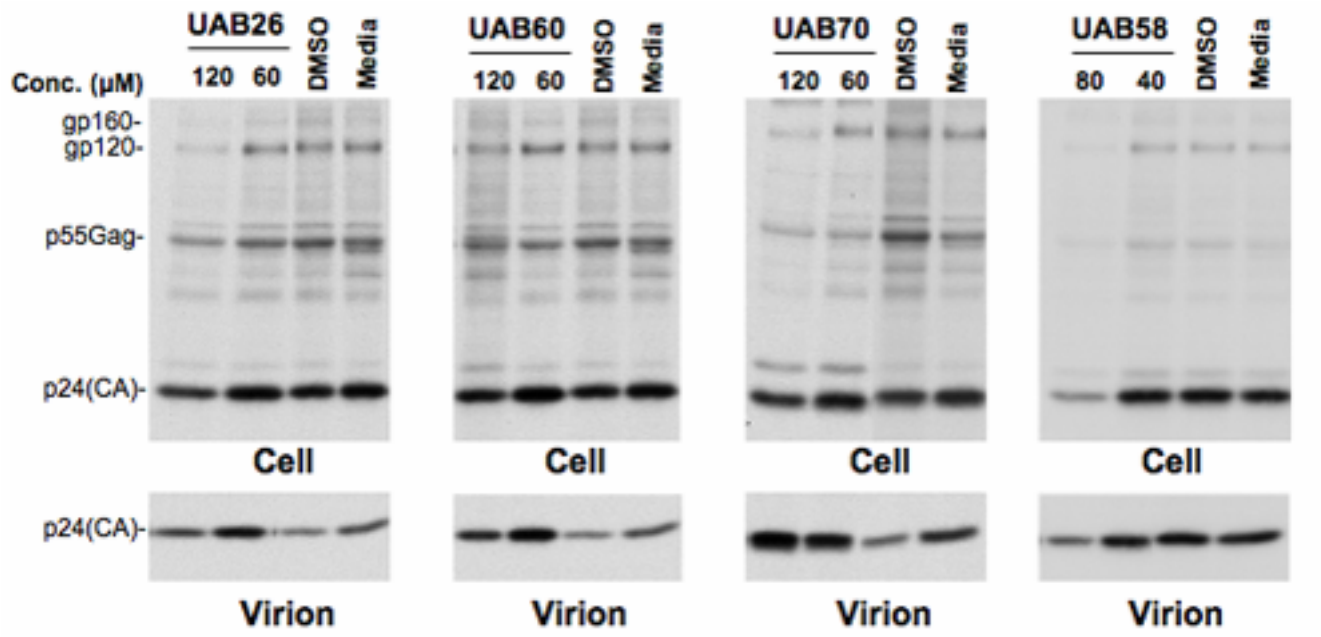
UAB26
UAB60
UAB70
UAB58
Conc. (μM)
120 60 DMSO Media
120 60 DMSO Media
120 60 DMSO Media
80 40 DMSO Media
gp160-
gp120-
p55Gag-
p24(CA)-
Cell
Cell
Cell
Cell
p24(CA)-
Virion
Virion
Virion
Virion

b)

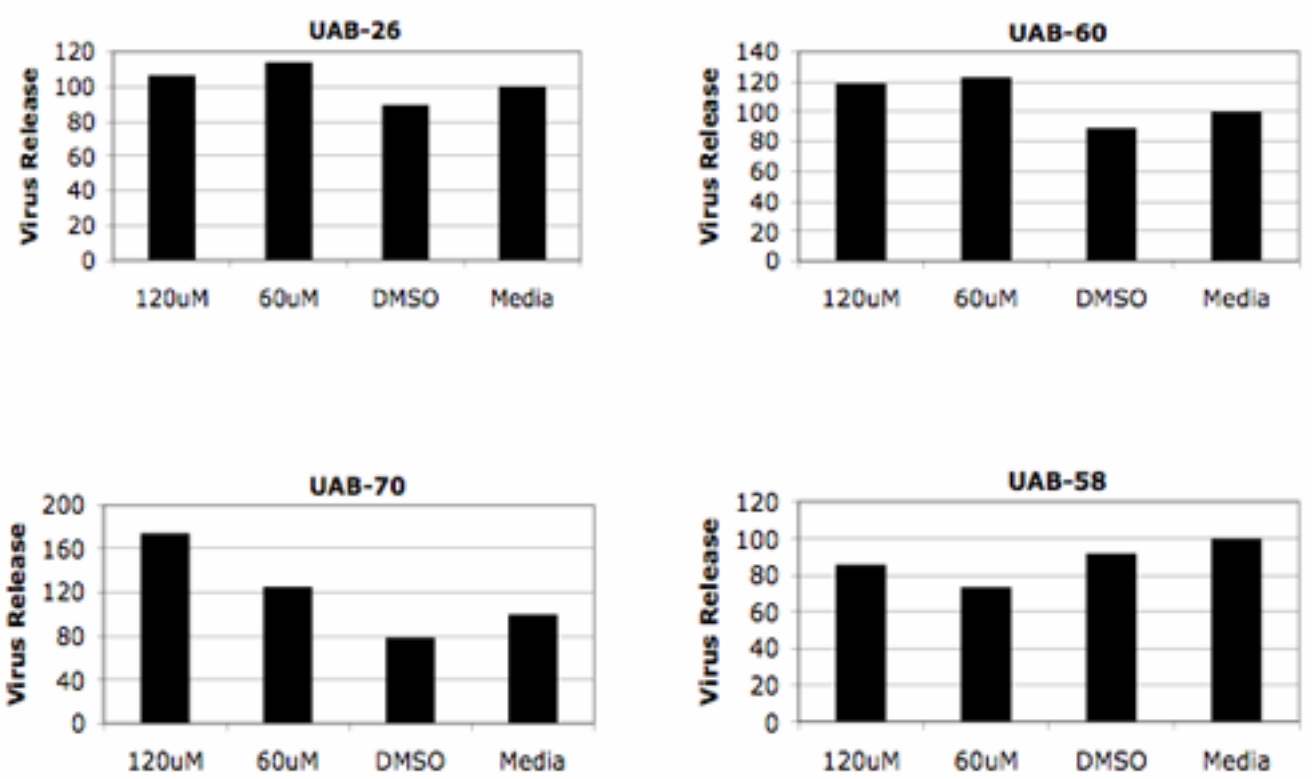
UAB-26
Virus Release
120
100
80
60
40
20
0
120uM
60uM
DMSO
Media
UAB-60
Virus Release
140
120
100
80
60
40
20
0
120uM
60uM
DMSO
Media
UAB-70
Virus Release
200
160
120
80
40
0
120uM
60uM
DMSO
Media
UAB-58
Virus Release
120
100
80
60
40
20
0
120uM
60uM
DMSO
Media

FIGURE LEGENDS

Figure 1 – Section of a 96-well plate for a set of *in-vitro* assembly reactions. Column 1 (black) contains DMSO only (no compound) controls. Position C3 (dark grey)-an assembly reaction in the presence of a compound that was scored in the strongly inhibitory category. Position B5 (light grey) - an assembly reaction in the presence of compound that was scored in the weakly inhibitory category.

Figure 2 – a) Titration curve of the strongly inhibitory compound shown in Fig. 1. The $IC_{50\%}$ for this compound is ~22 μM. b) Histogram of the in-vitro $IC_{50\%}$ distribution for 89 of the strongly inhibitory compounds

Figure 3- Viral spread (closed squares) and cell viability (open circles) for the top six compounds relative to the DMSO control. Experiment performed in triplicate. Error bars represent the standard deviation of the three readings.

Figure 4 – Chemical structures of the top six compounds.

Figure 5 – Assay for inhibition of integration and pre-integration steps. Infectivity (stripe light gray bars) relative to DMSO control and cell viability (dark gray bars) relative to DMSO on mock-infected cells. The data represents the mean from two independent experiments; error bars represent the standard deviation.

Figure 6 – Time of addition assay. Compounds were then added to parallel cultures at the indicated times post-infection in triplicate.

Figure 7 – Entry assay. SG3 Blam-Vpr infected SupT1 cells in the presence of compounds. Fluorescence ratio of blue (infected) and green fluorescence (uninfected) are indicated for each concentration of compound. Concentrations increase two fold for each factor. Base concentrations are 2.3 μM for UAB 41&59, 0.5 μg/ml for T-20 and 0.01 μM for 3TC.

Figure 8 –RT assay. Dose-dependant inhibition by UAB 41 and 59 of the *in-vitro* transcription of a poly-A template by recombinantly purified reverse transcriptase.

Figure 9 – a) Phosphoimages of SDS-PAGE of cell and virion associated immunoprecipated viral proteins. b) Graphical representation of the virus release efficiency determined from the SDS-PAGE in a). Efficiency calculated as Virus p24/ (cell p24+cell Pr55+ virus p24).

SUMMARY

The aim of this work was to build an understanding of the protein/protein interactions involved in HIV-1 capsid assembly as it relates to the condensation of capsid within the virion. The approach to accomplish this takes two divergent routes; 1) Armed with the knowledge that the forces involved in protein/protein interactions are similar to those in protein folding and that electrostatics can be used to determine specificity, docking orientation and may either act to stabilize or destabilize a protein complex we set out to unravel the role of electrostatics in HIV-1 capsid assembly. 2) Secondly, we searched for small molecules that could inhibit or alter the protein/protein interactions in capsid assembly as a means to; 1) use selected small molecules to find binding sites that would be deleterious to assembly and thus characterize sites of interactions important to assembly, 2) determine the feasibility of developing antivirals design to target protein/protein interactions involved in HIV-1 capsid condensation.

In the first section of the dissertation the reprinted article focused on the role of electrostatics in the assembly of HIV-1 capsid. Utilizing a then newly developed in-vitro assay capable of monitoring the process through the time-dependent increase in turbidity, we measured the effects of electrostatic mutants on the process of capsid assembly in-vitro. Some of these mutations were previously shown to affect viral infectivity through stabilization of the core (E45A, E128A/R132A). Focusing on these residues, mutations were made to determine the effect of their charge state on the process of assembly. In addition to the residues studied in-vivo, two previously unstudied mutations, K131A and K131E, were constructed. This charged amino acid was one that was centrally located in the structure of the N-domain of HIV-1 capsid to the other charged residues.

The paper starts by demonstrating that under identical assembly conditions the mutant proteins have varying rates of assembly. To ensure the validity of these differences, the assay was analyzed to verify the turbidity measures were proportional to the amount of polymerized CA for each mutant. In addition, since turbidity is a result of light scattering and in this case provides little information about the structure of the polymerizing protein the assembled mutant capsid were visualized by thin-section electron microscopy (Appendix 1) to confirm tube formation. Next to determine if the charge mutants were altering the assembly rate through changing the rate of subunit addition, the assembly pathway was described by elucidating the number of molecules involved in the rate determining step. This was done by calculating the dependence of the initial assembly rate to the initial protein concentration at constant salt in a manner analogous to chain polymerization in polymer chemistry. Although not explicitly presented in the reprinted article the assembly rate dependence on protein concentration is ~4. This estimate represents the average number of molecules involved in the rate-determining step which for the process of HIV-1 CA assembly in-vitro most likely is a nucleation step substantiated through the existence of a critical concentration for assembly. Interestingly, there is no sub-structure within the final complex that is made-up of four subunits. Isolation of dimers, formed through interactions in the C-domain has been extensively demonstrated (44, 140) and hexameric formation through the N-domain has been shown in the final tube structure (76). Perhaps, the interaction of the N-C interaction is one that occurs between pairs of dimers as modeled by Lanman et al.(68) and through the formation of this critical interaction, hexamers can form and tube elongation can occur.

Having proved that the assay was reliable, the next task undertaken was to prove that the effects seen were due solely to the addition or subtraction of charge and not to conformational changes of the protein. To do this the CD spectra and melting point at fixed ellipticity for each mutant was obtained at protein concentration where the capsid protein is monomeric. Furthermore the stability of the mutant proteins was reaffirmed through the ability to form dimers as assessed by sedimentation equilibrium.

Building on the fact that changes in charge state affected the rate of assembly without, a) influencing the fidelity of the assay, b) altering the conformation or stability of the monomeric protein, or c) modifying the stability of the dimer, we set out to conclusively prove that the changes where strictly a result of varying the electrostatic makeup of the protein. To do this the rate dependence of assembly on salt concentration was determined for each mutant. The ability of all but one mutant to assembly at the same rate once all charges on the protein were neutralized was also demonstrated. The exception was the K131A mutant whose dependent on salt was similar to wild type. In the last section of results this mutant is shown to posses a substantial higher critical concentration for assembly suggesting that impairment in the ability to nucleate is the cause for the differences in assembly rate. Additionally, the level of turbidity associated with the amount of capsid polymerized was lower for this mutant. With E45A, the level was higher and can be shown to be a result of the formation of shorter tubes, due presumably to the ability to form more nuclei. In a similar manner, K131A's inability to nucleate, likely resulted in the formation of longer tubes due to fewer nuclei. Although there is no direct evidence to support this it is suggested by the ability of K131A to participate in assembly when it is aided by E45A which may serve to nucleate the assembly reaction. If indeed

the rate limiting step is the nucleation step and it represents the formation of the N-C interaction, then the inability of this mutation, located away from the N-C interaction site to form this interaction would signify a crucial role of the entire electrostatic network of the protein on capsid condensation.

Lastly the affect of the mutations on the critical concentration of the reaction was measured by determining the concentration of unpolymerized protein remaining after one hour (approximately steady-state) over a range of protein concentration. This figure provides a value for comparing of the energetics of the intersubunit interactions since the critical concentration for polymerization reflects the equilibrium between subunit addition and dissociation. The mutations effect on the assembly rates correspond to their equilibrium positions; mutants with lower critical concentration show faster assembly. The exception to this is the double mutant which had a higher critical concentration than wild type but demonstrated similar assembly kinetics. One possible explanation to this phenomenon is both a reduce capability to form nuclei and shorter tube formation.

The paper finishes with a discussion of the purposed role of electrostatics in uncoating. Concentrating on the metastability of the virion that occurs as a result of maturation, a simplistic model for the role of electrostatics in the uncoating process is presented; surmised from the detrimental role it plays in capsid condensation.

As presented in the “Introduction” section one major conundrum for enveloped viruses is that they must both come together and fall apart in an identical environment. Biologically, the mechanism of maturation in enveloped viruses helps to solve this problem. It allows the virus to stably come together during assembly in the vast volume of a cell, after which a membrane encases the virion reducing that volume and shifts the equi-

librium to one that supports the maintenance of the matured core but primes it to come apart when reintroduced into a new cell. The resulting metastability would seem to be the effect of different or reduction in protein-protein interactions between the two states.

For HIV-1 core formation is aided by the assembly of intermediate structures that are subsequently cleaved. It seems intuitive that there would be more combining interactions in the polyprotein that forms the immature virus than when this protein is cleaved in the mature virus for each of the released proteins. However, concentration dilutions and reduction of interactions may not be enough to drive the disassembly of a formed complex however less stable it may be. Furthermore, the release of each of the sub-proteins undoubtedly results in the formation of new interactions as the protein relaxes and condenses from a stretched out state. Even though this release may allow for the formation of new interactions it is still questionable as to whether these interactions would equal or exceed the interactions present in the immature particle. There may be another reason for assembling through intermediate structures that are subsequently cleaved. In theory, it could allow the virus to overcome negative interactions either by preventing their formation until after maturation or by allowing more net positive interactions. These negative or rather repulsive properties may actually be a major driving force behind virus uncoating in the cell. The mechanism of action for the restriction faction Trim5α has been shown to be the acceleration of uncoating. With mutations located in the N-domain being resistant to this action and removal of charge residues activating the anti-viral activity of the human isoform of Trim5α to HIV-1 electrostatics may be the key to regulating capsid self-association.

In the second section of the dissertation is a manuscript in preparation for submission. Utilizing a library of 10,000 small molecules we screened for the ability of compounds to reduce the turbidity associated with the in-vitro assembly of HIV-1 capsid. One hundred and fourteen of the compounds exhibited strong inhibitory effects on the in-vitro assembly reaction. Equipped with 96 of the 114 compounds we advanced the study to within the virion and searched for compounds that would reduce viral production and spread in culture with limited toxicity to the cell. A series of cell culture assays were performed with the intentions of weeding out compounds with blatant toxicity or permeability problems. From these assays six of the 96 compounds showed anti-viral effect with a selectivity index of $\geq$15.

Next to correlate the compounds in-vitro anti-assembly properties to their anti-viral effects in the cell a number of experiments were performed to establish the stage in the virus life cycle being affected. Three of the six compounds exhibited anti-viral properties during the second half of the virus infectivity cycle, while two compounds demonstrated this ability in the first half. For these two compounds an attempt was made to attribute the antiviral effect to uncoating which is the main capsid related event taking place in this phase. Since, at the time there were no direct ways of monitoring or quantifying the process of uncoating the approach taken was one of elimination of all other possible stages. However, this was not accomplished, since the compounds were found to interfere with the activity of reverse transcriptase. Although unexpected, this does not absolutely eliminate the possibility that these compounds interfere with capsid related events, for which they were chosen, but rather introduces another possible function.

The three compounds affecting the second half of the replication cycle were also subjected to the elimination procedure to determine more concisely the process be affected. Data not including in the manuscript include, thin-section electron micrographs which show no deleterious effect on core structure. These were not included because none of the compound concentrations studied showed complete viral inhibition with little to no toxicity effects. Without this condition, we could not be certain that the viral particles observed were those incorporating compounds. Additionally, the fact that the conical core structure was retained did not eliminate capsid condensation as the compound target since the overall structure can be retained while weakening the complexes stability which in turn affects virus infectivity. Although compounds did not abrogate condensation as has been shown for some mutations and drugs they may alter the interactions present in the structure, a condition that is difficult to prove due to the inherent metastability of the core.

There are a number of capsid involved activities that take place in the second half of the replication cycle. All of which are subject to interference with compounds targeted to capsid. Focusing on these more plausible unintended targets an experiment was designed to investigate the effect of the compounds on Gag trafficking, virus assembly and release. This was accomplished by labeling virus infected cells with [35S] Met/Cys and quantifying the immunoprecipitation of Gag related proteins from both the cell and viral supernatant with HIV-IgG through phosphorimagery. Additionally, analysis of the SDS-PAGE of the extracted proteins revealed normal Gag processing in both the cell and released virus.

Although not mentioned in the text of the manuscript, there were several attempts made to determine the binding site for the compounds. Binding to the N-domain for some of the compounds was determined through NMR chemical shift mapping. UAB 26 binds to this domain in the region involved in the N-C interface, which may explain why the binding sites for some of the other compounds where harder to determine. Currently NMR of HIV-1 capsid is limited to the isolated domains. This is because CA proteins form dimers in solution, whose mass borders the upper limit achievable. Attempts at performing NMR determinations on largely monomeric mutants of the whole protein have been undertaken. However the results were ambiguous in the C-terminal domain due to the large degree of rotation that occurred (7). If the N-C site is the hot spot for binding both halves of the interaction may need to be present to form a sufficient binding pocket. The compounds may not be capable of holding on tight enough to just a fraction of the site. With the current structural information and technical limitations, conclusively demonstrating this region as the primary target for small inhibitory molecules will be difficult.

This manuscript demonstrates that small molecules selected for their ability to inhibit the in-vitro process of capsid assembly can also be used to disrupt viral spread in the cell. It has been more difficult to provide definitive evidence that this anti-viral effect is correlated to interference or alteration of capsid condensation within the virion. However, other stages in the viral replication cycle have been eliminated as targets increasing the probability that capsid condensation serves as the platform for the anti-viral effect exhibited by these compounds.

REFERENCES

1. **A. V. Veselovsky, Y. D. I., A. S. Ivanov, A. I. Archakov, P. Lewi, P. Janssen,.** 2002. Protein-protein interactions: mechanisms and modification by drugs. Journal of Molecular Recognition **15:**405-422.
2. **Alexander I. Archakov, V. M. G., Alexander V. Dubanov, Yuri D. Ivanov, Alexander V. Veselovsky, Paul Lewi, Paul Janssen,.** 2003. Protein-protein interactions as a target for drugs in proteomics. PROTEOMICS **3:**380-391.
3. **Anfinsen, C. B.** 1972. Presented at the Nobel Lecture, December 11, 1972, National Institutes of Health

Bethesda, Maryland.

4. **Arianna Loregian, H. S. M., Giorgio Palù,.** 2002. Protein-protein interactions as targets for antiviral chemotherapy. Reviews in Medical Virology **12:**239-262.
5. **BJERRUM, N.** 1923. Die konstitution der ampholyte, besonders der aminosauren,

und ihre dissoziationskonstanten. Z. physik. chem., **104:**147-173.

6. **Bosco, D. A., and D. Kern.** 2004. Catalysis and Binding of Cyclophilin A with Different HIV-1 Capsid Constructs. Biochemistry **43:**6110-6119.
7. **Briggs, J. A., M. N. Simon, I. Gross, H. G. Krausslich, S. D. Fuller, V. M. Vogt, and M. C. Johnson.** 2004. The stoichiometry of Gag protein in HIV-1. Nat Struct Mol Biol **11:**672-5.
8. **Bruinsma, R. F., W. M. Gelbart, D. Reguera, J. Rudnick, and R. Zandi.** 2003. Viral Self-Assembly as a Thermodynamic Process. Physical Review Letters **90:**248101.
9. **Bukrinskaya, A. G.** 2004. HIV-1 assembly and maturation. Archives of Virology **149:**1067-1082.
10. **Camacho, C. J., Z. Weng, S. Vajda, and C. DeLisi.** 1999. Free Energy Landscapes of Encounter Complexes in Protein-Protein Association. Biophys. J. **76:**1166-1178.
11. **Camarasa, M.-J., S. Velazquez, A. San-Felix, M.-J. Perez-Perez, and F. Gago.** 2006. Dimerization inhibitors of HIV-1 reverse transcriptase, protease and integrase: A single mode of inhibition for the three HIV enzymes? Antiviral Research

Special Issue To Honour Professor Erik De Clercq **71:**260-267.

12. **Casjens, S., and J. King.** 1975. Virus assembly. Annu Rev Biochem **44:**555-611.
13. **Caspar, D. L., and A. Klug.** 1962. Physical principles in the construction of regular viruses. Cold Spring Harb Symp Quant Biol **27:**1-24.
14. **Chatterji, U., M. D. Bobardt, P. Gaskill, D. Sheeter, H. Fox, and P. A. Gallay.** 2006. Trim5{alpha} Accelerates Degradation of Cytosolic Capsid Associated with Productive HIV-1 Entry

10.1074/jbc.M606066200. J. Biol. Chem. **281:**37025-37033.

15. **Chick, H.** 1910. On the "heat coagulation" of proteins. J Physiol **40:**404-30.
16. **Clackson, T., and J. A. Wells.** 1995. A hot spot of binding energy in a hormone-receptor interface. Science **267:**383-6.

17. **Crick, F. H., and J. D. Watson.** 1956. Structure of small viruses. Nature **177:**473-5.
18. **Daggett, V., and A. R. Fersht.** 2003. Is there a unifying mechanism for protein folding? Trends in Biochemical Sciences **28:**18-25.
19. **David C. Fry.** 2006. Protein-protein interactions as targets for small molecule drug discovery. Peptide Science **84:**535-552.
20. **del Alamo, M., J. L. Neira, and M. G. Mateu.** 2003. Thermodynamic dissection of a low affinity protein-protein interface involved in human immunodeficiency virus assembly. J Biol Chem **278:**27923-9.
21. **Downing, K. H.** 2000. STRUCTURAL BASIS FOR THE INTERACTION OF TUBULIN WITH PROTEINS AND DRUGS THAT AFFECT MICROTUBULE DYNAMICS
doi:10.1146/annurev.cellbio.16.1.89. Annual Review of Cell and Developmental Biology **16:**89-111.
22. **Edsall, J. T.** 1995. Wu,Hsien and the First Theory of Protein Denaturation (1931), p. 1-5, Advances in Protein Chemistry, Vol 46, vol. 46.
23. **Eiserling, F. A., and R. C. Dickson.** 1972. Assembly of viruses. Annu Rev Biochem **41:**467-502.
24. **Fersht, A. R.** 1997. Nucleation mechanisms in protein folding. Curr Opin Struct Biol **7:**3-9.
25. **Forshey, B. M., U. von Schwedler, W. I. Sundquist, and C. Aiken.** 2002. Formation of a Human Immunodeficiency Virus Type 1 Core of Optimal Stability Is Crucial for Viral Replication
10.1128/JVI.76.11.5667-5677.2002. J. Virol. **76:**5667-5677.
26. **Fraenkel-Conrat, H., and R. C. Williams.** 1955. Reconstitution of Active Tobacco Mosaic Virus from Its Inactive Protein and Nucleic Acid Components
10.1073/pnas.41.10.690. PNAS **41:**690-698.
27. **Freed, E. O.** 2001. HIV-1 replication. Somat Cell Mol Genet **26:**13-33.
28. **Fung, H. B., and Y. Guo.** 2004. Enfuvirtide: A fusion inhibitor for the treatment of HIV infection. Clinical Therapeutics **26:**352-378.
29. **Gallo, S. A., C. M. Finnegan, M. Viard, Y. Raviv, A. Dimitrov, S. S. Rawat, A. Puri, S. Durell, and R. Blumenthal.** 2003. The HIV Env-mediated fusion reaction. Biochimica et Biophysica Acta (BBA) - Biomembranes
Membrane Fusion **1614:**36-50.
30. **Gamble, T. R., S. Yoo, F. F. Vajdos, U. K. von Schwedler, D. K. Worthylake, H. Wang, J. P. McCutcheon, W. I. Sundquist, and C. P. Hill.** 1997. Structure of the carboxyl-terminal dimerization domain of the HIV-1 capsid protein. Science **278:**849-53.
31. **Ganser, B. K., S. Li, V. Y. Klishko, J. T. Finch, and W. I. Sundquist.** 1999. Assembly and Analysis of Conical Models for the HIV-1 Core
10.1126/science.283.5398.80. Science **283:**80-83.
32. **Ganser-Pornillos, B. K., U. K. von Schwedler, K. M. Stray, C. Aiken, and W. I. Sundquist.** 2004. Assembly Properties of the Human Immunodeficiency Virus Type 1 CA Protein
10.1128/JVI.78.5.2545-2552.2004. J. Virol. **78:**2545-2552.

33. **Garrus, J. E., U. K. von Schwedler, O. W. Pornillos, S. G. Morham, K. H. Zavitz, H. E. Wang, D. A. Wettstein, K. M. Stray, M. Cote, R. L. Rich, D. G. Myszka, and W. I. Sundquist.** 2001. Tsg101 and the Vacuolar Protein Sorting Pathway Are Essential for HIV-1 Budding. Cell **107:**55-65.
34. **Gomez, C., and T. J. Hope.** 2005. The ins and outs of HIV replication doi:10.1111/j.1462-5822.2005.00516.x. Cellular Microbiology **7:**621-626.
35. **Harrison, S. C., and R. Durbin.** 1985. Is there a single pathway for the folding of a polypeptide chain? Proc Natl Acad Sci U S A **82:**4028-30.
36. **HIV/AIDS, J. U. N. P. o.** 2006. Report on the global AIDS epidemic 2006.
37. **Hutchison, C. A., 3rd, S. Phillips, M. H. Edgell, S. Gillam, P. Jahnke, and M. Smith.** 1978. Mutagenesis at a specific position in a DNA sequence. J Biol Chem **253:**6551-60.
38. **Hvidt, A., and K. Linderstrom-Lang.** 1954. Exchange of hydrogen atoms in insulin with deuterium atoms in aqueous solutions. Biochim Biophys Acta **14:**574-5.
39. **Kauzmann, W.** 1959. Some factors in the interpretation of protein denaturation. Adv Protein Chem **14:**1-63.
40. **Kol, N., Y. Shi, M. Tsvitov, D. Barlam, R. Z. Shneck, M. S. Kay, and I. Rousso.** 2007. A Stiffness Switch in Human Immunodeficiency Virus 10.1529/biophysj.106.093914. Biophys. J. **92:**1777-1783.
41. **Kotov, A., J. Zhou, P. Flicker, and C. Aiken.** 1999. Association of Nef with the Human Immunodeficiency Virus Type 1 Core. J. Virol. **73:**8824-8830.
42. **Lanman, J., T. T. Lam, S. Barnes, M. Sakalian, M. R. Emmett, A. G. Marshall, and P. E. Prevelige, Jr.** 2003. Identification of novel interactions in HIV-1 capsid protein assembly by high-resolution mass spectrometry. J Mol Biol **325:**759-72.
43. **Lanman, J., T. T. Lam, M. R. Emmett, A. G. Marshall, M. Sakalian, and P. E. Prevelige, Jr.** 2004. Key interactions in HIV-1 maturation identified by hydrogen-deuterium exchange. Nat Struct Mol Biol **11:**676-7.
44. **Lanman, J., and J. Prevelige, Peter E.** 2005. Kinetic and Mass Spectrometry[hyphen (true graphic)]Based Investigation of Human Immunodeficiency Virus Type 1 Assembly and Maturation
Advances in Virus Research, p. 285-309. *In* P. Roy (ed.), Virus Structure and Assembly, Volume 64 ed. Academic Press.
45. **Levinthal, C.** 1968. Are There Pathways for Protein Folding? Journal de Chimie Physique, **65:**44-45.
46. **Li, S., C. P. Hill, W. I. Sundquist, and J. T. Finch.** 2000. Image reconstructions of helical assemblies of the HIV-1 CA protein. **407:**409-413.
47. **Linderstrom-Lang, K.** 1924. On the Ionization of Proteins. C. R. Trav. Lab. Carlsberg, Ser. Chim **15:**29.
48. **Lipinski, C. A., F. Lombardo, B. W. Dominy, and P. J. Feeney.** 2001. Experimental and computational approaches to estimate solubility and permeability in drug discovery and development settings. Adv Drug Deliv Rev **46:**3-26.
49. **Lundquist, D., N. Lundquis, and S. J. Linton.** 2007. How is persistent insomnia maintained? A prospective study on 50-60 years old adults in the general population. Br J Health Psychol.

50. **Markowitz, M., H. Mohri, S. Mehandru, A. Shet, L. Berry, R. Kalyanaraman, A. Kim, C. Chung, P. Jean-Pierre, A. Horowitz, M. L. Mar, T. Wrin, N. Parkin, M. Poles, C. Petropoulos, M. Mullen, D. Boden, and D. D. Ho.** Infection with multidrug resistant, dual-tropic HIV-1 and rapid progression to AIDS: a case report. The Lancet **365:**1031-1038.
51. **McCoy, A. J., V. Chandana Epa, and P. M. Colman.** 1997. Electrostatic complementarity at protein/protein interfaces. Journal of Molecular Biology **268:**570-584.
52. **Mirsky, A. E., and L. Pauling.** 1936. On the Structure of Native, Denatured, and Coagulated Proteins
10.1073/pnas.22.7.439. PNAS **22:**439-447.
53. **Morrison, K. L., and G. A. Weiss.** 2001. Combinatorial alanine-scanning. Current Opinion in Chemical Biology **5:**302-307.
54. **Nisole, S., and A. Saib.** 2004. Early steps of retrovirus replicative cycle. Retrovirology **1:**9.
55. **Pauling, L., and R. B. Corey.** 1951. Configurations of Polypeptide Chains With Favored Orientations Around Single Bonds: Two New Pleated Sheets. Proc Natl Acad Sci U S A **37:**729-40.
56. **Pauling, L., R. B. Corey, and H. R. Branson.** 1951. The structure of proteins; two hydrogen-bonded helical configurations of the polypeptide chain. Proc Natl Acad Sci U S A **37:**205-11.
57. **Perham, R. N.** 1975. Self-assembly of biological macromolecules. Philos Trans R Soc Lond B Biol Sci **272:**123-36.
58. **Pettit, S. C., L. E. Everitt, S. Choudhury, B. M. Dunn, and A. H. Kaplan.** 2004. Initial cleavage of the human immunodeficiency virus type 1 GagPol precursor by its activated protease occurs by an intramolecular mechanism. J Virol **78:**8477-85.
59. **Pettit, S. C., S. Gulnik, L. Everitt, and A. H. Kaplan.** 2003. The dimer interfaces of protease and extra-protease domains influence the activation of protease and the specificity of GagPol cleavage. J Virol **77:**366-74.
60. **Pettit, S. C., J. N. Lindquist, A. H. Kaplan, and R. Swanstrom.** 2005. Processing sites in the human immunodeficiency virus type 1 (HIV-1) Gag-Pro-Pol precursor are cleaved by the viral protease at different rates. Retrovirology **2:**66.
61. **Pettit, S. C., M. D. Moody, R. S. Wehbie, A. H. Kaplan, P. V. Nantermet, C. A. Klein, and R. Swanstrom.** 1994. The p2 domain of human immunodeficiency virus type 1 Gag regulates sequential proteolytic processing and is required to produce fully infectious virions. J. Virol. **68:**8017-8027.
62. **Prevelige, P. E., Jr.** 1998. Inhibiting virus-capsid assembly by altering the polymerisation pathway. Trends Biotechnol **16:**61-5.
63. **Ptitsyn, O. B.** 1973. [Stages in the mechanism of self-organization of protein molecules]. Dokl Akad Nauk SSSR **210:**1213-5.
64. **Reguera, J., A. Carreira, L. Riolobos, J. M. Almendral, and M. G. Mateu.** 2004. Role of interfacial amino acid residues in assembly, stability, and conformation of a spherical virus capsid. Proc Natl Acad Sci U S A **101:**2724-9.
65. **Rodriguez-Barrios, F., C. Perez, E. Lobaton, S. Velazquez, C. Chamorro, A. San-Felix, M. J. Perez-Perez, M. J. Camarasa, H. Pelemans, J. Balzarini, and**

F. Gago. 2001. Identification of a putative binding site for [2',5'-bis-O-(tert-butyldimethylsilyl)-beta-D-ribofuranosyl]-3'-spiro-5"- (4"-amino-1",2"-oxathiole-2",2"-dioxide)thymine (TSAO) derivatives at the p51-p66 interface of HIV-1 reverse transcriptase. J Med Chem **44:**1853-65.

66. **Roy, P.** 2005. Bluetongue Virus Proteins And Particles And Their Role In Virus Entry, Assembly, And Release
Advances in Virus Research, p. 69-123. *In* P. Roy (ed.), Virus Structure and Assembly, Volume 64 ed. Academic Press.
67. **Schreiber, G., and A. R. Fersht.** 1996. Rapid, electrostatically assisted association of proteins. Nat Struct Biol **3:**427-31.
68. **Schymkowitz, J. W. H., F. Rousseau, and L. Serrano.** 2002. Surfing on protein folding energy landscapes
10.1073/pnas.012686599. PNAS **99:**15846-15848.
69. **Sheinerman, F. B., R. Norel, and B. Honig.** 2000. Electrostatic aspects of protein-protein interactions. Current Opinion in Structural Biology **10:**153-159.
70. **Sinha, N., and S. J. Smith-Gill.** 2002. Electrostatics in Protein Binding and Function. Current Protein & Peptide Science **3:**601-614.
71. **Song, M.-c., S. Rajesh, Y. Hayashi, and Y. Kiso.** 2001. Design and synthesis of new inhibitors of HIV-1 protease dimerization with conformationally constrained templates. Bioorganic & Medicinal Chemistry Letters **11:**2465-2468.
72. **Stremlau, M., M. Perron, M. Lee, Y. Li, B. Song, H. Javanbakht, F. Diaz-Griffero, D. J. Anderson, W. I. Sundquist, and J. Sodroski.** 2006. From the Cover: Specific recognition and accelerated uncoating of retroviral capsids by the TRIM5{alpha} restriction factor
10.1073/pnas.0509996103. PNAS **103:**5514-5519.
73. **Stuchell, M. D., J. E. Garrus, B. Muller, K. M. Stray, S. Ghaffarian, R. McKinnon, H.-G. Krausslich, S. G. Morham, and W. I. Sundquist.** 2004. The Human Endosomal Sorting Complex Required for Transport (ESCRT-I) and Its Role in HIV-1 Budding
10.1074/jbc.M405226200. J. Biol. Chem. **279:**36059-36071.
74. **TANFORD, C.** 1997. How protein chemists learned about the hydrophobic factor. Protein Sci **6:**1358-1366.
75. **Tang, C., E. Loeliger, I. Kinde, S. Kyere, K. Mayo, E. Barklis, Y. Sun, M. Huang, and M. F. Summers.** 2003. Antiviral Inhibition of the HIV-1 Capsid Protein. Journal of Molecular Biology **327:**1013-1020.
76. **Tersoff, J.** 1992. Energies of fullerenes. Physical Review B **46:**15546 LP - 15549.
77. **Teschke, C. M., J. King, and P. E. Prevelige, Jr.** 1993. Inhibition of viral capsid assembly by 1,1'-bi(4-anilinonaphthalene-5-sulfonic acid). Biochemistry **32:**10658-65.
78. **Tiselius, A.** 1937. Electrophoresis of serum globulin. I. Biochem J **31:**313-7.
79. **Tiselius, A.** 1937. Electrophoresis of serum globulin: Electrophoretic analysis of normal and immune sera. Biochem J **31:**1464-77.
80. **VerPlank, L., F. Bouamr, T. J. LaGrassa, B. Agresta, A. Kikonyogo, J. Leis, and C. A. Carter.** 2001. Tsg101, a homologue of ubiquitin-conjugating (E2) enzymes, binds the L domain in HIV type 1 Pr55Gag

10.1073/pnas.131059198. PNAS **98:**7724-7729.
81. **von Schwedler, U. K., K. M. Stray, J. E. Garrus, and W. I. Sundquist.** 2003. Functional Surfaces of the Human Immunodeficiency Virus Type 1 Capsid Protein
10.1128/JVI.77.9.5439-5450.2003. J. Virol. **77:**5439-5450.
82. **Weber, G.** 1975. Energetics of ligand binding to proteins. Adv Protein Chem **29:**1-83.
83. **Wiegers, K., G. Rutter, H. Kottler, U. Tessmer, H. Hohenberg, and H. G. Krausslich.** 1998. Sequential steps in human immunodeficiency virus particle maturation revealed by alterations of individual Gag polyprotein cleavage sites. J Virol **72:**2846-54.
84. **Worthylake, D. K., H. Wang, S. Yoo, W. I. Sundquist, and C. P. Hill.** 1999. Structures of the HIV-1 capsid protein dimerization domain at 2.6 A resolution. Acta Crystallogr D Biol Crystallogr **55:**85-92.
85. **Wyma, D. J., J. Jiang, J. Shi, J. Zhou, J. E. Lineberger, M. D. Miller, and C. Aiken.** 2004. Coupling of human immunodeficiency virus type 1 fusion to virion maturation: a novel role of the gp41 cytoplasmic tail. J Virol **78:**3429-35.
86. **Xu, D., C. Tsai, and R. Nussinov.** 1997. Hydrogen bonds and salt bridges across protein-protein interfaces
10.1093/protein/10.9.999. Protein Eng. **10:**999-1012.
87. **Yon, J. M.** 2002. Protein folding in the post-genomic era. J Cell Mol Med **6:**307-27.
88. **Zlotnick, A., P. Ceres, S. Singh, and J. M. Johnson.** 2002. A small molecule inhibits and misdirects assembly of hepatitis B virus capsids. J Virol **76:**4848-54.

APPENDIX A

SUPPLEMENTAL HIV-1 CAPSID MUTATION DATA
(Data Referenced as Data Not Shown in Reprint)

Assembly of K131E at Various Concentrations Exhibiting Little Assembly Capabilities

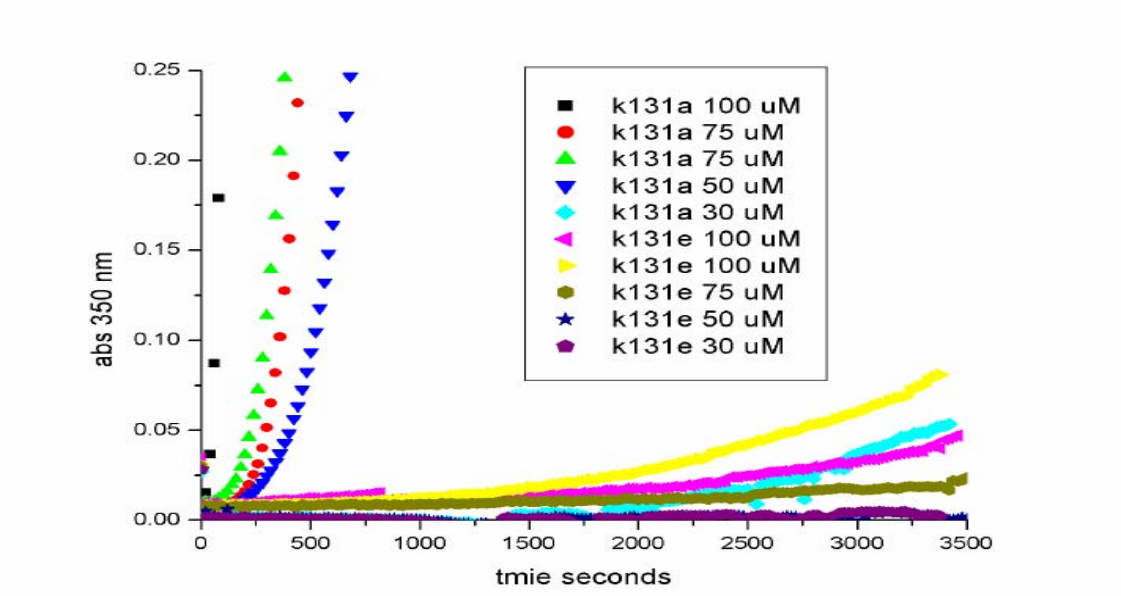

Thin-Section Electron Microscopy Showing Shorter Tubes for E45A Compared to Wild Type

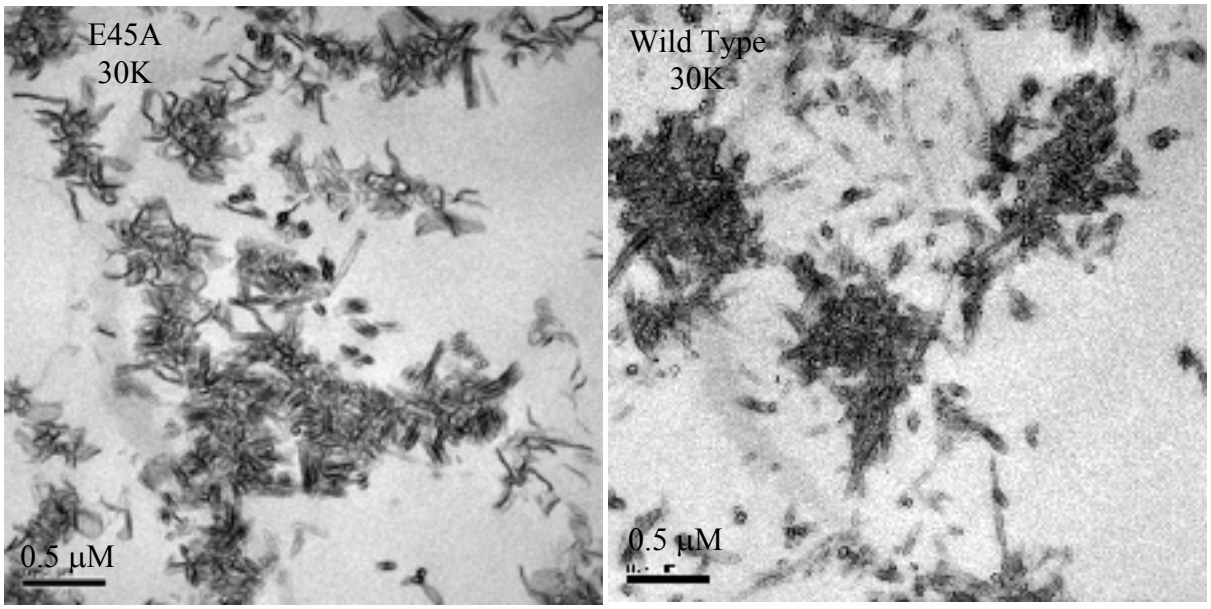

Assembly Reaction of K131E with E45A and Wild Type Protein

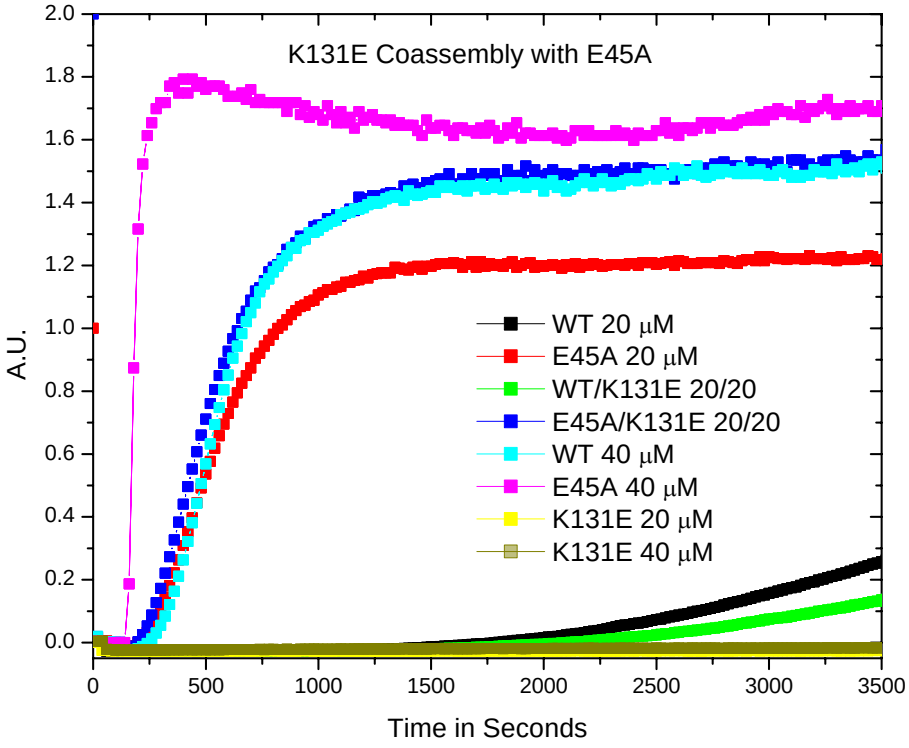

Equilibrium Sedimentation of E45A N-Domain in the Absence and Presence of High Salt

Model : Self Association 2/10/2004 14:27:50
Data Set: c:/xlada494/122303/151953/E45AN11

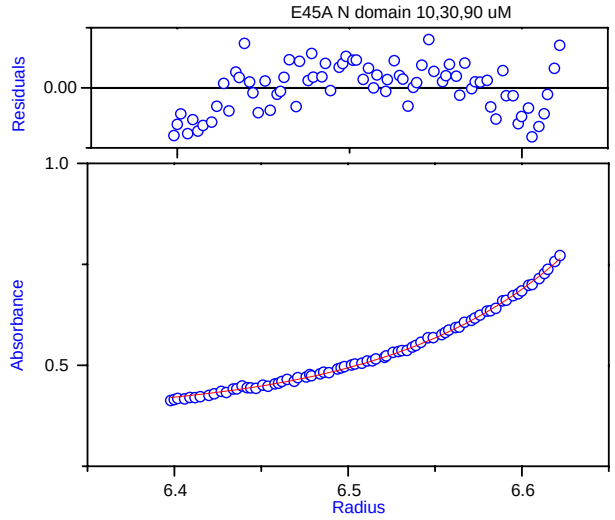

DOF = 548 Variance = 1.63236E-4

Fitted Parameters:

Co	Offset
0.004	0.045
0.026	0.065
0.422	0.521
0.007	0.160
0.044	0.377
0.192	0.879
0.003	0.161
0.013	0.427
0.068	1.187

M = 15578 B = 0
N2 = 2.00 Ka2 = 1E-20
N3 = 3.00 Ka3 = 1E-20
N4 = 4.00 Ka4 = 1E-20

Speed = 30000
Time = 580151
Temp = 20
V-bar = 0.7388
Rho = 1.0322

E45A N dom

Model : Self Association 2/10/2004 14:30:58
Data Set: c:/xlada494/122303/151953/E45ANS8

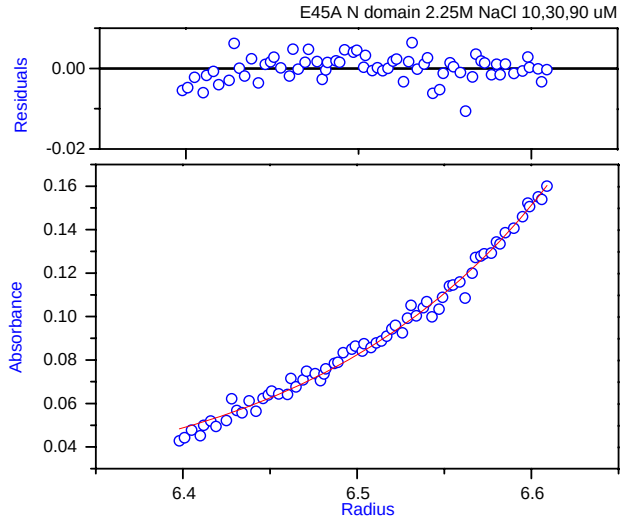

DOF = 571 Variance = 9.86678E-5

Fitted Parameters:

Co	Offset
0.023	0.020
0.047	0.017
0.870	0.035
0.021	0.017
0.033	0.015
1.571	0.076
0.003	0.006
0.004	0.004
0.398	0.128

M = [redacted] B = 0
N2 = 2.00 Ka2 = 1E-20
N3 = 3.00 Ka3 = 1E-20
N4 = 4.00 Ka4 = 1E-20

Speed = 30000
Time = 580975
Temp = 20
V-bar = 0.7385
Rho = 1.12044

E45A N dom w/ Salt

APPENDIX B

COMPILED CELL CULTURE DATA

Table of Cell Culture Luc-M7

Compound	TC50	IC50	SI
MS	76.4	4.8	15.8
UAB 1	114.6	>69.9	>1.6
UAB 3	120.0	>50.	>2.4
UAB 4	5.5	>50.	>0.1
UAB 5	59.6	41.3	1.4
UAB 6	39.4	16.5	2.4
UAB 7	55.1		
UAB 8	31.6	15.2	2.1
UAB 9	47.7		
UAB 10	78.3		
UAB 11	52.6		
UAB 12	34.9		
UAB 13	51.3	>65.3	>0.8
UAB 14	60.5	44.0	1.4
UAB 15	97.0	32.6	3.0
UAB 16	106.7	28.6	3.7
UAB 17	43.4		
UAB 18	5.5	3.5	1.6
UAB 19	44.7		
UAB 20	87.3	66.2	1.3
UAB 21	191.2		
UAB 22	191.3		
UAB 23	57.4	>49.9	>1.2
UAB 24	79.6	>63.	>1.3
UAB 25	7.1	5.4	1.3
UAB 26	48.9	3.2	15.4
UAB 27	44.0		
UAB 31	63.5		
UAB 32	45.0	>64.8	>0.7
UAB 33	75.4	35.9	2.1
UAB 34	30.9		
UAB 35	20.6		
UAB 36	0.9		
UAB 37	10.4		
UAB 38	32.3		
UAB 39	5.5		
UAB 40	18.0		
UAB 41	67.9	2.2	31.3
UAB 42	90.9		
UAB 43	147.6		
UAB 44	191.6		
UAB 45	76.9		
UAB 46	45.9	40.7	1.1

Compound	TC50	IC50	SI
UAB 47	57.1	82.3	0.7
UAB 48	348.2		
UAB 49	48.3		
UAB 50	34.0		
UAB 51	54.6		
UAB 52	34.2		
UAB 53	7.9		
UAB 54	52.3		
UAB 55	8.3		
UAB 56	85.7		
UAB 57	129.3		
UAB 58	11.7	0.1	145.0
UAB 59	86.8	4.6	18.7
UAB 60	165.1	9.2	18.0
UAB 61	226.6		
UAB 62	19.9		
UAB 65	25.0		
UAB 66	55.0		
UAB 67	20.8		
UAB 68	26.9		
UAB 69	15.2		
UAB 70	79.2	1.3	62.9
UAB 71	6.9		
UAB 72	90.6		
UAB 73	7.9	5.9	1.3
UAB 74	78.2		
UAB 75	194.7		
UAB 76	1.2		
UAB 77	110.9		
UAB 78	116.6		
UAB 79	15.1		
UAB 81	34.0		

293T Cell Culture Data

Compound	Infectivity 50%	p24 50%	TC50%	SI - Infectivity	SI - p24
UAB 14	N/A	62.8	102.0		1.6
UAB 18	43.2	1.8	9.1	0.2	5.1
UAB 25	17.7	10.4	174.0	9.8	16.7
UAB 26	17.6	60.2	193.0	11.0	3.2
UAB 47	34.2	24.6	202.0	5.9	8.2
UAB 58	10.0	1.7	5.0	0.5	3.0
UAB 70	32.9	67.5	135.2	4.1	2.0
UAB 73	32.0	70.0	178.4	5.6	2.5